

See discussions, stats, and author profiles for this publication at: <https://www.researchgate.net/publication/47792972>

# Magnetic Resonance Imaging Tracking of Stem Cells in Vivo Using Iron Oxide Nanoparticles as a Tool for the Advancement of Clinical Regenerative Medicine

ARTICLE in CHEMICAL REVIEWS · NOVEMBER 2010

Impact Factor: 46.57 · DOI: 10.1021/cr1001832 · Source: PubMed

---

CITATIONS

180

---

READS

383

8 AUTHORS, INCLUDING:



**Hossein Hosseinkhani**

122 PUBLICATIONS 2,366 CITATIONS

SEE PROFILE



**A. Simchi**

Sharif University of Technology

198 PUBLICATIONS 3,537 CITATIONS

SEE PROFILE



**Karthikeyan Subramani**

Roseman University of Health Sciences

41 PUBLICATIONS 472 CITATIONS

SEE PROFILE



**Sophie Laurent**

Université de Mons

251 PUBLICATIONS 10,050 CITATIONS

SEE PROFILE

# Magnetic Resonance Imaging Tracking of Stem Cells in Vivo Using Iron Oxide Nanoparticles as a Tool for the Advancement of Clinical Regenerative Medicine

Morteza Mahmoudi,<sup>\*,†,⊗</sup> Hossein Hosseinkhani,<sup>‡</sup> Mohsen Hosseinkhani,<sup>‡</sup> Sebastien Boutry,<sup>§</sup> Abdolreza Simchi,<sup>||</sup> W. Shane Journeay,<sup>#,▽</sup> Karthikeyan Subramani,<sup>○</sup> and Sophie Laurent<sup>§</sup>

National Cell Bank, Pasteur Institute of Iran, Tehran 1316943551, Iran, Cardiovascular Research Center, Mount Sinai School of Medicine, New York, New York 10029, United States, Department of General, Organic, and Biomedical Chemistry, NMR and Molecular Imaging Laboratory, University of Mons, Avenue Maistriau, 19, B-7000 Mons, Belgium, Institute for Nanoscience and Nanotechnology, Sharif University of Technology, Tehran 14588, Iran, Department of Biomedical Engineering, National Yang Ming University, No 155, Sec. 2, LiNong Street, Taipei 112, Taiwan, Nanotechnology Toxicology Consulting & Training, Inc., Nova Scotia, Canada, Faculty of Medicine, Dalhousie Medical School, Dalhousie University, Halifax, Nova Scotia, Canada, and Institute for Nanoscale Science and Technology (INSAT), University of Newcastle upon Tyne, Newcastle upon Tyne, NE1 7ER, U.K., <sup>⊗</sup>Nanotechnology Research Centre, Faculty of Pharmacy, Tehran University of Medical Sciences, Tehran, Iran

Received June 12, 2010

## Contents

1. Introduction	253	4.2. Surface Engineering of MRI Contrast Agents for Labeling MSCs	266
1.1. Mesenchymal Stem Cells (MSCs)	254	5. NSCs Labeling	269
1.2. Neural Stem Cells (NSCs)	256	6. In Vivo Tracking of Stem Cells	271
2. Magnetic Resonance Imaging (MRI) Technique	256	6.1. Animal Studies	271
2.1. Relaxation Times	258	6.2. Human Studies	272
2.2. Relaxation Mechanisms	258	7. Conclusions and Further Perspectives	274
3. Nanoparticles Delivery Systems	259	8. References	274
3.1. Advantages of Using Nanoparticles for Drug Delivery	260		
3.2. Nanoparticles in Drug Delivery	260		
3.2.1. Polymeric Biodegradable Nanoparticles	260		
3.2.2. Ceramic Nanoparticles	260		
3.2.3. Polymeric Micelles	261		
3.2.4. Dendrimers	261		
3.2.5. Liposomes	261		
3.3. Nanoparticles for Cellular Labeling	261		
3.3.1. Nanoparticles for Stem Cell Labeling	261		
3.3.2. Advantages of SPIONs	262		
3.4. Superparamagnetic Iron Oxide Nanoparticles for Stem Cell Labeling	262		
3.5. Applications of Nanoparticles in Imaging and Drug Delivery	262		
3.6. Nanotoxicology	263		
3.6.1. In Vitro Toxicity Assessment	265		
3.6.2. Cytotoxicity End-Points	265		
3.6.3. SPIONs Toxicity	265		
3.6.4. Considerations for In Vivo Applications	266		
4. MSCs Labeling	266		
4.1. MRI Contrast Agents for Labeling MSCs	266		

## 1. Introduction

Stem cells are primitive cells found in many multicellular organisms. Self-renewal and differentiation potency are two defining properties of stem cells. Self-renewal is the ability to perform numerous cell cycle divisions, each resulting in two identical daughter cells, while differentiation potency defines the capability of stem cells to develop into mature cell types. Mammalian stem cells are divided in three broad types including embryonic, fetal, and adult stem cells.<sup>1</sup>

Embryonic stem (ES) cells, which are derived from the inner cell mass of blastocyst, have the potential to differentiate into all mature cell types except extra embryonic tissue.<sup>2</sup> Because of this ability, ES cells are attractive for cell-replacement therapies. Despite their advantages, the major limitation for the use of ES cells is linked to their uncontrollable differentiation and proliferation, which may cause tumor formation and improper phenotype.

Fetal stem cells, which can be isolated from the organs of fetuses, differentiate along multiple lineages. Their advantages over their adult counterparts include better intrinsic homing and engraftment and lower immunogenicity, and they are less ethically contentious.<sup>3</sup> However, an important concern is that they are available in limited quantities.

Adult stem (AS) cells are comprised of undifferentiated cells found in many tissues of an adult organism. They have an extensive self-renewal capability and the ability to differentiate into various specialized cell types (i.e., blood, muscle, and nerve cells).<sup>4–10</sup> Adult stem cells are a particularly promising cell type, because they are easy to obtain, less controversial, and, if obtained autologously, less immunogenic than ES cells. It is noteworthy that the majority of the adult stem cells are lineage-restricted and entitled by

\* Corresponding author. Web: [www.biospion.com](http://www.biospion.com); e-mail: Mahmoudi@biospion.com.

<sup>†</sup> Pasteur Institute of Iran.

<sup>‡</sup> Mount Sinai School of Medicine.

<sup>§</sup> University of Mons.

<sup>||</sup> Sharif University of Technology.

<sup>‡</sup> National Yang Ming University.

<sup>#</sup> Nanotechnology Toxicology Consulting & Training, Inc.

<sup>▽</sup> Dalhousie University.

<sup>○</sup> University of Newcastle upon Tyne.

<sup>⊗</sup> Tehran University of Medical Sciences.



Dr. Morteza Mahmoudi obtained his Ph.D. in 2009 from Sharif University of Technology with specialization in the cytotoxicity of superparamagnetic iron oxide nanoparticles (SPIONs). He has received many awards such as the 2010 Dr. Mojtahedi Innovation Award for Distinguished Innovation in Research and Education at Sharif University of Technology and 2009 Kharazmi Young Festival Award. His current research involves the magic SPION for simultaneous diagnosis and therapeutic applications (<http://www.biospion.com>). He is the author of the book entitled *Superparamagnetic Iron Oxide Nanoparticles for Biomedical Applications*, which is published by Nova Science Publishers, NY, USA. He was a visiting scientist at Laboratory of Powder Technology (LTP) at Swiss Federal Institute of Technology (EPFL) under the supervision of Professor Heinrich Hofmann.



Dr. Hossein Hosseinkhani received his Ph.D. degree in Polymer Chemistry from Kyoto University, Japan, in 2002. He was JSPS Research Fellow at Institute for Frontier Medical Sciences, Kyoto University Hospital, Japan (2002–2004), Senior Researcher at International Center for Young Scientists, Notational Institute for Materials Science, Japan (2004–2008), Senior Research Fellow at International Research Institute for Integrated Medical Sciences, Tokyo Women's Medical University, Japan (2008–2009), and Visiting Scientist at Center for Biomedical Engineering, Massachusetts Institute of Technology (MIT), USA (2007–2009). In August 2009, he joined Department of Biomedical Engineering, National Yang-Ming University, Taiwan, as an Associate Professor. His research interests include: Biomaterials, Drug Delivery Systems, Biochip, Tissue Engineering, and novel 3D in vitro culture systems (<http://bme.ym.edu.tw/BioengStemCellsLab/>).

their tissue sources such as mesenchymal stem cells (MSCs). The adult somatic stem cells are also widely used in both animal and human models for the treatment of a broad range of diseases that involve the central nervous system (CNS).<sup>11,12</sup> Among various types of the somatic stem cells, neural stem cells (NSCs) have been recognized as the most promising candidate for treatment of CNS disorders.<sup>13</sup>

The development over the past decade of methods for delivering substances (e.g., genes, growth factors) to mammalian stem cells has stimulated great interest in the possibility of improving the treatment of human disease by drug-based therapies. However, despite substantial progress, a number of key technical issues need to be resolved before such drug-based therapies can be safely and effectively



Dr. Mohsen Hosseinkhani obtained his M.D. from Tehran Medical University in 1996 and subsequently completed his Ph.D. in the field of Regenerative Medicine and Stem Cell Biology from Kyoto University, Japan, in 2007. Dr. Hosseinkhani's research was focused on isolation and characterization of embryonic stem (ES) cells from primates. He established a system for efficient myocardial differentiation of nonhuman primate ES cells using an embryonic body (EB)-based approach. He discovered several cardiac inducer agents that significantly enhance myocardial differentiation of ES cells. An important aspect of Dr. Hosseinkhani's research has been in the area of tissue engineering and biomaterials. For potential clinical use of stem cells, Dr. Hosseinkhani established several 2D and 3D micro and nanoculture systems to scale up the expansion of stem cells for clinical cell therapy. His achievements include publications in peer-reviewed journals, presentations (oral and posters), and being honored by the professional associations. Dr. Hosseinkhani is a cardiology fellow at Mount Sinai Hospital, New York. Currently, his research focuses on cardiac regeneration, the role of cell cycle regulation of cardiomyocytes, and endogenous cardiac progenitor cells.



Sébastien Boutry was born in 1978 in French-speaking Belgium. He graduated with a Ph.D. in Biology from the University of Mons (Belgium) in 2007. He completed his Ph.D. in the NMR laboratory of Prof. Robert N. Muller, studying the magnetic labelling of cells with iron oxide nanoparticles. As a senior researcher in this laboratory, he was enrolled in the Center for Microscopy and Molecular Imaging that was set up by the Free University of Brussels and the University of Mons, where he is currently in charge of the Magnetic Resonance Imaging (MRI) and Optical Imaging investigations.

applied in clinical settings. This review provides a critical view of these drug-based therapies with a major focus on advanced nanoparticle technologies to control the in vitro and in vivo location and function of administered SPIONs.

### 1.1. Mesenchymal Stem Cells (MSCs)

There are three broad types of multipotent adult progenitor cells in the bone marrow, one of which is mesenchymal stem cells. These cells have a great capability for differentiating into bone,<sup>14</sup> cartilage,<sup>15</sup> muscle,<sup>16</sup> and fat cell<sup>17</sup> phenotypes. MSCs have a large capacity for self-renewal while maintain-



Dr. Abdolreza (Arash) Simchi is a Distinguished Professor in Department of Materials Science and Engineering and Institute for Nanoscience and Nanotechnology at Sharif University of Technology (SUT). He received his Ph.D. in Materials Science from SUT in 2001. He was a visiting researcher at the Vienna University of Technology in the period of 1998–1999 and employed at Fraunhofer Institute for Manufacturing and Advanced Materials IFAM (Bremen, Germany) during 1999–2001 as a scientist and in the summers of 2004–2008 as a visiting professor. He is the fellow of the Alexander von Humboldt Foundation (Bonn, Germany) and holds the 2002 Kawrazmi International Award (the highest national award) and World Intellectual Property Award (as the Best Young Inventor, United Nations Organization). He has also received the prestigious Royal Society Fellowship (UK) to visit Imperial College London as an Academic Visitor in 2009. The activities of Dr. Simchi are in the broad areas of nanostructured materials, metal matrix composites and nanocomposites, nanoparticles, nanoceramics, biomaterials, and functional structures. During the last eight years, he has been the author and coauthor of two books, four patents, and about 200 papers which have been cited many times (average citation per journal paper, 5.8; *h* index = 11).



A native of Nova Scotia, Canada, Dr. W. Shane Journeay is a recognized expert on the toxicological aspects of nanomaterials. Journeay received his BSc and Masters degrees at the University of Ottawa and earned his Ph.D. in Toxicology at the University of Saskatchewan. He was also awarded a Certificate in Space Studies from the International Space University. Dr. Journeay is a toxicologist with specialization in the potential human and environmental health risks associated with nanotechnology. An author of numerous peer-reviewed articles and technical papers related to nanotoxicology, Dr. Journeay has served as an invited presenter and expert to the media and organizations including the United States Environmental Protection Agency, Health Canada, and American Industrial Hygiene Association, and represented Canada at the International Space University in Strasbourg, France. He is also on the Editorial Board of the *Journal of Occupational Medicine and Toxicology* and served as the Editor-in-Chief of the *Dalhousie Medical Journal* from 2008–2010. He is currently the President and CEO of Nanotechnology Toxicology Consulting and Training.

ing their multipotency and can differentiate into a variety of cell types in vitro or in vivo including adipocytes,  $\beta$ -pancreatic islets, chondrocytes, endothelium, myocytes, and osteoblasts.<sup>18</sup> Therefore, MSCs are recognized as candidates for the repair of damaged tissues. Furthermore, comprehen-



Dr. Karthikeyan Subramani received his MSc in Biomedical Nanotechnology from University of Newcastle upon Tyne in 2004 following the Bachelor of Dental Surgery (BDS) degree from India in 2003. His MSc thesis work, entitled "Fabrication of poly(ethylene glycol) hydrogel micropatterns with osteoinductive growth factors and evaluation of effects on bone cell activity and function" is aimed at exploring the applications of nano/microfabrication techniques in the fabrication of poly(ethylene glycol) hydrogel micropatterns that can be used as an interface at the bone-implant interface for guided tissue (bone) generation. His current research interests include surface micropatterning of hydrogels and evaluation of effects on osteoblasts, nanofabrication of titanium dental implants, dental nanocomposites and nanoindentation studies of tooth surface, and biomedical applications of nanotechnology.



Dr. Sophie Laurent was born in 1967. Her studies were performed at the University of Mons-Hainaut (Belgium) where she received her Ph.D. in Chemistry in 1993. She then joined Prof R. N. Muller's team and was involved in the development (synthesis and physicochemical characterization) of paramagnetic Gd complexes and superparamagnetic iron oxide nanoparticles as contrast agents for magnetic resonance imaging. She is currently working on the vectorization of contrast agents for molecular imaging. She is lecturer and coauthor of around 90 publications and more than 180 communications in international meetings.

sive studies have proved that human MSCs (hMSCs) avoid allorecognition and interference with both T-cell and dendritic cell function; hence, they have the potential to generate a local immunosuppressive microenvironment via cytokines activity.<sup>19</sup> Moreover, the immunomodulatory function of hMSCs is excelled due to the exposure of cells to an inflammatory environment.<sup>20</sup>

It is noteworthy that MSCs can be activated and mobilized at the site of damaged tissue. Since vascular delivery suffers from a pulmonary first pass effect, direct or systemic injection of MSCs into the damaged tissue is preferred, particularly in the case of versatile tissue ischemia.<sup>21</sup> Upon reaching the desired tissue, MSCs may produce essential factors to inhibit both fibrotic and apoptotic phenomena. As a result, angiogenesis stimulates host progenitors to repair the damaged



site. Therefore, there is an increasing interest in culture-expanded MSCs as a promising cell source for clinical use such as regeneration of bone defects,<sup>22,23</sup> spinal cord injury,<sup>24</sup> stroke,<sup>25</sup> and myocardial infarction.<sup>26</sup> In vivo animal tests have already proved the ability of the MSCs to repair large full-thickness defects in the formal condyle.<sup>27</sup> Trans-differentiation of bone marrow derived MSCs (BM-MSCs) into a neuronal-like phenotype suggested that MSCs are potential candidates for cell therapy in the CNS.<sup>28</sup> Several studies have shown that implanting of MSCs in rodent brain leads to functional improvement in damaged areas of adult rat brain.<sup>29–33</sup> Human umbilical cord MSCs (hUC-MSCs) have also been considered as attractive candidates for regenerative medicine because these stem cells have faster proliferation and greater ex vivo expansion capabilities compared with BM-MSCs.<sup>34</sup> Therefore, the treatment of patients with CNS injuries, neurodegenerative diseases, and bone defects by transplantation of hUC-MSCs is promising. Moreover, these cells can be used to induce heart, skeletal muscle, endothelium, cartilage, and adipose.<sup>35</sup>

## 1.2. Neural Stem Cells (NSCs)

NSCs are a heterogeneous population of immature progenitor, self-renewing, and multipotent cells derived from the nervous system as well as more primitive ES cells, and have the potential to generate the neural lineages of the nervous system. The derivation of mouse and human ES cells has opened up exciting possibilities for their therapeutic use for the treatment of neurodegenerative diseases. Several studies have described the long-term maintenance of NSCs derived from mouse or human ES cells in adherent monolayer culture.<sup>36,37</sup> Such cultures are easier to maintain and manipulate compared with Neurospheres, which require manual dissection for subcultivation and are more difficult to examine microscopically than cells grown in a monolayer.

Adult NSCs and restricted progenitors are found in several regions of the CNS throughout life. The isolation of neural progenitor and stem cells from the striata tissue of the brains of adult mice was first reported by Reynolds and Weiss.<sup>38</sup> NSCs can be cultured (via the Neurosphere culture system<sup>38</sup>) and grown in vitro. After injection in vivo, NSCs enable the repair of damaged neural tissue via their extensive self-renewal ability and multipotency during their residence time. Moreover, after systemic injection to the host part of the brain, NSCs migrate into the damaged sites (even from far distances) where the engrafting and differentiation into the appropriate neuronal cell type occurs.<sup>39</sup> It is noteworthy that the rate of migration of SPION-labeled NSCs is correlated with the degree of inflamed tissue.<sup>40</sup> NSCs have been successfully transplanted into animal models in order to treat brain diseases such as demyelinating<sup>41</sup> and lysosomal storage disorders,<sup>42</sup> acute spinal cord injury,<sup>43</sup> and Parkinson's<sup>44</sup> and Huntington's<sup>45</sup> diseases. Furthermore, intravenous injection of NSCs has been confirmed to be able to induce markers of recovery in a murine model of multiple sclerosis.<sup>41</sup> Frisen and his colleagues showed that NSCs from the adult mouse brain can contribute to the formation of chimeric chick and mouse embryos and give rise to cells of all germ layers. This result indicates that NSCs have multipotent capacities and can generate a wide range of cell types for transplantation in a variety of diseases.<sup>46</sup>

Recently, Schöler et al. described direct reprogramming of adult mouse NSCs by Oct4 and either Klf4 or c-Myc. The NSCs subsequently expressed Sox2, c-MYC, and Klf4

endogenously.<sup>47–49</sup> They also found that Oct4 itself is sufficient to directly reprogram NSCs to pluripotency and plasticity amenable to genetic programming and epigenetic reprogramming during normal differentiation. Recent evidence suggests that adult NSCs significantly contribute to specialized neural functions under physiological and pathological conditions.<sup>46</sup> Therefore, understanding the biology of adult NSCs will provide pivotal insights into both the etiology of and potential therapeutic interventions for major neurological disorders.

## 2. Magnetic Resonance Imaging (MRI) Technique

Since ancient times, visualization of the detailed inner spaces of the body, without surgery, was a physician's dream. Diagnostic imaging modalities are currently one of the most rapidly expanding domains in the field of medicine, with several methods for imaging internal structures and functions of the body including X-ray, computed tomography (CT), positron emission tomography (PET), single-photon emission computed tomography (SPECT), ultrasound (US), and MRI.<sup>50</sup> Each method has its advantages and disadvantages according to the physical phenomena that are being employed to create imaging information.<sup>51</sup> In CT, an X-ray beam is sent through an object and is differentially attenuated by the various structures of the object according to their densities. For example, in living organisms, bones impede most of the incident X-rays, while soft tissues and fluids do not. X-rays blunting across the object are detected from multiple angles around the circumference of the scanner and a two-dimensional (2D) image of each slice of the object can be reconstructed by a computer. PET is an imaging method that uses a radioactive isotope incorporated in a metabolically active molecule, commonly fluorodeoxyglucose (FDG). These radioactive tracers are injected into the circulating blood and decay by emitting a positron, which rapidly meets an electron, resulting in a pair of annihilation photons moving in nearly opposite directions. When the photons reach a scintillator material in the scanning device, a burst of light is created and detected by photomultiplier tubes. Thus, the image collected represents the accumulation of the compound. SPECT also studies the distribution of a radiolabeled compound. SPECT images are collected using gamma cameras; multiple 2D images are acquired from multiple angles. Then, a tomographic reconstruction algorithm is applied to the multiple projections to obtain a three-dimensional (3D) data set.

Ultrasound applies acoustic energy with a frequency above human hearing (20 kHz). Ultrasound imaging (or sonography) scanners operate between 2 and 13 MHz. The frequency determines the image's spatial resolution and the penetration depth into the examined patient. For example, lower frequencies give a lower resolution and a greater imaging depth. Ultrasound contrast agents made of gas-filled microbubbles can be injected intravenously. They have a high degree of echogenicity (in other terms, they reflect the ultrasound waves), and can be conjugated to ligands that specifically bind to intravascular receptors. Thus, the generated contrast is due to the echogenicity difference between the microbubbles and the surrounding tissues. The maximum spatial resolution in MRI is around 50  $\mu\text{m}$ , whereas CT, ultrasound imaging and the two nuclear imaging methods have a lower resolution (on the order of millimeter). However, micro-CT and micro-US imaging technologies, having a resolution of 50  $\mu\text{m}$  and higher, are now being developed. Although

ultrasound is an ideal target for miniaturization (in comparison with other imaging techniques), it suffers from weak imaging of small abnormal matter in the tissue due to a loss of energy signal caused by the overlapping of waves, which arise from variations in acoustic impedance.<sup>52</sup> Nuclear medicine imaging techniques (e.g., PET and SPECT) have the advantages of an excellent sensitivity and the possibility to create 3D images showing the radiotracers' biodistribution.<sup>53,54</sup> These methods have the capability to track the specific disease process and to detect metabolic activity in vivo.<sup>55,56</sup> However, the side effects of the radiotracers cannot be ignored.

MRI is a very safe method for human in vivo imaging that uses a powerful magnetic field to align the nuclear magnetization of hydrogen atoms which are responsible for the majority of MRI signals;<sup>57–59</sup> hence, the water distribution in the body is shown by MRI to correlate with the anatomy of the body.<sup>50,60</sup> It is noteworthy that the principles of nuclear magnetic resonance (NMR) are used for MRI signal acquisition (i.e., interactions between nuclear spin and magnetic field). In order to track body functions, which are sensitive to the flow in the body, functional MRI (fMRI) was developed.<sup>60,61</sup> It is worth noting that fMRI is a technique to monitor brain activation due to a stimulus.<sup>50</sup> The principle of this mapping relies on different magnetic properties of the oxygenated and deoxygenated hemoglobin in the blood.<sup>62</sup> In addition, MRI has the capability to show blood flow with one of its techniques, called magnetic resonance angiography (MRA). Furthermore, tracking of blood flow through capillaries in tissue (i.e., tissue perfusion) is now possible via arterial spin labeling and dynamic contrast enhanced MRI techniques.<sup>50</sup> It is noteworthy that in order to gather adequate information, which is needed for better image construction, radio frequency fields are employed.<sup>63–65</sup> The distinguishing feature of MRI, in comparison with other available methods, is its unique potential to probe the in vivo molecular diffusion of water (i.e., its molecular movement along random

paths).<sup>66–71</sup> MRI is a relatively new technique and its progress is schematically illustrated in Figure 1 according to refs 63, 72–78.

Multimodality imaging techniques are now combining different “anatomical” and “functional” methods; CT/PET, CT/SPECT, and MRI/PET are examples of combinations. A coupling between MRI and optical imaging methods is also being experimented on animals. Long circulating iron oxide nanoparticles (MION), able to reach lymph nodes, have been conjugated to probes emitting a “near-infrared fluorescence” (NIRF) detectable by an optical camera.<sup>79</sup> Furthermore, the fluorescence of the probe can also be activated by certain enzymes (e.g., tumor-associated proteases), which can provide further information about the environment of the accumulated nanoparticles.<sup>79</sup> However, the in vivo visualization of fluorescent dyes sometimes requires surgical or invasive procedures because deep tissue penetration is not allowed by this optical approach. Femurs of mice have been exposed to visualize intravenously injected fluorescently labeled bone marrow cells homing to the bone marrow.<sup>80,81</sup> A catheter has also been used for optical imaging of the human coronary artery. In this case, the catheter emits ultrasounds and a back-reflected infrared light is measured. This method is called optical coherence tomography (OCT).<sup>82,83</sup> Among the microscopic optical imaging techniques, one can mention light and fluorescence microscopy, confocal microscopy, and two photon microscopy.

Advancements in nanotechnology over the last 20 years have led to the development of novel magnetic nanoparticles. Such nanoscale agents have led to a wide array of biomedical applications in concert with MRI, including “theragnostics” (therapeutic and diagnostic) applications such as hyperthermia.<sup>84,85</sup> stem cell tracking,<sup>86–88</sup> gene expression,<sup>89–91</sup> angiogenesis,<sup>92–95</sup> cancer detection,<sup>96–98</sup> inflammation,<sup>99–101</sup> apoptosis detection,<sup>102–104</sup> and atherosclerosis.<sup>105,106</sup>

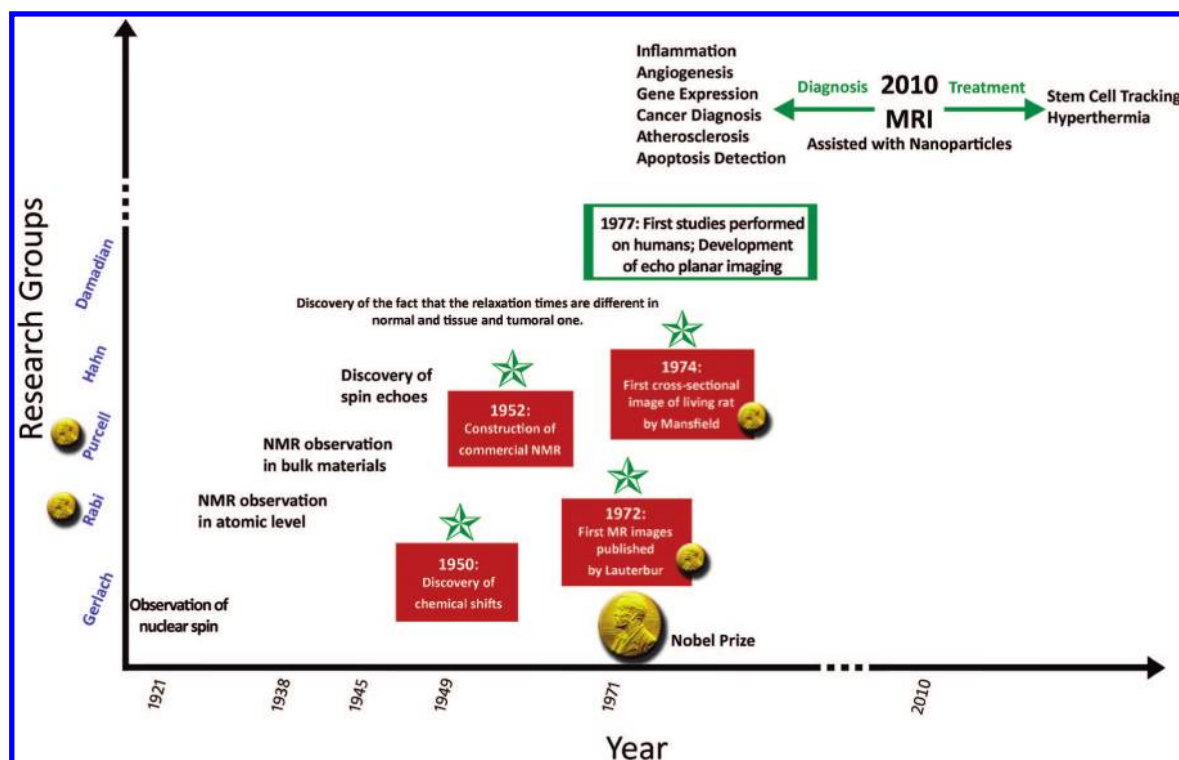
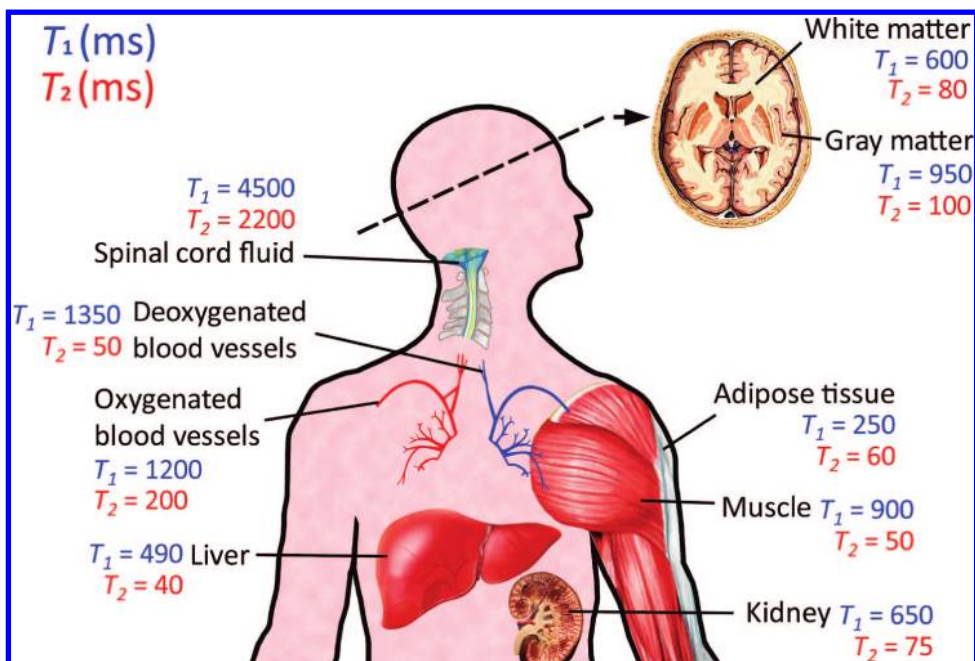


Figure 1. Progress in MRI technology.



**Figure 2.** Approximate values of the two relaxation time constants of various tissues in the human body at a field of 1.5 T.

## 2.1. Relaxation Times

The most common foundations of contrast in MRI are spin–lattice relaxation time ( $T_1$ ) and spin–spin relaxation time ( $T_2$ ). The signal enhancement produced by contrast agents depends on their longitudinal  $r_1$  or transverse  $r_2$  relaxivities, which are defined as the increase of relaxation rates ( $R_1 = 1/T_1$  and  $R_2 = 1/T_2$ ) produced by 1 mM of magnetic center per liter. The terms  $r_1$  and  $r_2$  are expressed as per second per millimole and are characteristic of the contrast agent efficacy. The observed relaxation rate  $R_i(\text{obs})$  ( $= 1/T_i(\text{obs})$ ) of a water solution or a tissue is given by the equation:

$$R_{i(\text{obs})} = \frac{1}{T_{i(\text{dia})}} + \frac{1}{T_{i(\text{para})}} = \frac{1}{T_{i(\text{dia})}} + r_i C$$

with  $i = 1$  or  $2$  where  $T_i(\text{dia})$  is the relaxation time of the system before adding the contrast agent, also called the diamagnetic contribution;  $T_i(\text{para})$  is the paramagnetic relaxation time, that is, the relaxation time resulting from the presence of the contrast agent;  $C$  is the concentration of the magnetic center (millimole per liter); and  $r_i$  is the relaxivity (per second per millimole liter).

Various  $T_1$  and  $T_2$  times for different tissues are schematically illustrated in Figure 2.

## 2.2. Relaxation Mechanisms

A general theory of nuclear relaxation in the presence of paramagnetic substances was developed by Bloembergen, Solomon, and Freed.<sup>107–113</sup> According to this theory, paramagnetic complexes induce an increase of both the longitudinal and transverse relaxation rates,  $R_1$  and  $R_2$ . The paramagnetic relaxation of water protons originates from the dipole–dipole interactions between the nuclear spins and the fluctuating local magnetic fields caused by the unpaired electron spins. Paramagnetic relaxation can be explained by three mechanisms called the inner sphere (IS), second sphere (SS), and outer sphere (OS) contributions.<sup>114</sup>

In superparamagnetic colloids, the IS relaxation mechanism does not contribute significantly to proton relaxation, which occurs because of the fluctuations of the dipolar magnetic coupling between the nanocrystal magnetization and the proton spin. This mechanism is modulated by the translational correlation time that takes into account the relative diffusion of the paramagnetic center and the solvent molecule, as well as their distance of closest approach. The relaxation is described by an OS model where the dipolar interaction fluctuates because of both the translational diffusion process and the Neel relaxation process.<sup>115–118</sup>

Negative contrast agents shorten the  $T_2$  and  $T_2^*$  (same as  $T_2$  but also contains heterogeneities in the environment) much more than the  $T_1$  of nuclei situated in their neighborhood, generating a signal darkening on MR images. They are based on a monocrystalline or polycrystalline iron oxide core with a diameter of 5–30 nm embedded within a polymer coating (usually dextran or another polysaccharide). These nanoparticles are also called superparamagnetic contrast agents. They differ from ferromagnetic agents in their size. Ferromagnetic particles show a permanent magnetism, but if their size is reduced, although fully magnetized, they lose their permanent magnetic properties and become superparamagnetic particles.

Superparamagnetism occurs when the regions of unpaired spins contained in iron oxide crystals are small enough to be considered as single-domain particles, named magnetic domains. The net magnetic dipole of such a magnetic domain is larger than the sum of its individual unpaired electrons. An external magnetic field can induce a reorientation of the magnetic dipoles, analogous to paramagnetic materials. Thus, each magnetic domain has a magnetic moment reflecting its interacting unpaired electrons. Compared to paramagnetic substances, the resultant magnetic moment of superparamagnetic particles is greater, and responsible for a phenomenon of magnetic susceptibility that disrupts the homogeneity of the external magnetic field.  $T_2$  will be reduced because of the water diffusion through the created field gradients, and  $T_2^*$  effects will appear because of field inhomogeneities, leading to a signal loss in the regions capturing the iron oxide nanoparticles on MR images. Several types of these negative



contrast agents accumulate in the liver when intravenously injected. After binding of plasma proteins (opsonins) to their surface, Endorem (Guerbet, France) or Feridex (Berlex Inc., USA), coated with dextran, and Resovist (SHU 555A, Bayer Schering Pharma AG, Germany), coated with carboxydextran, are easily captured by Kupffer cells within minutes. Because of their relatively large size, they are called small particles of iron oxide (SPIO). For Endorem (or Feridex), the iron oxide crystal size is 4.8–5.6 nm, and the apparent (hydrodynamic) diameter varies from 80 to 150 nm. Resovist is smaller (crystal size: 4.2 nm; hydrodynamic diameter: 62 nm). These SPIO are approved for clinical use in the detection of liver metastases. Since they are not retained in metastases and in hepatocytes, the darkening of liver signal on  $T_2$ -weighted MR images will only be observed in healthy parts of the organ. SPIO sequestration also occurs in spleen and bone marrow macrophages.

Another category of iron oxide nanoparticles exists: the ultrasmall particles of iron oxide (USPIO). Sinerem (Guerbet, France) is a USPIO composed of a crystalline core of 4–6 nm surrounded by a dextran coating. Because of their relatively small hydrodynamic diameter (20–40 nm), USPIO have a stronger  $T_1$  relaxation as compared to SPIO and are less likely to be captured by macrophages. As they circulate longer, they can be used as blood pool agents for  $T_1$ -weighted MRA during the early phase of intravenous administration. In the later phase, USPIO accumulate in liver and spleen, but also become potent contrast agents for lymphography. Indeed, their small size enables them to reach the lymphatic system by crossing the capillary wall.

Endocytosis of the nanoparticles by the macrophages contained in normal lymph nodes leads to a reduction of the signal intensity. As metastases do not take up USPIO, these nanoparticles will be useful to detect metastatic involvement of lymph nodes. Carbohydrate-polyethyleneglycol-coated NC100150 (Clariscan from General Electric Healthcare, UK), carboxydextran-coated SHU 555C (Supravist from Bayer Schering Pharma AG, Germany), and citrate-coated VSOP-C184 (Ferropharm, Germany) also belong to this category. Monocrystalline iron oxide nanoparticles (MION) are dextran-coated and have a very small size (8–20 nm). They differ from other iron oxide nanoparticles in their monocrystallinity.<sup>119–123</sup>

The high  $T_2$  relaxivity of iron oxide based contrast agents is a significant advantage for molecular MRI, as they produce strong negative  $T_2$  contrast at nanomolar concentrations. Molecular targeting with negative contrast agents was attempted by conjugating specific ligands to iron oxide nanoparticles. Several cell surface receptors, such as the leukocyte common antigen of normal lymphocytes (the Her-2/neu receptor in malignant breast cancer cells) or the E-selectin in inflammatory stimulated endothelial cells, were imaged in vitro after labeling with adequate antibodies conjugated to superparamagnetic nanoparticles.<sup>124–127</sup> However, a problem arises in the context of in vivo use of iron oxide nanoparticles because of the rapid capture of the largest particles by macrophages after intravenous injection. This can be overcome by reducing the particle size which delays the clearance.

Indeed, the use of USPIO conjugated to the C2 fragment of synaptotagmin (a protein binding to phosphatidylserine present on the outer leaflet of the plasma membrane of apoptotic cells) allowed for molecular MRI of apoptosis in an animal model of implanted tumors treated with a chemotherapeutic drug, and confirmed results obtained on

cultured cells.<sup>128</sup> A sialyl-LewisX (sLeX) synthetic mimetic, covalently bound to the coating of USPIO, has been successfully tested on endothelial cells expressing E-selectin. MRI results obtained with this contrast agent in mouse models of hepatitis and muscular inflammation suggested an interaction between the sLeX mimetic and endothelial E-selectin.<sup>129,130</sup> In the context of in vivo targeting of tumors, MION linked to a monoclonal antibody specific for a cell surface antigen expressed on human small-cell lung carcinoma, breast carcinoma, and colon carcinoma, have been successfully used to detect tumors after intravenous injection in a rodent model of intracranial human small-cell lung carcinoma.<sup>131–135</sup> Another way to reduce the uptake of nanoparticles by macrophages is to coat them with a hydrophilic polymer, such as polyethyleneglycol (PEG), which helps to reduce their opsonization by plasma proteins.<sup>136</sup>

In order to accumulate nanoparticles at the desired sites, the targeting ligands (e.g., peptides, antibodies, or aptamers) are attached to the surface of nanoparticles.<sup>103,137–140</sup> Among all types of nanoparticles, SPIONs are the most promising candidates for use as contrast agents not only for their suitable magnetic saturation and superparamagnetic properties, but also due to their colloidal stability and biocompatibility.<sup>141–143</sup> Furthermore, the nanoscale size and the shape of SPIONs can be controlled by optimization of their synthesis parameters.<sup>144,145</sup> Nanoengineering of the particles can not only generate new applications for SPIONs, but also produce characteristics that might improve the biocompatibility profile of the particles. Not only can nanoengineering of the particles generate new applications for SPIONs, but we can also engineer characteristics that might hinder the biocompatibility profile of the particles. This has significant implications for targeted therapies as well as for addressing challenges related to in vivo toxicity.

### 3. Nanoparticles Delivery Systems

The current methods of drug delivery pose specific problems that can be overcome by applying nanotechnology. Drugs are administered into the human body through various means: by enteral route (oral, buccal, sublingual, rectal), parenteral route (intramuscular, intravenous, subcutaneous), and other routes (topical, inhalation).<sup>146,147</sup> The potency and therapeutic effects of many drugs are reduced due to the partial degradation of the drug that occurs in the body before it reaches the desired target tissue. For example, a drug administered orally may undergo changes in the stomach due to the action of gastric enzymes. Drugs administered through enteral routes undergo a first-pass effect, which is the term used for the hepatic metabolism of a pharmacological agent when it is absorbed from the gut and delivered to the liver via the portal circulation. These processes lead to premature drug loss due to drug metabolism and rapid clearance from the body.

Lack of target specificity is one of the major disadvantages of many drugs. When a drug is administered parenterally, it is distributed to all parts of the human body through the bloodstream, rather than to the specific target organ which needs the pharmacological treatment. Biochemical and physiological barriers of certain organs also limit drug delivery to the specified organ, like the human brain. Certain drugs such as anticarcinogenic (chemotherapeutic) drugs may destroy healthy tissue along with destroying the cancer cells and carcinomatous tissue. The cytotoxic effect of these



chemotherapeutic drugs is greatest in organs like bone marrow, gonads, hair follicles and digestive tract that contain rapidly proliferating cells. The adverse effect of chemotherapy includes fatigue, nausea, vomiting, alopecia (loss of hair), gastrointestinal disturbance, impaired fertility, impaired ovarian function and bone marrow suppression resulting in anemia, leucopenia, and thrombocytopenia. Drug interaction with other pharmacological agents may also alter the efficacy of a particular drug. To overcome these disadvantages, newer and effective methods should be developed to safely shepherd a pharmacological agent to avoid specific organs, such as stomach or liver, or areas of the human body where healthy tissue might be adversely affected.<sup>148</sup> The application of nanotechnology can be an answer toward the discovery and use of efficient and improved drug delivery systems. These disadvantages and limiting factors of the currently available drug delivery systems necessitate the application of nanotechnology toward the discovery and use of efficient and improved nanoparticle-based drug delivery systems.

The aim of such sophisticated drug delivery systems should be to deploy medication in the desired form to a specific target in the human body without causing any adverse effects.<sup>149–151</sup> This is where nanotechnology comes into play. Extensive research is being conducted worldwide to exploit nanoparticles or nanosystems as drug delivery systems. These nanoparticles can be used as effective carriers of drug molecules. The carrier can be a carbon nanotube, a carbon nanohorn, or a silica nanoparticle with drug molecules bound to its surface. It can be a nanomagnetic particle which can be drawn to a particular part of the human body under the influence of a magnetic field. It can also be an implantable nanoscale device filled with drug molecules encapsulated by a nanoporous membrane which can act as a tiny turnstile for releasing the drug.

### 3.1. Advantages of Using Nanoparticles for Drug Delivery

Nanoparticle-based drug delivery systems have the following advantages over the conventionally available ones:

- Pharmacological agents can be targeted to a specific area of the human body by adding nanoreceptors on the surface. These receptors specifically recognize the target tissue, bind to it, and release the drug molecules.<sup>151,152</sup>
- Healthy tissues are not affected due to cytotoxic effects of drugs.
- Drugs can be protected from degradation by encapsulating them with nanoparticle coatings.<sup>153</sup>
- As nanoparticles are extremely small, they can penetrate through smaller capillaries and are easily captured by affected cells. This causes efficient drug accumulation at the target sites.<sup>154</sup>
- Use of biodegradable nanoparticles allows sustained drug release within the target site over a period of time.<sup>155</sup>
- Nanosystems with enhanced drug delivery and target specificity lead to superior performance and improved efficacy.<sup>156</sup>

### 3.2. Nanoparticles in Drug Delivery

There has been a remarkable progress over the past decade in the development of nanoparticles as effective drug delivery systems.<sup>157–160</sup> The various types of nanoparticles that are currently studied for use as drug delivery systems are

- Polymeric biodegradable nanoparticles that include nanospheres and nanocapsules
- Ceramic nanoparticles
- Polymeric micelles
- Dendrimers
- Liposomes

To make these nanoparticles function as effective drug delivery systems, specific biological molecules such as antibodies, enzymes, hormones, and pharmaceutical drugs can be coupled structurally.

#### 3.2.1. Polymeric Biodegradable Nanoparticles

These are solid, colloidal particles consisting of macromolecular substances that vary in size from 10 to 1000 nm. Depending on the methods of preparation, these nanoparticles can be of two types: nanospheres or nanocapsules. These two nanostructures have completely different properties and release characteristics for the encapsulated drug.<sup>161–163</sup>

A nanosphere is a matrix system in which the drug is physically and uniformly dispersed, while nanocapsules are vesicular systems in which the drug is confined to a cavity surrounded by a unique polymer membrane. These drug deliverers degrade into biologically acceptable compounds by hydrolysis thus delivering the encapsulated medication to the target tissues. The erosion process occurs either in bulk, where the matrix degrades uniformly, or at the polymer's surface, where the release rate is related to the polymer's surface area. The polymer is degraded into lactic and glycolic acids which are eventually reduced to carbon dioxide and water by the Krebs cycle. Earlier research focused on using naturally occurring polymers such as collagen, cellulose, etc. as biodegradable systems. The focus has now moved to chemically synthesize biodegradable polymers with improved characteristics. Examples include polyanhydrides, polyacrylic acids, polyurethanes, polyesters and poly (methyl methacrylates). One group of researchers have synthesized polymeric nanospheres based on methoxy poly (ethylene glycol) and DL-lactide diblock copolymers.<sup>164</sup> The cytotoxicity tests showed that the nanospheres exhibited sustained drug release and no cell damage. Collagen gels are flowable, suggesting the possibility of an easily injectable, biocompatible drug delivery matrix.<sup>165</sup> Wallace and Rosenblatt reported systems utilizing collagen for drug and protein delivery. Binding interactions to FC can retard release but are specific to each drug and hard to predict. Modified collagens may be useful in this regard since they may have additional binding sites for drugs, but the complexity of such systems is a disadvantage from a commercial perspective. For tissue engineering applications, collagen gels are more attractive, since they can act as a "cage" to retain cells or as gene delivery complexes, which are larger than drugs and therapeutic proteins. The gels have limitations in terms of strength, but reinforcement with solid components and alignment during gelation and culture can improve performance.

#### 3.2.2. Ceramic Nanoparticles

Ceramic nanoparticles are made from calcium phosphate, silica, alumina, or titanium. These nanoparticles have certain advantages such as easier preparative processes, high biocompatibility, ultralow size (less than 50 nm), and good dimensional stability.<sup>166</sup> They effectively protect the doped drug molecules against denaturation caused by changes in external pH and temperature. Their surfaces can be easily

modified with different functional groups and can be conjugated with a variety of ligands or monoclonal antibodies to target them to desired sites. These nanoparticles can be manufactured with the desired size, shape, and porosity. A ceramic nanoparticle does not undergo swelling or porosity changes caused by changes in the surrounding environment. Self-assembling ceramic nanoparticles have been tested for the parenteral delivery of insulin.<sup>166</sup> A calcium phosphate nanoparticle core was used as the insulin carrier, and the particles were characterized and studied *in vivo*. The *in vivo* performance of this drug delivery system gave better results than the standard porcine insulin solution.

### 3.2.3. Polymeric Micelles

These are supramolecular networks composed of cross-linked combinations of hydrophobic and hydrophilic ligands which self-assemble in an aqueous medium. These copolymers are only tens of nanometers in diameter and are thus ideally suited for enclosing an individual drug molecule.<sup>167</sup> On the basis of their structural conformation, there are two types: block and random copolymer micelles. Because of their minute size, these drug carriers can avoid renal exclusion and the reticuloendothelial system (RES) thus enhancing the absorption by tumor cells. Their hydrophilic outer shell protects the core and its contents from the surrounding aqueous medium in the human body while delivering the drug. They are very useful in delivering water-insoluble drugs and can be administered intravenously. The distribution of these drug carriers mainly depends on their size and surface characterization. For example, micelles containing sugar group ligands attached to their surface have been shown to specifically target glucose receptors in cell membranes.<sup>167</sup> Most micelle-based delivery systems are made from a poly (ethylene dioxide) triblock network or along with a polypeptide combination.

### 3.2.4. Dendrimers

Dendrimers were discovered in the early 1980s by Donald.<sup>168</sup> These molecules are monomers comprised of a series of branches around an inner core<sup>169</sup> and share the advantages of polymeric micelles. Dendrimers can be easily synthesized in the nanometer scale level. In addition to this, they have a unique globular structure with internal cavities in which drug molecules can be housed safely protected by the hydrophobic exterior surface. Drug molecules can be attached also to the outer surface. They can be built from the core to the periphery, called a divergent synthesis (bottom-up approach) or vice versa, called a convergent synthesis (top-down approach).

### 3.2.5. Liposomes

Liposomes were first described in 1968.<sup>170</sup> These are small artificial spherical vesicles made from naturally occurring nontoxic phospholipids and cholesterol. Because of their size, biocompatibility, hydrophobicity, and ease of preparation, liposomes serve as promising systems for drug delivery. Their surfaces can be modified by attaching polyethylene glycol units (PEG) to enhance the circulation time in the bloodstream. Liposomes can also be conjugated with ligands or antibodies to improve their target specificity.

## 3.3. Nanoparticles for Cellular Labeling

Labeling of cells has been a key application in biomedical research for many years. The use of fluorescent molecules, radioactive isotopes, immunohistological assays, and colorimetric methods, to name a few, have traditionally been employed *in vitro* and *in vivo* to improve our understanding of physiology and pathophysiology. Many of these methods involve the conjugation of molecules to the cell surface for real-time tracking or the incubation of such molecules after considerable tissue processing. As the field of nanotechnology moves forward and we better understand the interaction of nanoscale particles with cells, an increasing number of methods for labeling cells with nanoparticles are evolving. The use of nanoparticles has many applications including tracking of cells and diagnostic imaging.

### 3.3.1. Nanoparticles for Stem Cell Labeling

In recent years, nanoparticles have gained increasing attention for the tracking of stem cells. In fact, they may offer stem cell research a tool with which to perform long-term noninvasive imaging of transplanted cells *in vivo* to monitor their survival, migration, differentiation, and regenerative impact.<sup>171</sup> For this purpose, a wide variety of nanoparticles have been exploited, including quantum dots, liposomes, organic and inorganic particles, and carbon nanotubes. Specifically, nanoparticles have a number of applications in stem cell biology, such as (i) noninvasive tracking of stem cells and progenitor cells transplanted *in vivo*, (ii) intracellular delivery of DNA, RNAi, proteins, peptides and small drugs for stem cell differentiation or survival, and (iii) biosensing of the physiological status of stem cells.<sup>172</sup>

Central to the future application of nanoparticles in stem cell labeling is our understanding of particle–cell interaction. Nanoparticles are particularly adept at being internalized by a variety of cell types and uptake is dependent on a number of factors.<sup>173,174</sup> The currently proposed mechanisms of uptake are discussed elsewhere in this manuscript; however, science is constantly evolving with methods to best engineer nanoparticles for favorable uptake and elimination pathways. This is particularly important given our current understanding of the role of particle surface chemistry on uptake by stem cells.<sup>175</sup>

While cellular uptake is crucial for the labeling of stem cells, a number of factors are particularly important when considering the long-term implications for the use of nanoparticles in stem cell technology. They include factors related to labeling efficiency, stem cell differentiation impact, cell function, and toxicity from particles or breakdown products. Frank et al. outlined key features that would likely be required by the FDA for ferumoxide-protamine sulfate nanoparticles for labeling of stem cells.<sup>176</sup> These features could reasonably apply to most nanoparticles proposed for stem cell labeling and include (i) labeling technique is reproducible, (ii) labeled cells have similar viability to unlabeled cells, (iii) the stem cell or other mammalian cell phenotype is not altered as a result of labeling, (iv) once labeled with nanoparticles the stem cells are able to differentiate and their functional capacity is the same as unlabeled cells, and (v) there are no toxins present in the resultant product. Nearly all classes of nanoparticles will need to adhere to these criteria in order to be successfully integrated in clinical stem cell treatment. Further research

is required to delineate the specific nanoparticle features that will make them most amenable to stem cell labeling and application to modern imaging methods such as MRI.

### 3.3.2. Advantages of SPIONs

Given that the focus of this review is on SPIONs, we will consider some of their positive attributes in stem cell labeling. Most labeling strategies use one of two methods: (i) conjugating magnetic nanoparticles to the cellular surface of the stem cell or (ii) internalization of the particles.<sup>171</sup> SPIONs can work in both these methods since the potential to manipulate their surface chemistry is plentiful and their sizes along with other attributes promote their successful uptake into cells. The SPIO class of nanoparticles also interfaces well with MRI technology, thus moving us closer to the noninvasive tracking of migrating stem cells *in vivo*. This is crucial to the further application and study of stem cells using an already accepted diagnostic imaging modality. SPION toxicity has also been shown to be favorable thus far, as supported by the FDA-approved formulations of SPIONs already on the market. However, as more modifications and novel formulations of SPIONs become available, toxicity considerations remain important for researchers. SPIONs with low iron content also show good contrast enhancement on MRI.<sup>171</sup> In fact, most studies demonstrate that the iron liberated during SPION breakdown does not cause significant toxicity but it is rather the coatings and transfection agents that tend to influence the cells in a greater proportion.<sup>177</sup> This is in contrast to some of the early studies on quantum dots where the *in vivo* stability and leaching of cadmium demonstrated significant cytotoxicity.<sup>178</sup> At present, there are data to demonstrate the degradation of polymeric and SPIO nanoparticles for MRI contrast agents, whereas for other nanoparticles such as quantum dots, carbon nanotubes, and gold particles the elimination profiles show a less defined degradation.<sup>172</sup>

SPION research for application to stem cell research has exploded in recent years. Given that this class has successfully made it to the market for use in humans supports preliminary attributes related to biocompatibility, which will drive further application in stem cell clinical trials.

### 3.4. Superparamagnetic Iron Oxide Nanoparticles for Stem Cell Labeling

Among all types of nanoparticles, SPIONs with proper surface architecture and conjugated targeting ligands/proteins have attracted great attention during the past decade for biomedical applications.<sup>141,143–145,179–184</sup> More specifically, the number of publications on stem cell labeling with all kinds of nanoparticles in comparison to those with SPIONs clearly confirms the latter's ability for stem cell tracking (see Figure 3a). Because of their special magnetic properties, SPIONs are recognized as a promising contrast agent candidate for MRI techniques.<sup>137,140,185–197</sup> Fabrication of ferrofluids can be named as one of the oldest applications for magnetic nanoparticles; however, relatively new and promising applications are being explored for biocompatibility, such as using Fe<sub>3</sub>O<sub>4</sub> for contrast enhancement in MRI, drug/gene delivery, molecular/cellular tracking, magnetic separation technologies (e.g., rapid DNA sequencing), magnetotransfections, and ultrasensitive diagnostic assays. Since each biomedical application needs specific physical and chemical properties, several synthesis methods are available. Figure

3b shows the crystal structure (inverse spinel), different synthesis methods (see Table 1), and prominent bioapplications of SPIONs. For instance, hyperthermia (thermotherapy) needs very uniform magnetic saturations<sup>198–200</sup> in order to have colloids with very specific physical and chemical properties. In addition, for SPIONs' most recent application in stem cell tracking (see Figure 3c), the labeling efficacy or "SPIONs wrapping" by the stem cells is highly dependent on interactions between SPIONs and cell membranes.<sup>201</sup> These interactions are influenced by targeting agents (e.g., antibodies and aptamers) and cell receptors, coating properties (e.g., charge and hydrophobicity/hydrophilicity) and cell membrane negative charge. In addition to the nanobio interface, both the physical and chemical properties of nanoparticles (such as size, surface charge, roughness and surface curvature) are involved in the endocytosis/labeling process.<sup>173,202,203</sup> For instance, by controlling the size of nanoparticles, their endocytic pathways (e.g., caveolin- and clathrin-coated vesicles) could be predicted.<sup>185,204</sup> Figure 4 schematically shows the mentioned interactions and the uptake pathways. It is worth noting that according to the thermodynamics of the reactions, the total free energy of the membrane will be decreased after endocytosis.

There are many distinct endocytic pathways that coexist in mammalian cells. Currently, pathways are best defined through their differential dependencies on certain lipids and proteins, including clathrin,<sup>205–207</sup> caveolin1,<sup>208</sup> flotillin1,<sup>209</sup> GRAF1 kinases,<sup>210</sup> small G proteins,<sup>211</sup> actin,<sup>212</sup> and dynamin.<sup>213</sup> Although some cargoes enter exclusively by one pathway, most cargoes can enter by several pathways. Any endocytic mechanism requires the coordinated action of proteins that are capable of deforming the plasma membrane to produce highly curved endocytic intermediates and proteins that can induce scission of these intermediates from the plasma membrane. Such proteins include ENTH domain-containing proteins, BAR superfamily proteins, ARF family small G proteins, proteins that nucleate actin polymerization, and dynamin superfamily proteins. The best-understood mechanism is clathrin-mediated endocytosis (CME). Although caveolae have been extensively reported as endocytic intermediates, their contributions to endocytosis are uncertain. However, many questions still need to be elucidated, such as how is clathrin-coated pit (CCP) formation coupled to cargo incorporation? What controls CCP size and how is CCP fission regulated by dynamin? How is the spatiotemporal coordination of the membrane curvature-modulating proteins that act in CME?

### 3.5. Applications of Nanoparticles in Imaging and Drug Delivery

Quantum dot technology and magnetic nanoparticles can be employed to enhance fluorescent markers used for diagnostic imaging procedures. There are several disadvantages in current fluorescent imaging techniques, including the need for color-matched lasers, fluorescent bleaching, and lack of discriminatory capacity of multiple dyes. These disadvantages can be overcome by the use of fluorescent quantum dots. Quantum dots are crystalline clumps of nanocrystals of a few hundred atoms, coated with an outer shell of a different material.<sup>351</sup> The applications and advantages of nanocrystals (quantum dots) for *in vivo* drug delivery and imaging have been extensively discussed in recent studies.<sup>352</sup>



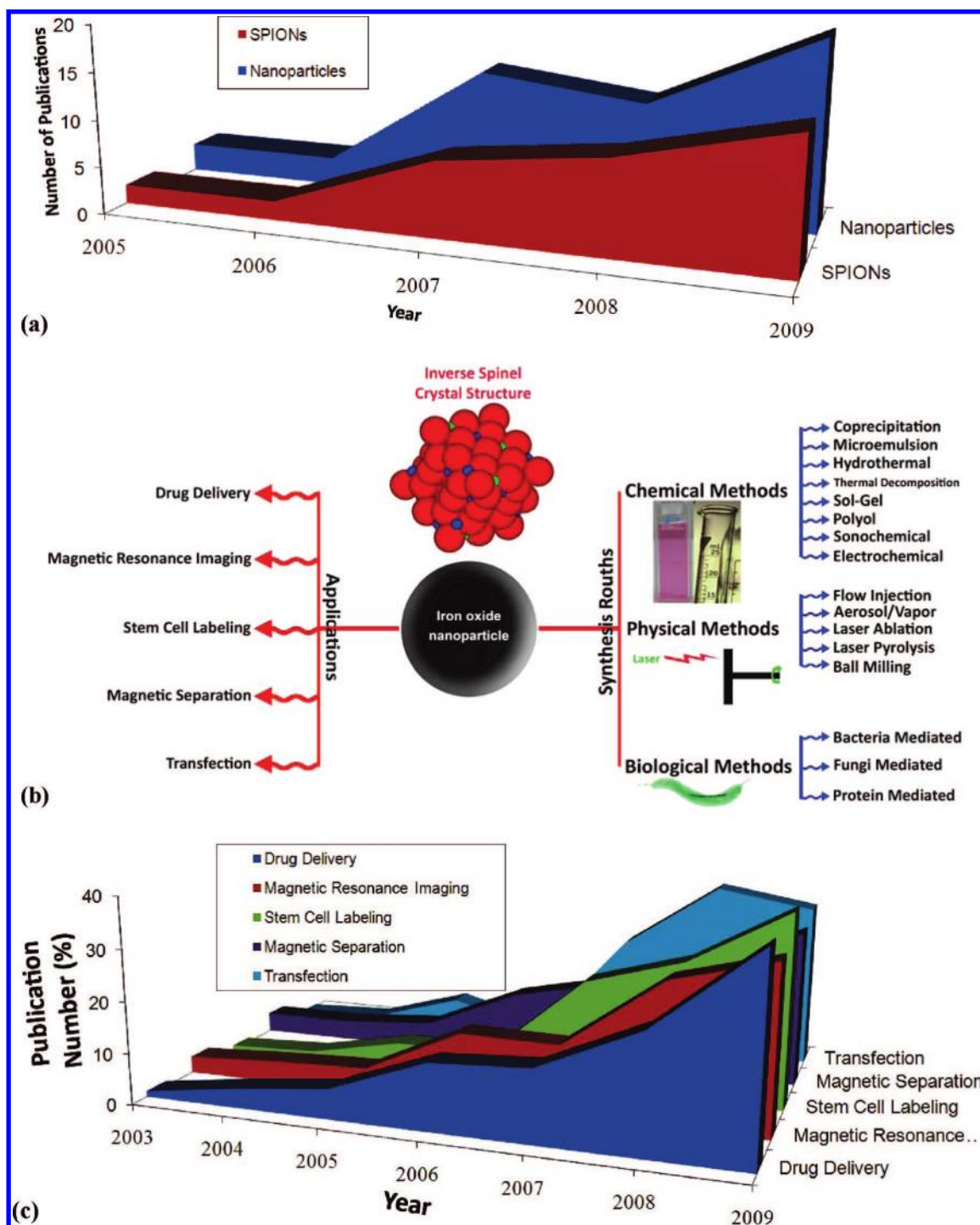


**Figure 3.** (a) Number of publications in stem cell labeling with all kind of nanoparticles in comparison with those with SPIONs; (b) crystal structure, various synthesis methods, and well-known biomedical applications of SPIONs; (c) number of publications (percentage) for the important biomedical applications of SPIONs.

Magnetic nanoparticles (ferrofluids with iron oxide nanoparticles) have been tested for their use in imaging and treatment of colon cancer.<sup>353</sup> These iron oxide nanoparticles were found to have a higher affinity for the tumor cells than for the normal cells. Another group of researchers have developed SPIONs and studied their interaction with human cancer cells.<sup>354</sup> When the iron oxide nanoparticle core was coated with amino group, the human cancer cells showed significant cellular uptake. Dextran-coated iron oxide nanoparticles can be utilized toward the treatment of breast cancer by magnetic heating.<sup>355</sup> Treatment methodologies like these

will make the increasing demand for breast conserving therapies more feasible in the future.

### 3.6. Nanotoxicology

Nanotoxicology, defined as the “science of engineered nanodevices and nanostructures that deals with their effects in living organisms”,<sup>356</sup> has been launched on a platform based upon our understanding of ultrafine particle research. This has raised the issue of whether conventional toxicology approaches are sufficient to establish the relative toxicity of

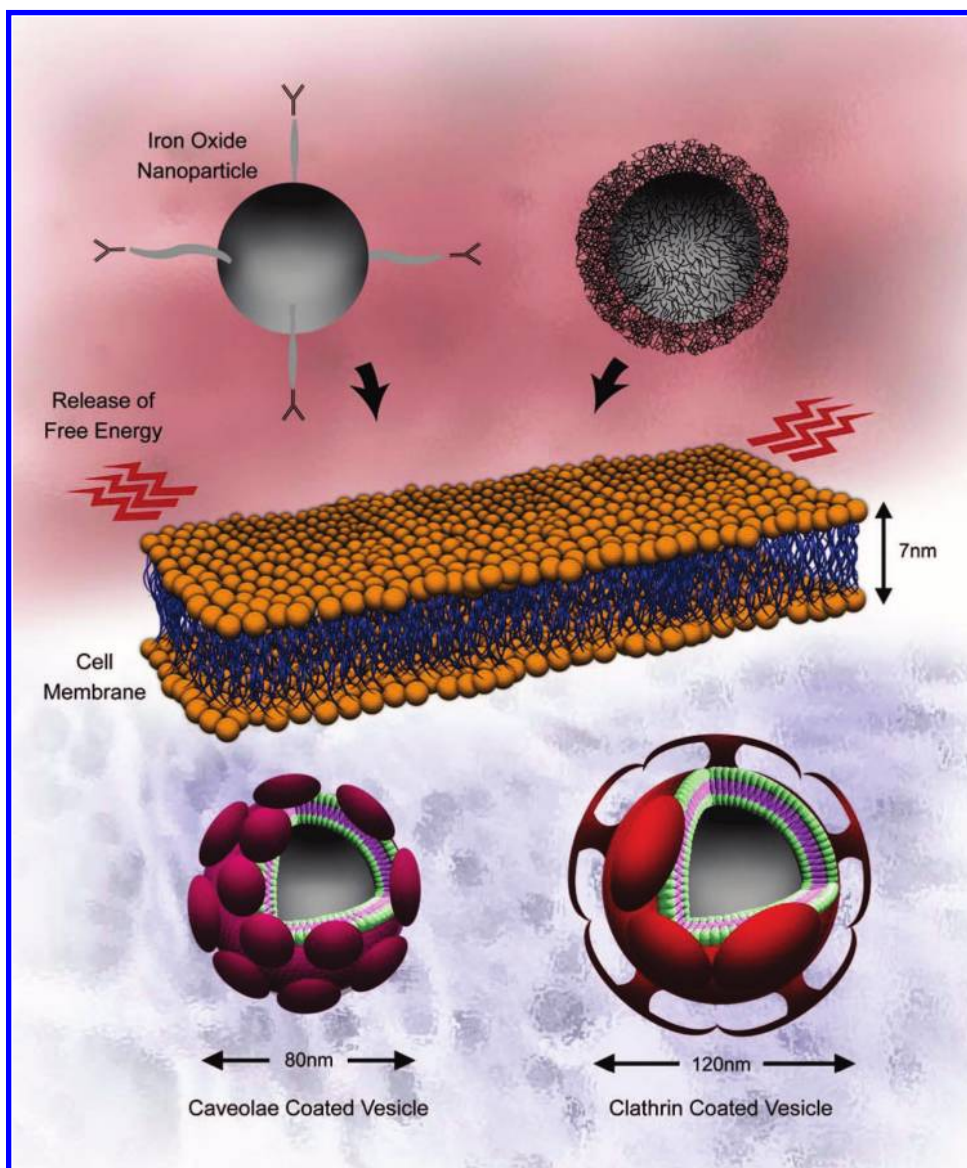
**Table 1. Various Procedures for the Synthesis of Bare SPIONs**

routes	main advantage/ main disadvantage	methods	size range/distribution	morphology	refs
physical	continuous methods/ <i>no shape and size control</i>	flow injection	$\leq 10$ nm/narrow	spherical	214–219
		aerosol/vapor	5–60 nm/broad	spherical but large aggregates	220–226
		laser ablation	nano particulate		227–232, 230 233
chemical	scale up possibility/ <i>needs surfactant removal process</i>	laser pyrolysis	nano particulate		234–239
		ball milling	nano particulate	irregular	240–246
		coprecipitation	10 to 200 nm/broad	rhombic or spherical	143, 144, 179–182, 247–250
		microemulsions	4–15 nm/narrow	cubic or spherical	251–265, 254, 265–278
		hydrothermal	15–200 nm/broad	spherical	279–288, 283, 284, 286, 288–293
		thermal decomposition	10–40 nm/narrow	spherical	294–309
		sol–gel	3–20 nm/narrow	spherical	310–320
		polyol	$\leq 20$ nm/narrow	spherical	321–327, 321–323
		sonochemical	30 nm or 48/14 nm/narrow	spherical or rod shaped	328–334
		electrochemical	3–8 nm/narrow	spherical	335–342, 335
biological	fully biocompatible/ <i>very low yield</i>	using bacteria, fungus, proteins	different sizes/very narrow	cluster/folded chains/ cubo-octahedral/spherical	343–350

engineered nanostructures with traditional particulate toxicants. Recent work has highlighted the difficulties of working with nanostructures which include characterization, batch variation, aggregation and agglomeration states, and the most appropriate dose metric.<sup>356–359</sup> At present, a tiered testing strategy<sup>358,360</sup> is being encouraged due to the lack of toxicity data available. However, the interpretation of the data must

recognize the unique properties of nanostructures before making general conclusions.

The precise mechanisms of nanostructure induced inflammation are complex given the range of compositions and our evolving understanding of the role of oxidative stress and aspect ratio in toxicity.<sup>360–365</sup> The traditional model for understanding ultrafine particle toxicity is based in an

**Figure 4.** Schematic representation of the SPIONs and the cell membrane together with the uptake pathways.

oxidative stress paradigm.<sup>366–369</sup> Therefore, depending upon the synthetic process employed and the subsequent chemical content of a nanostructure, it is reasonable to assume that oxidative stress is a primary mechanism of toxicity.<sup>361</sup>

It is therefore a reasonable hypothesis that SPIONs may generate reactive oxygen species in a manner similar to combustion-derived carbon particles or other metal oxides.<sup>363,370</sup> Additionally, there is no evidence to suggest that SPIONs would act through innate receptor responses such as Toll-like receptors; although other innate immune recognition responses can be modulated by some nanoscale particles.<sup>371</sup> Nanoparticles in general can have a wide array of immunological effects.<sup>372</sup>

### 3.6.1. *In Vitro* Toxicity Assessment

*In vitro* models to screen for possible *in vivo* toxicity are presently in demand as the development of new nanomaterials is outpacing the capacity to test their toxicity or biocompatibility. The unique issues associated with nanostructure dosimetry<sup>359</sup> have made it difficult to develop a suite of *in vitro* tests with comparative capacity to *in vivo* responses.<sup>373</sup> Moreover, the incredibly complex interrelationship among cell populations *in vivo* and the redundant physiological nature of the inflammatory response can make it difficult to find accordance between *in vivo* and *in vitro* toxicity data. To this end, water-soluble C<sub>60</sub> has been shown to cause no difference in lung toxicity relative to control animals which contradicts *in vitro* data.<sup>374</sup> This is likely due to the complex interplay of cellular and molecular responses involved in the inflammatory response, which includes the interaction of *in vivo* biology with exposure to and fate of toxicants. The long-term toxicity outcomes are integral to understanding the possible health effects of nanomaterials. At present, *in vitro* approaches do not afford reliable long-term predictions.

From a risk assessment standpoint, *in vitro* studies should be used in combination with an evaluation of exposure scenarios, epidemiology, and *in vivo* toxicity studies.<sup>375</sup> Unfortunately, inadequate consideration of dosing and experimental design has led to artifacts and some poor interpretations of *in vitro* data in nanotoxicology research.<sup>376,377</sup> Nevertheless, *in vitro* work is extremely valuable for isolating the responses of specific cell types, as well as for studying subcellular localization and uptake mechanisms.<sup>173,174,363,378</sup> While *in vitro* nanotoxicology studies may not adequately predict the global *in vivo* responses or possible pathology, they are essential to answer some of the fundamental questions pertinent to toxicology such as specific cellular responses, including cytokine activation, signaling pathways, genotoxicity and induction of oxidative stress and associated reactive oxygen species.<sup>377</sup>

### 3.6.2. *Cytotoxicity End-Points*

While phenomenological doses *in vitro* can provide useful data for comparison with other studies, caution should be used in making broad conclusions from these dose—responses alone. Dosing of *in vitro* systems has particularly unique considerations when studying nanoparticles.<sup>379</sup> For a comprehensive evaluation of nanoparticle cytotoxicity and the advantages and disadvantages of experimental methods, the reader is directed to excellent reviews by Lewinski et al.<sup>380</sup> and Stone et al.<sup>377</sup> It is of particular concern to take a critical approach to cytotoxicity assays, as some nanoparticles can

directly confound some of the traditional methods of assessment such as colorimetric assays.<sup>376,382</sup>

For example, while Trypan blue counting is an accepted method for determining cell viability in a tiered toxicity screening approach,<sup>358</sup> it should be interpreted cautiously as this technique indicates grossly disrupted membranes<sup>381</sup> and therefore is not specific to other forms of cell death or injury. It has also been shown with molecular nano-onions in skin fibroblasts that the mechanisms of cell death are affected by the dose used *in vitro*.<sup>383</sup> Alamar Blue, MTT, WST, and LDH cytotoxicity assays are also commonly used and can have discordant results with some classes of nanoparticles.<sup>376,380,382</sup> Cytokines and chemokines are also important factors in assessing cellular responses to nanoparticles since they can have significant pleiotropic and proinflammatory effects. For example, interleukin-8 and its rodent analogue MIP-2<sup>384</sup> are chemokines often associated with oxidative stress and can lead to significant inflammatory cell recruitment *in vivo*.<sup>385</sup>

### 3.6.3. *SPIONs Toxicity*

Despite a relatively large body of literature on the chemical synthesis and characterization of SPIONs, little work exists on their toxicity *in vitro* and *in vivo*. SPIONs are in the class of metal oxide nanoparticles, but they can be modified significantly which can alter their disposition in biological environments. The manner in which SPIONs are chemically modified will indeed impact cytotoxicity outcomes *in vitro* and also their toxicokinetics and dynamics *in vivo*.<sup>386</sup> While there are many unanswered toxicity questions concerning SPIONs, they are some of the first magnetic nanoparticles approved for clinical application.<sup>387</sup> However, the toxicity studies on SPIONs are discordant and can be influenced by many factors. A comprehensive section on the cytotoxicity of SPIONs has been included in a review by Lewinski et al.<sup>380</sup> More recent studies pertinent to the present manuscript are highlighted in the following section.

Nanoparticle toxicity outcomes continue to be influenced by many factors including size, shape, charge, surface modification, agglomeration state, etc. While nanotechnology can afford particles a range of different properties, it also allows us to manipulate such nanoscale properties and therefore the potential toxicity. Indeed, SPIONs have been manipulated to modify their chemical properties,<sup>303</sup> and this has been shown to influence toxicity.<sup>386,388,389</sup> Mahmoudi et al. generated magnetic nanoparticles such as spheres, nanoworms (rough elongated), rod-shaped (smooth elongated), and beads (random dispersion of iron oxide nanoparticles in polymeric beads).<sup>390</sup> It was then observed that the toxicity of SPIONs even at the same molarity was enhanced when mouse L929 fibroblast cells were exposed to nanobeads, nanoworms, and nanospheres. It was also noted that a critical mass ratio (*r*-ratio) of ~3 is key to functional magnetic saturation and biocompatibility. Indeed, by studying cytotoxicity with the MTT assay, it was noted that cell viability was enhanced as the *r*-ratio increased. That is, with an increased hydrodynamic diameter the SPIONs showed lower toxicity.

Nanomaterials can also interact with cell media under *in vitro* conditions and possibly impact toxicity results, as has been shown with single-walled carbon nanotubes.<sup>391</sup> Mahmoudi et al. have been utilizing this technology with a variety of nanoparticles, specifically with SPIONs.<sup>392</sup> In another study by these researchers, it was demonstrated that SPIONs can impact the cell media by interacting with proteins and



in turn influencing toxicity.<sup>392,393</sup> By modifying the exposure protocol to account for particle-media interactions, it was observed that PVA-coated nanoparticles induced lower toxicity, which is likely due to the particles having less adsorption sites for biomolecules in the media.

Further *in vitro* work on SPIONs has compared combustion synthesized SPIONs with commercially available SPIONs and has found no difference in endothelial cell viability at exposures of up to 0.1 mg/mL of SPIONs in concentration.<sup>394</sup> This study employed the live-dead cell assay as the determinant of cytotoxicity and also studied an endothelial cell line (PAEC) which is different from previously discussed studies.

#### 3.6.4. Considerations for *In Vivo* Applications

In many ways, SPIONs may face the same hurdles as quantum dots for further applications *in vivo*.<sup>395</sup> SPIONs have immense physicochemical versatility which makes them attractive for tailoring to specific nanomedical applications. However, with each new SPION formulation there are new toxicity considerations that will impact both *in vitro* and *in vivo* data. Indeed, the modifications made to the surface chemistry of SPIONs will have a significant influence on particle stability and the *in vivo* fate.<sup>386</sup> Different physicochemical properties such as final size, surface charge, and coating density are key factors. At present, there is no single property–activity relationship that predicts the stability, toxicity, as well as pharmacokinetics and overall safety of SPIONs.<sup>396</sup> While important information has been gained from cytotoxicity studies of SPIONs, further purpose-specific toxicity testing is required prior to other clinical applications of SPIONs.

### 4. MSCs Labeling

Besides the numerous advantages of using MSCs in cell therapy and their potential applications, the characteristics of the stem cells in repairing defects is not well understood. In fact, further evaluation of the cells' behavior in tissue repair, migratory dynamics, degree of cell survival, integration into the newly formed tissue, and fate *in vivo* is needed. Evidently, the development of tissue engineering therapies requires noninvasive techniques for tracking MSCs after transplantation in order to monitor the cells' fate in both animal models and in clinical trials. So far, procedures including bioluminescence, radioactive substrates, near-infrared fluorescence, post-mortem histological analysis, and MRI contrast agents have been utilized to detect migration and homing of the transplanted cells.<sup>397,398</sup> Among these methods, only labeling with MRI contrast agents and radioactive agents are currently suitable for clinical use.

#### 4.1. MRI Contrast Agents for Labeling MSCs

Gadolinium chelates, which are widely used in MRI, have been utilized recently by Yang et al.<sup>399</sup> for labeling hMSCs without the aid of a transfection agent. In this study, hMSCs were incubated with paramagnetic gadodiamide complexes ( $R_1/R_2 = 3.9 \text{ s}^{-1} \text{ mM}^{-1}$ ) at different concentrations of 0.95, 2.87, 9.53, and 28.7 mg/mL. Although mass cell death at the highest concentration of gadodiamide complexes was observed, revealing the possible toxicity of the chelate, no cell death or morphological change in hMSCs were noticed at a 9.53 mg/mL concentration. Flow cytometric measure-

ment also confirmed no change in cell size and granularity due to the labeling. MR cell labeling can be done with Gd-based contrast agent.<sup>400</sup> They suggested that the lower stability of gadodiamide (Gd-DTPA-BMA) is responsible of a net transfer of  $\text{Gd}^{3+}$  ions on the cell membrane followed by a slower internalization process. Furthermore, *in vitro* MR imaging of labeled cells showed that more than 50 000 cells were detectable by MRI. As compared to the gadodiamide-labeled hMSCs, SPIONs are more effective as MRI contrast agents and thus most approaches use them for stem cell labeling. It is noteworthy that Heyn et al.<sup>401</sup> showed that single cells labeled with SPIONs could be tracked *in vivo* using MRI. Without a transfection agent, a concentration of 10  $\mu\text{g Fe/mL}$  does not yield apoptosis and thus can be used for MR imaging of at least 12 500 cells which is 25% of the cells required for gadodiamide-labeled hMSCs. Transfection agents like Superfect, DOTAP, Lipofectamin, poly-L-Lysine (PLL), and protamine are usually required to achieve intracellular uptake of SPIONs.<sup>402</sup> It has been shown that without a transfection agent, negligible uptake of SPIONs occurs. Nevertheless, these agents are mostly cationic and toxic at high concentrations and are not approved for clinical use (with the exception of protamine). Therefore, there is great interest in surface engineering of SPIONs to avoid a transfection agent in the process of stem cell labeling.

#### 4.2. Surface Engineering of MRI Contrast Agents for Labeling MSCs

After intracellular labeling, commercially available MRI contrast agents of a large size (120–180 nm) usually tend to be biodegraded by intracellular enzymes and acids and then diluted by rapid cell division. In order to solve this problem, nanoparticles for MSCs tracking with MRI need to be engineered to (a) label stem cells with a “larger” number of nanoparticles of a “smaller” size, so that after cell proliferation the nanoparticles will be enough to be distributed in the off-spring cells, and (b) coat nanoparticles with chemically inert substances, which are resistant to intracellular enzymes and acid. Mailänder et al.<sup>402</sup> studied the efficiency of two commercially available SPIONs (Resovist and Feridex) without transfection agents for hMSCs labeling. They showed that the uptake of Resovist (generic name: ferucarbotran), in which the particles are stabilized by carboxydextran, is more efficient. Huang et al.<sup>403</sup> reported that ferucarbotran is not toxic to hMSCs and increases cell growth. They showed that the promoted cell growth is due to the ability of ionic SPIONs to diminish cellular  $\text{H}_2\text{O}_2$  through intrinsic peroxidase-like activity and to affect protein regulators of the cell cycle (Figure 5).

The major shortcoming of SPIONs for labeling MSCs is their low intracellular labeling efficiency. This limitation has evoked great interest in developing new labeling methods. In order to increase the efficacy of cellular-internalization of SPIONs, several researchers have explored invasive modifications on the surface of SPIONs, including polymeric coatings and utilizing transfection agents. In this regard, the internalizing efficiency has been slightly increased, but it is still very low to be detected by MRI. A long-term incubation together with high concentration of nanoparticles per cell<sup>29,404,405</sup> and/or using MRI systems<sup>406,407</sup> with higher field strengths than clinical MR imagers (i.e., 1.5 T) are reported as alternative methods to increase the MRI detection of labeled MSCs. Enhancing the internalizing efficiency is also achieved by linking the SPIONs to an HIV tat peptide or

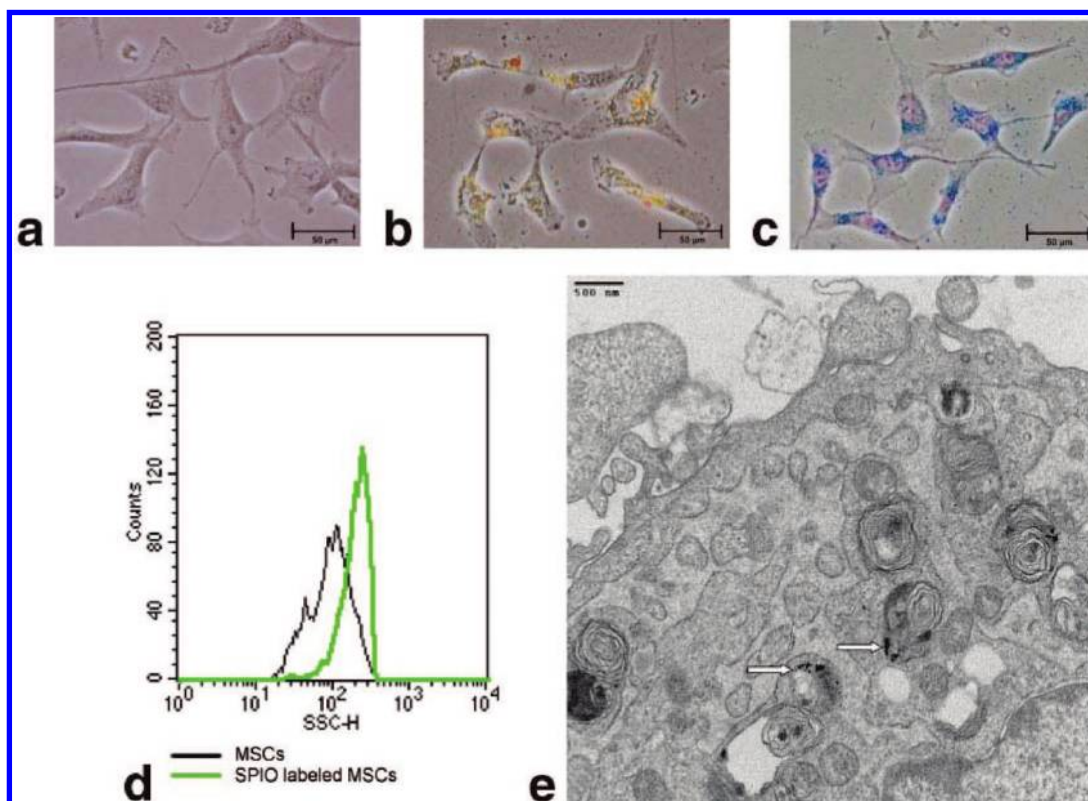


**Figure 5.** Microscopic appearance of hMSCs. (a) Nonlabeled hMSCs. (b) SPIO-labeled hMSCs at 24 h. Some brownish-colored, shining granules are evident at the cytoplasm near nuclei. Most cells were labeled with these granules. Morphology of these SPIO-labeled stem cells is not changed. (c) Prussian blue staining of SPIO-labeled stem cells. Several blue granules were evident at the cytoplasm around the nuclei. (d) Flow cytometry of nonlabeled and labeled hMSCs. Labeled hMSCs contained SPIO, manifesting as granules. SSC distribution of labeled hMSCs was shifted to the right. (e) Electron microscopic appearance of hMSCs after SPIO labeling. These ingested SPIOs manifest as clusters of dense spots detected at the cytoplasmic membrane-bound organelles (white arrows). The results suggest the location of SPIO is in the intracellular organelles. No SPIO was found at the cell membrane; reprinted with permission from ref 403. Copyright 2009 Elsevier.

monoclonal antibodies.<sup>408</sup> However, these methods suffer from the biosafety of a xenogeneic protein. Lu et al.<sup>409</sup> reported that hMSCs can be efficiently labeled with SPIONs and can be monitored *in vitro* and *in vivo* with a clinical 1.5 T MR imager under low incubation concentration of SPIONs together with short incubation time, and low detection cell numbers at the same time. Electron microscopy studies<sup>402</sup> revealed intracellular deposits of nanoparticles mainly inside of endosomal/lysosomal compartments without cytoplasmic localization or deposition in cell core, Golgi, or mitochondria. As a result, the intercellular SPIONs accelerate the cell cycle progression through the production of iron from the lysosomal metabolism of the nanoparticles.

Experiments have shown that the amount of iron in living cells is remarkably increased by increasing the concentration of SPIONs in the cell culture media and no toxicity was noticed up to 250  $\mu\text{g Fe/mL}$ .<sup>268</sup> It was therefore demonstrated that the presence of carboxyl groups increases the cellular uptake as compared with nonfunctionalized particles. Although a high amount of SPIONs without transfection agent resulted in poor iron uptake, as compared with a low concentration of SPIONs with transfection agent, extracellular agglomeration of nanoparticles by serum proteins occurred. As a result, it became questionable whether the signals detected by MRI represented cell migration, nanoparticle agglomeration, or macrophage phagocytosis. Yang et al.<sup>399</sup> found that even at a low concentration of ferucarbotran (10  $\mu\text{g/mL}$ ), the MRI signal intensity drops in the areas surrounding the cells, which might interfere with the interpretation of anatomical structure. SPIONs coated with

charged monomers are another class for efficient magnetic labeling of MSCs. These particles have a small hydrodynamic diameter (<50 nm) and are stabilized by electrostatic surface charges in a wide range of pH, ranging from 3 to 11, due to a negative zeta potential. Anionic citrate-coated SPIONs with an ultrasmall iron core size (4 nm) have been shown to be incorporated by macrophages much faster and with a better efficiency than carboxydextran-coated SPIONs.<sup>410</sup> Fluorescein isothiocyanate (FITC)-incorporated silica-coated core-shell SPIONs, SPIONs@SiO<sub>2</sub>(FITC), with diameters of 50 nm (see Figure 6a) have been synthesized and used as a bifunctionally magnetic vector that can efficiently label hMSCs via clathrin- and actin-dependent endocytosis with subsequent intracellular localization in late endosomes/lysosomes.<sup>399</sup> It is important to mention that silica is biocompatible and stable in biological environments, possessing a protective shell to prevent the dissolution and release of toxic ions (i.e., Fe<sup>2+</sup>) from SPIONs.<sup>201,405,411</sup> Indeed, as more and more nanoparticles become interfaced with biological systems in medicine the question of *in vivo* particle stability will need to be addressed. This is particularly true for particles which consist of multiple core-shell components that might be destabilized by various physiological environments.

In the mentioned study by Yang et al.,<sup>399</sup> although the uptake process displayed a time- and dose-dependent behavior, SPIONs@SiO<sub>2</sub>(FITC) yielded adequate cell MRI contrast at an incubation dosage as low as 0.5  $\mu\text{g}$  of iron/mL of culture medium with  $1.2 \times 10^5$  hMSCs. Additionally, the *in vitro* detection threshold of cell number was found to

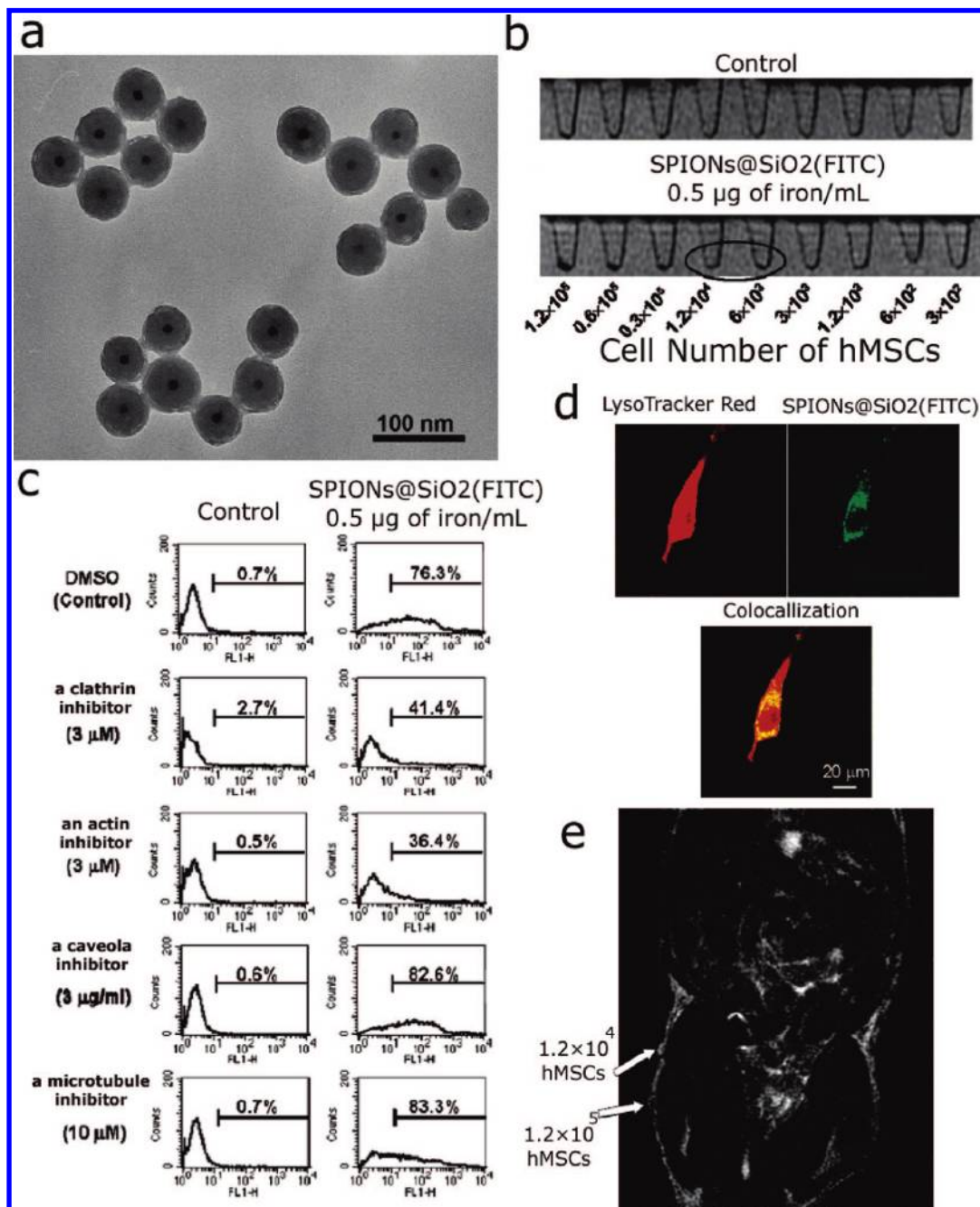


**Figure 6.** (a) TEM image of SPIONs@SiO<sub>2</sub>(FITC) with an average overall size of 50 nm, 10 nm core, and about 5 nm ring related to the presence of the organic group. (b) Sensitivity of in vitro MRI of SPION@SiO<sub>2</sub>(FITC)-labeled hMSCs. Cells ranging from  $3 \times 10^2$  to  $1.2 \times 10^5$  after treatment with 30  $\mu$ g/mL SPIONs@SiO<sub>2</sub>(FITC) for 1 h were scanned. (c) hMSCs were treated with a vehicle (DMSO, control) or the indicated inhibitors in the absence (left panels as negative control) or presence of 30  $\mu$ g/mL SPIONs@SiO<sub>2</sub>(FITC) (right panels) for 1 h. After treatment, uptake was detected by flow cytometry. The number of positively labeling cells is represented as the percentage of total counting cells in each panel. (d) Colocalization of green fluorescent SPIONs@SiO<sub>2</sub>(FITC) with late endosomes/lysosomes. The hMSCs were treated with 30  $\mu$ g/mL SPIONs@SiO<sub>2</sub>(FITC) for 30 min and then incubated with LysoTracker Red for another 30 min. (e) T<sub>2</sub>-weighted MRI study of SPION@SiO<sub>2</sub>(FITC)-labeled hMSCs was performed by injecting  $1.2 \times 10^4$  or  $1.2 \times 10^5$  cells mixed with Matrigel into subcutaneous tissue of the flanks (unlabeled cells at left flank and labeled cells at right flank, respectively) of a nude mouse; reprinted with permission from ref 399. Copyright 2009 American Institute of Physics.

be  $\sim 1 \times 10^4$  cells. Furthermore,  $1.2 \times 10^5$  labeled cells could be MRI-detected in a subcutaneous model in vivo (Figure 6b). The pathway of digested nanoparticles was determined via flow cytometry analysis and colocalization of LysoTracker Red (i.e., a marker for late endosomes and lysosomes with red fluorescence). Flow cytometry data (Figure 6c) showed that the SPIONs@SiO<sub>2</sub>(FITC)-labeled hMSCs treated with clathrin or actin inhibitors yield a lower MRI signal intensity, indicating the inhibition of particle uptake by these inhibitors rather than caveolae or microtubule inhibitors. The entrance

of SPIONs@SiO<sub>2</sub>(FITC) via endocytosis phenomena was also confirmed by colocalization of LysoTracker Red and SPIONs@SiO<sub>2</sub>(FITC) in late endosomes and lysosomes (Figure 6d). In order to track the labeled cells, MR imaging was performed in a nude mice model using hMSCs-treated SPIONs ( $1.2 \times 10^4$  and  $1.2 \times 10^5$  cells in 30  $\mu$ g/mL SPIONs). The functionalized nanoparticles were suspended in 10  $\mu$ L of Matrigel and injected subcutaneously and separately into the dorsal flanks of each nude mouse (Figure 6e). According to the results, by employing T<sub>2</sub>-weighted



images, the  $1.2 \times 10^5$  labeled hMSCs were detected in a 1.5 T MRI at the dorsal flanks of the nude mouse and presented as a dark, protruding mass mimicking a subcutaneous tumor. By contrast, the  $1.2 \times 10^4$  labeled hMSCs could only be detected as a bright dot, a signal which only reflects Matrigel. The authors concluded that the labeled cells could be detected in vivo in a dose-responsive manner under a clinical MRI system.

In another study, Wang et al.<sup>412</sup> developed amine-coated  $\text{Fe}_3\text{O}_4/\text{SiO}_2$  core/shell nanoparticles for MSCs labeling. Almost complete labeling of rabbit MSCs was achieved through 18 h incubation with  $4.5\text{--}9 \mu\text{g Fe/mL}$  for  $\text{Fe}_3\text{O}_4/\text{SiO}_2\text{--NH}_2$  nanoparticles. The nanoparticles were located in lysosomes postexposure. In vitro 3.0 T MR imaging revealed a significant enhancement in the sensitivity of the core/shell nanoparticles (2–5 fold) compared to the commercial Resovist. It has already been shown that anionic monomer-coated SPIONs can be used for labeling of various cells after a short incubation time (20 min to 2 h) without impairment of the cell viability and functionality.<sup>413</sup> It is suggested that the pathway of the coated nanoparticles includes attachment to the plasma membrane at the early stage, followed by endosomal formation and finally conveyance to the cytoplasm to fuse with late endosomes. The iron uptake mechanism is thus based on electrostatic adsorptive endocytosis. It is noteworthy that the nanoparticles do not behave as “single particles” but are clustered into agglomerates. Both in vitro and in vivo examinations revealed that the anionic monomer-coated SPIONs did not alter cell specificity and toxicity by the labeling procedure. Babic et al.<sup>414</sup> developed and used poly(L-lysine)-coated SPIONs for labeling of rMSCs and hMSCs. They found that a very high uptake (more than 92%) could be obtained for the PLL with a molecular weight of 388 100 due to the interaction of positively charged PLL with the negatively charged cell surface and subsequent endosomolytic uptake. The increased endocytosis was thought to be induced by the relatively higher amount of serum protein adsorption of PLL-coated SPIONs. Results of MR imaging both in vitro (200 cells/ $\mu\text{L}$ ) and in vivo (500 cells/ $\mu\text{L}$ ) demonstrated the possibility of imaging to detect a low number of cells. However, aggregation of PLL-modified SPIONs in the presence of electrolytes is a limitation. Moreover, their modification with antibodies, enzymes, and proteins is difficult at present.

In order to improve the colloidal stability and to enable the subsequent covalent attachment of biomolecules, Babic et al.<sup>415</sup> developed poly(*N,N*-dimethylacrylamide) (PDMAAm)-coated SPIONs for MSCs labeling. As compared with dextran-modified SPIONs (Feridex), higher labeling efficiency was obtained for both hMSCs and rat MSCs. For instance, after 72 h incubation with  $15 \mu\text{g Fe}_2\text{O}_3/\text{mL}$ , the amount of uptake for hMSCs was 82% and 68% for PDMAAm-coated SPIONs and Feridex, respectively (20% improvement). Electron microscopy studies revealed intracellular uptake and large accumulation in endosomes. Moreover, in vivo MR imaging of labeled hMSCs in rat brain demonstrated a higher sensitivity and better resolution of the PDMAAm-coated SPIONs compared with commercially available Feridex. Very recently, Suh et al.<sup>416</sup> synthesized SPIONs conjugated with a nontoxic protein transduction domain, termed a low molecular weight protamine (LMWP), in order to generate a powerful MSCs labeling tool. The average particle size and zeta potential of the functionalized particles were  $\sim 27 \text{ nm}$  and  $\sim 17 \text{ mV}$ , respectively. An

effective internalization into hMSCs by LMWP-SPIONs was shown with the highest iron incorporation at  $2.3 \pm 0.25 \text{ pg/cell}$ . Interestingly, the labeled hMSCs presented a similar osteogenic and adipogenic differentiation to the unlabeled cells. Schwarz et al.<sup>417</sup> compared the uptake of synthetic lipid-shell SPIONs (core size of 8–10 nm) with that of magnetosomes from magnetotactic bacteria into hematopoietic  $\text{Flt}3^+$  stem cells. Magnetosomes comprise magnetic crystals (40–45 nm) enveloped by a biological membrane composed of phospholipids and specific proteins. Both synthetic and biogenic SPIONs exhibited internalization into the stem cells without any evidence of cytotoxicity. The intracellular iron concentration was  $13.6 \pm 1.6 \text{ pg/cell}$  and  $16.8 \pm 1.7 \text{ pg/cell}$  for the lipid-shell and magnetosomes nanoparticles, respectively. MR relaxometry experiments revealed values of 4.0 and  $3.2 \text{ s}^{-1} \text{ mM}^{-1}$  for  $R_1$  and 729 and  $1198 \text{ s}^{-1} \text{ mM}^{-1}$  for  $R_2$  relaxivities for the synthetic and biogenic SPIONs, respectively. Interestingly, the lower  $R_1$  and higher  $R_2$  values of the magnetosomes demonstrate the potential of biogenic nanoparticles as contrast agents for both  $T_1$  and  $T_2^*$ -weighted MR imaging. Gold has also been used as a rigid shell in order to minimize the potential toxic effects of  $\text{Fe}^{2+}$  ions originating from dissolved SPIONs in the cell cytoplasm.<sup>418</sup>

## 5. NSCs Labeling

The investigation of endogenous neural progenitor cell migration in the rodent brain by MRI may greatly aid the study of NSCs response to brain injury and disease. Iron-oxide particles, as an agent for cellular MRI, have previously been utilized to label endogenous NSCs in situ in rats and mice. For example, core–shell structures (e.g., SPIONs as core and Au as the shell) were prepared by Wang et al.<sup>418</sup> and were shown to interact with NSCs isolated from an adult rat spinal cord. A dose-dependent attenuation of MRI signals was observed for both SPIONs@Au and SPIONs@dextran (examined for comparison). The Au-coated SPIONs showed a clear suppression of  $T_2$ -weighted spin echo signals by about 17% of the control (water/agar) levels at a concentration of  $0.001 \mu\text{g Fe}/\mu\text{L}$ . The dextran-coated SPIONs (examined for comparison) induced a similar effect (13% attenuation) at a concentration of  $0.01 \mu\text{g Fe}/\mu\text{L}$  (see Figure 7a). However consequently, at a concentration of  $0.03 \mu\text{g Fe}/\mu\text{L}$ , the Au-coated SPIONs caused an almost complete attenuation in MRI signal intensity, whereas dextran-SPION still permitted about 35% of  $T_2$ -weighted signals originating from the medium carrier (water/agar gel). In order to track the cells in vivo via MRI, the labeled cells were infused into the spinal cord of anaesthetized rats and the  $T_2$ -weighted signal intensities (reflecting diffusion and clearance of the SPIONs from the spinal cord) were monitored at 1 h, 48 h, and 1 month postinjection (see Figure 7b). According to the results, for dextran-coated SPIONs the diffusion volume quickly increased along the longitudinal axis of the spinal cord with time. Consequently, the corresponding MRI signal was markedly attenuated already after two days and completely disappeared one month postinjection. In contrast, the diffusion volume of Au-coated SPIONs did not change and the particles showed intensive suppression on  $T_2$ -weighted spin echo signals even one month after injection. Histological analysis (i.e., staining of Au-coated SPIONs with silver enhancement and green fluorescence protein (GFP) immunoreactivity for GFP-labeled NSCs) also revealed that MRI signals were well correlated with gold-positive staining of transplanted cells (Figure 7c). Focke et al.<sup>419</sup> labeled human

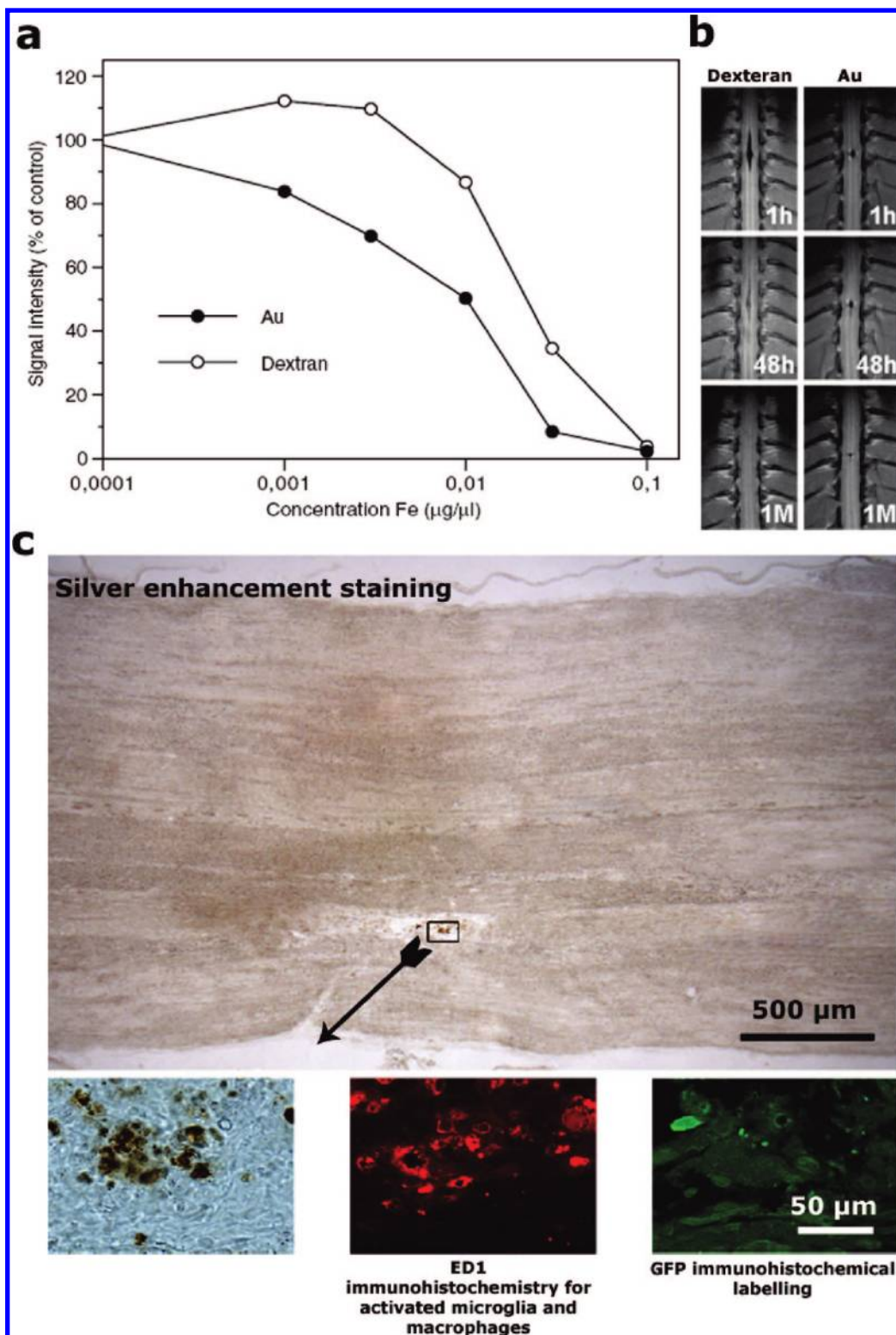


**Figure 7.** (a) A dose-dependent attenuation of  $T_2$ -weighted MRI signals induced by Au- and dextran-coated SPIONs in suspension. (b) In vivo MRI tracking of dextran- and Au-coated SPION-labeled GFP-NSCs injections in the rat's spinal cord 1 h, 48 h, and 1 month postgrafting. (c) Au@SPION-labeled GFP-NSCs in the rat's spinal cord 1 month postgrafting; reprinted with permission from ref 418. Copyright 2006 IOP Publishing.

mesencephalic neural precursor cells (hmNPCs) with SPIONs (core size of 5 nm; Ferropharm, Teltow, Germany) and investigated, on the one hand, the effect of these SPIONs on the survival, proliferation, and differentiation of the stem cells and, on the other, the sensitivity of 1.5 T MRI to detect labeled cells in living rats following transplantation. According to the results, about 95% of the treated hmNPCs (with 1.5 mM of SPIONs) were labeled without detectable

inverse effect on cell viability or proliferative capacity which were measured by the expression of proliferating cell nuclear antigen and cell cycle distribution, respectively. It is interesting to note that the labeled hmNPCs showed great potency (about 30%) of differentiation into neurons and glia with no detectable difference compared to control cells. The transplanted (into rat striata) labeled hmNPCs were detectable via MRI even after three months postsurgery, confirming the

high labeling stability. NSCs (derived from the brain of embryonic 14-day rat) have also been labeled with SPIONs via poly-L-lysine and bromodeoxyuridine (BrdU) and monitored via MR scanning 1, 3, 5, 7 weeks after transplantation into the ischemic rat.<sup>420</sup> It is noteworthy that the two types of labeled NSCs were transplanted into the ipsilateral caudate nucleus (group 1) and the contralateral caudate nucleus (group 2), respectively. After the first postimplantation image, a well-defined hyperintensity of the cortical infarct lesion was observed. The implanted labeled cells were visible on MR images as a hypointense area at the injection site caudate nucleus. Three weeks later, linear hypointensity was observed in the subcortical infarct lesion in group 1. After five weeks, the low signal intensity could be seen in the corpus callosum and formed a triangle-like loop with its tip directed to the lesion side in group 2. Seven weeks later, hypointensity was observed in the lesion of the second group. According to their results, the labeled-NSCs and BrdU could migrate into the lesions after transplanted into rats' brains. SPION-labeled nerve growth factor- $\beta$  (NGF- $\beta$ ) gene-modified spinal cord-derived NSCs were prepared by Lei et al.<sup>421</sup> The distinguishing markers for stem cells (nestin), neuron ( $\beta$ -III-tubulin), oligodendrocyte (CNPase) and astrocyte (GFAP) were used to assess the differentiation ability of the labeled cells. From their results, the authors concluded that the SPION-labeled NGF- $\beta$  gene-modified spinal cord-derived NSCs were effectively recognized and they were multipotent and capable of self-renewal.

## 6. In Vivo Tracking of Stem Cells

### 6.1. Animal Studies

Jing et al.<sup>27</sup> used Feridex suspension and protamine sulfate (Fe-Pro complex) as the transfection agent to track MSCs by in vivo MRI following injection into the knee joint cavity in rabbit articular cartilage defect models. No significant change in the viability, cell death, proliferation, differentiation, and morphology of the labeled cells as compared to the unlabeled cells was observed at a concentration of 25  $\mu\text{g/mL}$ . Nevertheless, the signal intensity of GRE  $T_2$ -weighted images was found to depend on the number of labeled cells and significantly decreased over time. Similar results were reported by Hu et al.<sup>35</sup> when transplantation of human umbilical cord mesenchymal stem cells (hUC-MSCs) into focal areas in an adult rat spinal cord was performed. They incubated hUC-MSCs with 22.4  $\mu\text{gFe/mL}$  for 24 h (Feridex suspension) and observed a good correlation between the number of labeled cells and optical density of GRE  $T_2$ -weighted and SE  $T_2$ -weighted images. In vivo MR imaging revealed that SPION-labeled MSCs ( $5 \times 10^4$  cells) can be efficiently detected 2 weeks after transplantation into the rat spinal cord. The possible application of BM-MSCs for cardiac regeneration has recently been studied in adult rats through MRI and positron emission tomography (PET) by Chapon et al.<sup>86</sup> These authors used dextran-coated nanoparticles (15–20 nm) conjugated with TAT-fluorescein isothiocyanate peptide as a marker and showed that, after 6 h incubation with 10  $\mu\text{g}$  SPIONs/ $10^5$  cells per mL of culture medium, 98% of BM-MSCs were labeled. After injection in rat hearts, it was possible to track live labeled stem cells over a 6-week period. Stucky et al.<sup>422</sup> reported an even longer time (16 weeks) for detection of BM-MSCs labeled with relatively large SPIONs (900 nm). A long detectability (12 weeks) of MSCs labeled with Fe-Pro complex (120–150

nm) in knee joint cavity in rabbit has also been observed.<sup>27</sup> Lee et al.<sup>423</sup> studied a complex formation between negatively charged fluorescent SPIONs and positively charged peptides (protamine sulfate) with an ability to improve the MR imaging of MSCs. The fluorescent nanoparticles (10 or 15 nm core) were synthesized by conjugating fixable fluorescent dextran to various SPIONs. For the 15 nm core size particles, the iron concentration in hMSCs was found to be  $17.2 \pm 0.2$  pg/cell. A strong fluorescent signal and enhanced  $T_2^*$ -weighted MR images were obtained in vitro and in vivo in a flank tumor model.

Although BM-MSCs have the ability to differentiate into cardiomyocytes and improve cardiac function,<sup>424–428</sup> several lines of evidence<sup>86,422</sup> reveal that a combination of variable degrees of infarction size and differential tissue remodeling over the period of study influences the global functional recovery following implantation. PET has revealed a higher 2-deoxy-2-[F-18]fluoro-D-glucose (FDG) uptake in infarcted areas in MSCs-treated animals, reflecting macrophage activity and changing glucose metabolism. Amsalem et al.<sup>429,430</sup> examined the functionality of SPION-labeled MSCs into the injured myocardium by injection of the stem cells directly into immunocompetent Sprague–Dawley rat hearts after ischemic injury. Four weeks after delivery, the SPIONs were only observed in cardiac macrophages and not within MSCs by MRI (Figure 8). Although this study raised concerns regarding the potential of SPIONs in cardiac cell therapy, many studies revealed cellular rejection of MSCs as the immune system of the rat recognizes MSCs as foreign in the absence of immunocompetent agents.<sup>431</sup>

Besides the labeling capacity and biocompatibility of SPIONs, their utility to monitor stem cells migration in vivo is an important clinical application of this tool. Portet et al.<sup>432</sup> developed SPIONs coated with 1-hydroxyethylidene-1,1-bisphosphonic acid (HEDP), allowing the targeting and uptake of MSCs with the ability to transdifferentiate into neural cells in vitro. Very recently, Delcroix et al.<sup>433</sup> used HEDP-coated SPIONs to study the potential effects of labeling rat MSCs (rMSCs) on their viability and functions as well as their osteogenic and neuronal differentiation potentials in vitro. The migratory potential of these iron-labeled MSCs in vivo in response to brain neurogenic stimuli was also studied. No effect on the viability, morphology, and differentiation functionality of rMSCs was noticed when using up to 50  $\mu\text{g}$  Fe/mL incubated for 48 h. Spectroscopic iron titration also revealed an average concentration of  $5.6 \pm 1.6$  pg iron/cell, which is in the same range as obtained when labeling hMSCs with Resovist.<sup>402</sup> It is interesting to note that the rate of stem cells migration can be defined through MRI.<sup>434</sup> Similar results were obtained by Guzman et al.<sup>435</sup> who demonstrated that labeling of human CNS stem cells grown as neurospheres with SPIONs did not adversely affect survival, migration, and differentiation or alter neuronal electrophysiological characteristics. Furthermore, they proved that the transplanted stem cells either to the neonatal, the adult, or the injured rodent brain respond to cues characteristic of the microenvironment resulting in distinct migration patterns. Meanwhile, a higher labeling efficiency of a subpopulation of hMSCs (MIAMI cells) by HEDP-coated SPIONs has been reported by D'Ippolito.<sup>436</sup> The application of MRI tracking for clinical cell therapy using iron-labeled hMSCs has been shown by Tatard et al.<sup>437</sup>

Delcroix et al.<sup>433</sup> reported on an in vivo examination of labeled rMSCs with no response to the subventricular zone



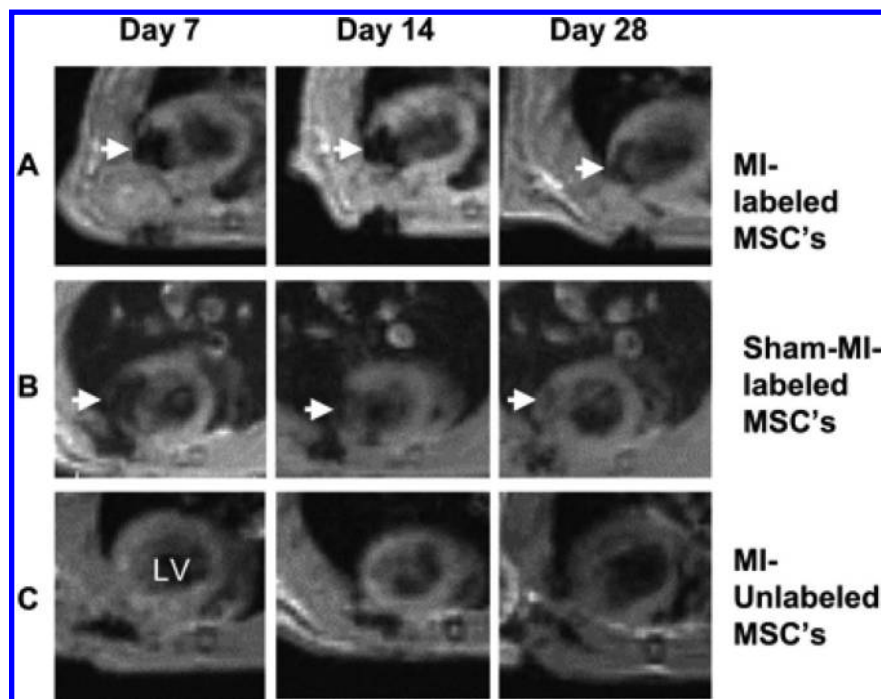


**Figure 8.** Serial in vivo tracking of MSCs by MRI. (A) Injection of  $2 \times 10^6$  SPIO-labeled MSCs 7 days after left coronary artery ligation created a wide intramural area of hypointensity (arrows) at the anterior LV wall. (B) Positive signals are still visible after 28 days. Similar magnetic signals (arrows) were produced by labeled cells injected to normal hearts. (C) Injection of unlabeled MSCs did not alter the magnetic signal of the myocardium; Reprinted with permission from refs 429 and 430. Copyright 2007 and 2008 Lippincott Williams & Wilkins.

(SVZ) microenvironment and no migration toward the olfactory bulb (OB) via the rostral migratory system. Nevertheless, when a mechanical lesion of the OB was performed, a long distance migration from the SVZ toward the OB was observed. This may be attributed to the chemoattractive molecules present in a damaged environment<sup>438</sup> that can promote cell migration via an interaction with MSCs surface receptors. In spite of this finding, no migration of injected iron-labeled MSCs to the adjacent cartilage defects in knee joint of rabbits has been observed.<sup>27</sup> The reason could be the stiff and strong collagen networks and proteoglycan matrix which resist cell migration. In this particular case, the repair of cartilage is mainly caused by host cells that are recruited to the defect in response to the implant. Recently, Pawelczyk et al.<sup>439</sup> studied the migration of SPION-labeled BM-MSCs in a modified Boyden chamber as a localized model of inflammation. In this model, activated macrophages were used as inflammatory cells and mouse or human fibroblasts as a surrogate host cells. Dextran-coated SPIONs (Feridex) with an approximate size of 120–150 nm and a total iron content of 11.2 mg/mL were used for labeling the stem cells. An abundant uptake of SPIONs into the cytoplasm in an amount of  $34.75 \pm 0.32$  pg per cell was obtained. Nevertheless, less than 10% of the total iron from the iron-labeled BM-MSCs was found in the activated macrophages depending on the ratio of labeled cells to inflammatory cells and microenvironment conditions. Therefore, direct implantation of the labeled stem cells into target tissue may lead to the uptake of label by the macrophages which can confound the interpretation of MRI results.

## 6.2. Human Studies

Noninvasive imaging techniques for in vivo tracking of transplanted human stem cells offer real-time insight into

the underlying biological processes of new stem cell based therapies, with the aim to depict stem cell migration, homing, and engraftment at organ, tissue and cellular levels. The evidence thus far indicates that human embryonic and adult stem cells can be labeled effectively with contrast agents and that the labeled cells can be tracked noninvasively and repetitively with MRI and optical imaging (OI).<sup>440–442</sup> Clinical studies are recognized as an essential stage in order to transfer the findings from animal experiments to human applications. Since there are many physiological parameters to consider, for instance, the organism's weight, blood volume, cardiac output, circulation time, as well as factors associated with a tumor's volume/location/microenvironment,<sup>138</sup> the step from animal trials to human trials is not straightforward.<sup>139</sup> Safe and feasible clinical studies of SPION-labeled stem cells were first carried out by de Vries et al.<sup>443</sup> According to their results, very low numbers of dendritic cells in conjugation with detailed anatomical information could be detected in vivo using 3T MRI. SPION-labeled autologous dendritic cells were injected intranodally as a cancer vaccine in melanoma patients. Evaluation of the accuracy of the dendritic cells delivery and the pattern of their migration was performed by MRI. The literature reports that SPION-labeled stem cells have been used for the regeneration of damaged brain tissues. Zhu et al.<sup>444</sup> explored the tracking-feasibility of SPION-labeled NSCs via MRI. Two patients were examined: a 34-year-old man with a brain trauma in the left temporal lobe and a 42-year-old man, as a control patient, with a brain trauma in the right temporal lobe. In the test patient, the neural tissue was collected from his brain during an emergency operation and cultured in a suitable medium. The autologous cultured NSCs were implanted stereotactically around the area of the damaged tissue of the brain. A 3 T MRI with a gradient reflection echo with a recovery time of 200 ms, an echo time of 20

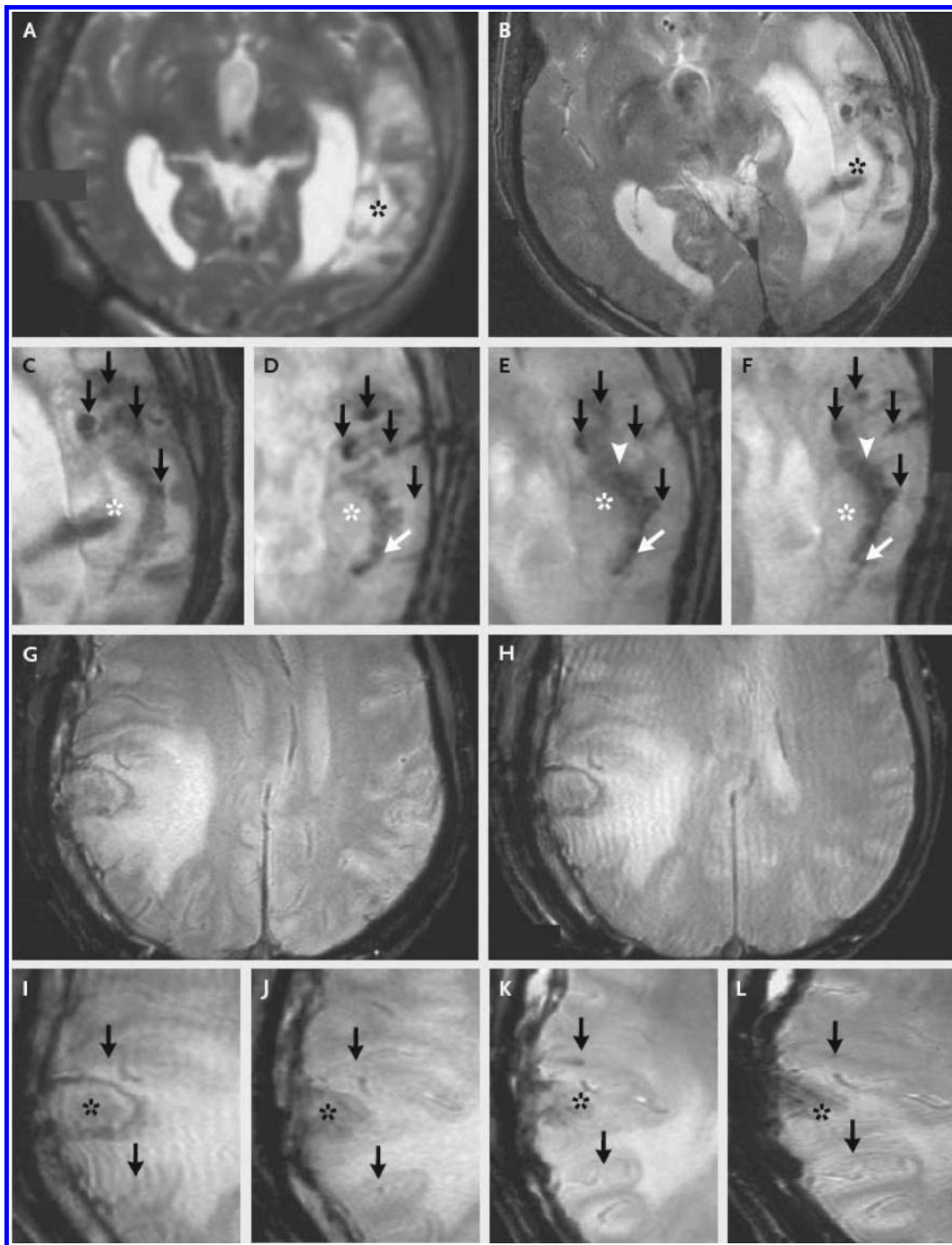


**Figure 9.** MRI scans from the test (A–F) and the control patients (G–L). The scan obtained before the implantation of the SPION-labeled NSCs (A) did not show a pronounced hypointense signal around the lesion (asterisk) in the left temporal lobe, whereas circular areas of hypointense signal were visible at the injection sites 1 day after implantation (B). Magnified images are shown in C–F. Four hypointense signals (black arrows) were observed at injection sites around the lesion on day 1 (C), day 7 (D), day 14 (E), and day 21 (F). On day 7 (D), dark signals (white arrow) were observed posterior to the lesion, a finding that was consistent with the presence of the labeled cells. By day 14 (E), the hypointense signals at the injection sites had faded, and another dark signal (white arrowhead) had appeared and spread along the border of the damaged brain tissue. By day 21 (F), the dark signal had thickened and extended further along the lesion (white arrow). The scans in panels G and H, from the patient who underwent implantation of unlabeled cells, were obtained on days 0 and 1, respectively, and the magnified views in panels I, J, K, and L were obtained on days 1, 7, 14, and 21, respectively. A slightly hypointense signal is present around the injection sites in panels I, J, K, and L. In these panels, the black arrows indicate the hypointense signal, and the asterisks indicate the lesion; Reprinted with permission from ref 444. Copyright 2006 Massachusetts Medical Society.

ms, and a flip range of 20 deg at 24 h and then every 7 days (for a period of 10 weeks) after implantation was employed. Pronounced hypointense signals were not found at the injection sites before implantation (Figure 9A). In contrast,

the injection sites were visible on the first day after implantation (Figure 9B). The hypointense signal at each injection site faded thereafter (Figure 9C–F). NSCs accumulation and proliferation caused detectable changes in

**Table 2. Efficiency and Toxicity of MRI Contrast Agents for Stem Cell Labeling**

cell type	MRI contrast agent	nanoparticle coating	environment	ref
hMSCs	gadodiamide chelate compared to iron oxide nanoparticles	N/C	in vitro	399
hMSCs	ferucarbotran (Resovist)	carboxydextran-coated SPIONs	in vitro	402, 403
rMSCs	Fe <sub>3</sub> O <sub>4</sub> @SiO <sub>2</sub>	silica-coated core–shell SPIONs	in vitro	412
R & hMSCs	SPION	poly( <i>N,N</i> -dimethylacrylamide) (PDMAAm)-coated SPIONs	in vitro	308
R & hMSCs	SPION	PDMAAm-coated	in vitro	415
hMSCs	SPION	low molecular weight protamine (LMWP)-coated SPIONs	in vitro	416
rNSCs	gold-coated SPIONs compared to dextran-coated SPIONs	SPIONs@Au/ SPIONs@dextran	in vitro	418
hMSCs	very small superparamagnetic iron oxide particles (VSOP)	citrate-coated SPIONs	in vitro	419
hNSCs	SPIONs	poly-L-lysine	in vitro	445
rNSCs	SPIONs	NGF- $\beta$ labeling achieved with SPIONs+fugene	in vitro	421
rMSCs	Fe-Pro complex	SPIONs (Feridex)-protamine sulfate complex	in vivo	27
hMSCs	Feridex suspension	dextran-coated SPIONs	in vivo (rat brain)	35
BM-MSCs	SPIONs	Tat peptide-derivatized dextran-coated nanoparticles	in vivo (rat heart)	86
BM-MSCs	SPIONs	Fe-Pro complex	in vivo (rabbit knee)	27
rMSCs	SPIONs	1-hydroxyethylidene-1, 1-bisphosphonic acid (HEDP)-coated SPIONs	in vitro	432
hMSCs	Resovist	carboxydextran-coated SPIONs	in vivo	399
dentritic stem cell	Endorem (Feridex)	dextran-coated SPIONs	in vivo (intranodally)	443
HNSCs	SPIONs	N/C	in vivo (human brain)	444

the signals during 1–10 weeks after implantation (Figure 9D). An interesting result was noted on the migration of NSCs from the injected site to the area of the damaged site (Figure 9E,F). The same procedure was applied for the control patient, in which the cultured NSCs were not labeled with SPIONs. After injection of NSCs to the brain tissue, there was no trace of a pronounced change in the signal around his lesion; instead, a slightly hypointense signal around the injection sites was detected (Figure 9G–L). No considerable change was observed in the signal intensity during the testing period.

## 7. Conclusions and Further Perspectives

Stem cells have enormous potential for therapeutic and pharmaceutical applications because they can give rise to various cell types. Given that clinical trials are ongoing or about to start with many different categories of stem cells, there is a need for in vivo stem cell imaging to monitor cell motility after inoculation, and to follow the location and expansion of the stem cells thereafter. Despite their therapeutic potential, many challenges, including the monitoring of cell fate in vivo, remain to be elucidated. Thus, a greater understanding of stem cell biology that can be used to expand and differentiate embryonic and adult stem cells in a directed manner offers great potential for tissue repair and regenerative medicine. These challenges may be addressed by using magnetic labeling approaches such as iron derivative nanoparticles.

As can be seen by the increasing number of examples in the application of magnetic techniques for stem cell biology, many advances have already been made; however, much

progress still remains to be made to fully utilize these technologies in a safely and efficiently manner. Moreover, the rejection of transplanted stem cells is another concern that needs further investigation.

We provided examples of a variety of MRI contrast agents with different nanoparticle coatings on rodent and human mesenchymal and neural stem cells in different environmental conditions that would help other investigators to access updated published data (Table 2).

## 8. References

- (1) Sykova, E.; Jendelova, P. *Cell Death Differ.* **2007**, *14*, 1336.
- (2) Thomson, J. A. *Science* **1998**, *282*, 1145–1147.
- (3) Bongso, A.; Lee, E. H. *Stem Cells*; World Scientific Publishing Co: Singapore, 2005.
- (4) Taupin, P. *Curr. Opin. Mol. Ther.* **2006**, *8*, 345.
- (5) Tholpady, S. S.; Llull, R.; Ogle, R. C.; Rubin, J. P.; Futrell, J. W.; Katz, A. *Clin. Plast. Surg.* **2006**, *33*, 55.
- (6) Watt, F. M.; Lo Celso, C.; Silva-Vargas, V. *Curr. Opin. Genet. Dev.* **2006**, *16*, 518.
- (7) Morigi, M.; Benigni, A.; Remuzzi, G.; Imberti, B. *Cell Transplant.* **2006**, *15*, 111.
- (8) Ratajczak, M. Z.; Machalinski, B.; Wojakowski, W.; Ratajczak, J.; Kucia, M. *Leukemia* **2007**, *21*, 860.
- (9) Fruehauf, S.; Seeger, T.; Topaly, J. *Cytotherapy* **2005**, *7*, 438.
- (10) Bobis, S.; Jarocha, D.; Majka, M. *Folia Histochem. Cytobiol.* **2006**, *44*, 215.
- (11) Biffi, A.; De Palma, M.; Quattrini, A.; Del Carro, U.; Amadio, S.; Visigalli, I.; Sessa, M.; Fasano, S.; Brambilla, R.; Marchesini, S.; Bordignon, C.; Naldini, L. *J. Clin. Invest.* **2004**, *113*, 1118.
- (12) Biffi, A.; Capotondo, A.; Fasano, S.; Del Carro, U.; Marchesini, S.; Azuma, H.; Malaguti, M. C.; Amadio, S.; Brambilla, R.; Grompe, M.; Bordignon, C.; Quattrini, A.; Naldini, L. *J. Clin. Invest.* **2006**, *116*, 3070.
- (13) Flax, J. D.; Aurora, S.; Yang, C.; Simonin, C.; Wills, A. M.; Billingham, L. L.; Jendoubi, M.; Sidman, R. L.; Wolfe, J. H.; Kim, S. U.; Snyder, E. Y. *Nat. Biotechnol.* **1998**, *16*, 1033.



- (14) Haynesworth, S. E.; Goshima, J.; Goldberg, V. M.; Caplan, A. I. *Bone* **1992**, *13*, 81.
- (15) Yoo, J. U.; Nishimura, K.; Solchaga, L.; Caplan, A. I.; Goldberg, V. M.; Johnstone, B. J. *Bone Joint Surg. Am.* **1998**, *80*, 1745.
- (16) Wakitani, S.; Saito, T.; Caplan, A. I. *Muscle Nerve* **1995**, *18*, 1417.
- (17) Nakagami, H.; Morishita, R.; Maeda, K.; Kikuchi, Y.; Ogiwara, T.; Kaneda, Y. *J. Atheroscler. Thromb.* **2006**, *13*, 77.
- (18) Chen, L. B.; Jiang, X. B.; Yang, L. *World J. Gastroenterol.* **2004**, *10*, 3016.
- (19) Ryan, J. M.; Barry, F. P.; Murphy, J. M.; Mahon, B. P. *J. Inflammation* **2005**, *2*, 1.
- (20) Ryan, J. M.; Barry, F.; Murphy, J. M.; Mahon, B. P. *Clin. Exp. Immunol.* **2007**, *149*, 353.
- (21) Fischer, U. M.; Harting, M. T.; Jimenez, F.; Monzon-Posadas, W. O.; Xue, H.; Savitz, S. I.; Laine, G. A.; Cox, C. S. J. *Stem Cells Dev.* **2009**, *18*, 683.
- (22) Kaveh, K.; Ibrahim, R.; Bakar, M. Z. A.; Ibrahim, T. A. *J. Anim. Vet. Adv.* **2009**, *8*, 1616.
- (23) Strube, P.; Mehta, M.; Baerenwaldt, A.; Trippens, J.; Wilson, C. J.; Ode, A.; Perka, C.; Duda, G. N.; Kasper, G. *Bone* **2009**, *45*, 1065.
- (24) Jung, D. I.; Ha, J.; Kang, B. T.; Kim, J. W.; Quan, F. S.; Lee, J. H.; Woo, E. J.; Park, H. M. *J. Neurol. Sci.* **2009**, *285*, 67.
- (25) Hayase, M.; Kitada, M.; Wakao, S.; Itokazu, Y.; Nozaki, K.; Hashimoto, N.; Takagi, Y.; Dezawa, M. *J. Cereb. Blood Flow Metab.* **2009**, *29*, 1409.
- (26) Roobrouk, V. D.; Ulloa-Montoya, F.; Verfaillie, C. M. *Exp. Cell Res.* **2008**, *314*, 1937.
- (27) Jing, X.; Yang, L.; Duan, X.; Xie, B.; Chen, W.; Li, Z.; Tan, H. *Jt. Bone, Spine* **2008**, *75*, 432.
- (28) Delcroix, G. J.-R.; Jacquart, M.; Lemaire, L.; Sindji, L.; Franconi, F.; Le Jeune, J.-J.; Montero-Menei, C. N. *Brain Res.* **2009**, *1255*, 18.
- (29) Jendelova, P.; Herynek, V.; Urdzkova, L.; Glogarova, K.; Kroupova, J.; Andersson, B.; Bryja, V.; Burian, M.; Hajek, M.; Sykova, E. *J. Neurosci. Res.* **2004**, *76*, 232.
- (30) Kopen, G. C.; Prockop, D. J.; Phinney, D. G. *Proc. Natl. Acad. Sci. U. S. A.* **1999**, *96*, 10711.
- (31) Zhao, L. R.; Duan, W. M.; Reyes, M.; Keene, C. D.; Verfaillie, C. M.; Low, W. C. *Exp. Neurol.* **2002**, *174*, 11.
- (32) Chen, X.; Li, Y.; Wang, L.; Katakowski, M.; Zhang, L.; Chen, J.; Xu, Y.; Gautam, S. C.; Chopp, M. *Neuropathology* **2002**, *22*, 275.
- (33) Zhang, J.; Li, Y.; Chen, J.; Cui, Y.; Lu, M.; Elias, S. B.; Mitchell, J. B.; Hammill, L.; Vanguri, P.; Chopp, M. *Exp. Neurol.* **2005**, *195*, 16.
- (34) Troyer, D. L.; Weiss, M. L. *Stem Cells Dev.* **2008**, *26*, 591.
- (35) Hu, S.-L.; Zhang, J.-Q.; Hu, X.; Hu, R.; Luo, H.-S.; Li, F.; Xia, Y.-Z.; Li, J.-T.; Lin, J.-K.; Zhu, G.; Feng, H. *J. Cell. Biochem.* **2009**, *108*, 529.
- (36) Conti, L.; Pollard, S. M.; Gorba, T.; Reitano, E.; Toselli, M.; Biella, G.; Sun, Y.; Sanzone, S.; Ying, Q. L.; Cattaneo, E.; Smith, A. *PLoS Biol.* **2005**, *3*, 1594.
- (37) Shin, S.; Mitalipova, M.; Noggle, S.; Tibbitts, D.; Venable, A.; Rao, R.; Stice, S. L. *Stem Cells* **2006**, *24*, 125.
- (38) Reynolds, B. A.; Weiss, S. *Science* **1992**, *255*, 1707.
- (39) Park, K. I.; Ourednik, J.; Ourednik, V.; Taylor, R. M.; Aboody, K. S.; Augustine, K. I.; Lachyankar, M. B.; Redmond, D. E.; Snyder, E. Y. *Gene Ther.* **2002**, *9*, 613.
- (40) Ben-Hur, T.; Bulte, J. W. *Proc. Int. Soc. Magn. Reson. Med.* **2004**, *12*, 159.
- (41) Pluchino, S.; Zanotti, L.; Rossi, B.; Brambilla, E.; Ottoboni, L.; Salani, G.; Martinello, M.; Cattalini, A.; Bergami, A.; Furlan, R.; Comi, G.; Constantin, G.; Martino, G. *Nature* **2005**, *436*, 266.
- (42) Kawabata, K.; Migita, M.; Mochizuki, H.; Miyake, K.; Igarashi, T.; Fukunaga, Y.; Shimada, T. *Brain Res.* **2006**, *1094*, 13.
- (43) Teng, Y. D.; Lavik, E. B.; Qu, X.; Park, K. I.; Ourednik, J.; Zurakowski, D.; Langer, R.; Snyder, E. Y. *Proc. Natl. Acad. Sci. U. S. A.* **2002**, *99*, 3024.
- (44) Rafuse, V. F.; Soundararajan, P.; Leopold, C.; Robertson, H. A. *Neuroscience* **2005**, *131*, 899.
- (45) McBride, J. L.; Behrstock, S. P.; Chen, E. Y.; Jakel, R. J.; Siegel, I.; Svendsen, C. N.; Kordower, J. H. *J. Comp. Neurol.* **2004**, *475*, 211.
- (46) Clarke, D. L.; Johansson, C. B.; Wilbertz, J.; Veress, B.; Nilsson, E.; Karlström, H.; Lendahl, U.; Frisén, J. *Science* **2000**, *288*, 1660.
- (47) Kim, J. B.; Greber, B.; Arauzo-Bravo, M. J.; Meyer, J.; Park, K. I.; Zaehres, H.; Schöler, H. R. *Nature* **2009**, *461*, 649.
- (48) Kim, J. B.; Sebastiano, V.; Wu, G.; Arauzo-Bravo, M. J.; Sasse, P.; Gentile, L.; Ko, K.; Ruau, D.; Ehrlich, M.; van den Boom, D.; Meyer, J.; Hübner, K.; Bernemann, C.; Ortmeier, C.; Zenke, M.; Fleischmann, B. K.; Zaehres, H.; Schöler, H. R. *Cell* **2009**, *136*, 411.
- (49) Kim, J. B.; Zaehres, H.; Wu, G.; Gentile, L.; Ko, K.; Sebastiano, V.; Arauzo-Bravo, M. J.; Ruau, D.; Han, D. W.; Zenke, M.; Schöler, H. R. *Nature* **2008**, *454*, 646.
- (50) Iniewski, K. *Medical Imaging*; John Wiley & Sons: Hoboken, NJ, 2009.
- (51) Cho, Z. H.; Jones, J. P.; Singh, M. *Foundations of Medical Imaging*; John Wiley & Sons: New York, 1993.
- (52) Krestel, E. *Imaging Systems for Medical Diagnostics*; Siemens Aktiengesellschaft: Berlin, 1990.
- (53) Cherry, S. R.; Sorenson, J. A.; Phelps, M. E. *Physics in Nuclear Medicine*; Elsevier Science: Philadelphia, 2003.
- (54) Wernick, M. N.; Aarsvold, J. N. *Emission Tomography, The Fundamentals of PET and SPECT*; Elsevier, Academic Press: Amsterdam, Boston, 2004.
- (55) Tsien, R. Y. *Nat. Rev. Mol. Cell Biol.* **2003**, *4*, SS16.
- (56) Piwnica-Worms, D. R. *J. Am. Col. Radiol.* **2004**, *1*, 2.
- (57) Schroeder, T. *Nature* **2008**, *453*, 345.
- (58) Leach, M. O. *NMR Biomed.* **2009**, *22*, 17.
- (59) Sinha, S.; Sinha, U. *NMR Biomed.* **2009**, *22*, 3.
- (60) Logothetis, N. K. *Nature* **2008**, *453*, 869.
- (61) Duong, T. Q.; Pardue, M. T.; Thulé, P. M.; Olson, D. E.; Cheng, H.; Nair, G.; Li, Y.; Kim, M.; Zhang, X.; Shen, Q. *NMR Biomed.* **2008**, *21*, 978.
- (62) Ogawa, S.; Lee, T. M.; Kay, A. R.; Tank, D. W. *Proc. Natl. Acad. Sci. U. S. A.* **1990**, *87*, 9868.
- (63) Lauterbur, P. C. *Nature* **1973**, *242*, 190.
- (64) Lauterbur, P. C. *Clin. Orthop. Relat. Res.* **1989**, *3*.
- (65) Nelson, F.; Poonawalla, A.; Hou, P.; Wolinsky, J. S.; Narayana, P. A. *Mult. Scler.* **2008**, *14*, 1214.
- (66) Le Bihan, D. *Magn. Reson. Med.* **1988**, *7*, 346.
- (67) Le Bihan, D. *Radiology* **2008**, *249*, 748.
- (68) Le Bihan, D.; Breton, E.; Lallemand, D. *Radiology* **1986**, *161*, 401.
- (69) Le Bihan, D.; Breton, E.; Lallemand, D.; Aubin, M. L.; Vignaud, J.; Laval-Jeantet, M. *Radiology* **1988**, *168*, 497.
- (70) Le Bihan, D.; Turner, R. *Magn. Reson. Med.* **1992**, *27*, 171.
- (71) Turner, R.; Le Bihan, D.; Maier, J.; Vavrek, R.; Hedges, L. K.; Pekar, J. *Radiology* **1990**, *177*, 407.
- (72) Gerlach, W.; Stern, O. *Z Phys.* **1921**, *8*, 110.
- (73) Rabi, I. I.; Zacharias, J. R.; Millman, S.; Kusch, P. *Phys. Rev.* **1938**, *53*, 318.
- (74) Purcell, E. M.; Torrey, H. C.; Pound, R. V. *Phys. Rev.* **1946**, *69*, 37.
- (75) Bloch, F.; Hansen, W. W.; Packard, M. *Phys. Rev.* **1946**, *69*, 127.
- (76) Damadian, R. *Science* **1971**, *171*, 1151.
- (77) Mansfield, P. *J. Phys. C: Solid State Phys.* **1977**, *10*, L55.
- (78) Mansfield, P.; Grannell, P. K. *J. Phys. C: Solid State Phys.* **1973**, *6*, L422.
- (79) Josephson, L.; Kircher, M. F.; Mahmood, U.; Tang, Y.; Weissleder, R. *Bioconjugate Chem.* **2002**, *13*, 554.
- (80) Askenasy, N.; Farkas, D. L. *Stem Cells* **2002**, *20*, 501.
- (81) Modo, M.; Hoehn, M.; Bulte, J. W. M. *Mol. Imaging* **2005**, *4*, 143.
- (82) Tearney, G. J.; Brezinski, M. E.; Boppart, S. A.; Bouma, B. E.; Weissman, N.; Southern, J. F.; Swanson, E. A.; Fujimoto, J. G. *Circulation* **1996**, *94*, 3013.
- (83) Tearney, G. J.; Brezinski, M. E.; Boppart, S. A.; Bouma, B. E.; Weissman, N.; Southern, J. F.; Swanson, E. A.; Fujimoto, J. G. *Circulation* **1996**, *94*, 3013.
- (84) Gellermann, J.; Faehling, H.; Mielec, M.; Cho, C. H.; Budach, V.; Wust, P. *Int. J. Hyperthermia* **2008**, *24*, 327.
- (85) Wyatt, C.; Soher, B.; MacCarini, P.; Charles, H. C.; Stauffer, P.; MacFall, J. *Int. J. Hyperthermia* **2009**, *25*, 422.
- (86) Chapon, C.; Jackson, J. S.; Aboagye, E. O.; Herlihy, A. H.; Jones, W. A.; Bhakoo, K. K. *Mol. Imaging Biol.* **2009**, *11*, 31.
- (87) Loebinger, M. R.; Kyrtatos, P. G.; Turmaine, M.; Price, A. N.; Pankhurst, Q.; Lythgoe, M. F.; Janes, S. M. *Cancer Res.* **2009**, *69*, 8862.
- (88) Thu, M. S.; Najbauer, J.; Kendall, S. E.; Harutyunyan, I.; Sangalang, N.; Gutova, M.; Metz, M. Z.; Garcia, E.; Frank, R. T.; Kim, S. U.; Moats, R. A.; Aboody, K. S. *PLoS One* **2009**, *4*.
- (89) Jiang, Y.; Chen, L.; Tang, Y.; Ma, G.; Shen, C.; Qi, C.; Zhu, Q.; Yao, Y.; Liu, N. *Basic Res. Cardiol.* **2009**, *1*.
- (90) Klose, A. D.; Beattie, B. J.; Dehghani, H.; Vider, L.; Le, C.; Ponomarev, V.; Blasberg, R. *Med. Phys.* **2010**, *37*, 329.
- (91) Wang, K.; Shen, B.; Huang, T.; Sun, X.; Li, W.; Jin, G.; Li, L.; Bu, L.; Li, R.; Wang, D.; Chen, X. *Mol. Imaging Biol.* **2009**, *12*, 520–529.
- (92) Hermus, L.; van Dam, G. M.; Zeebregts, C. J. *Eur. J. Vasc. Endovasc.* **2009**, *39* (2), 125.
- (93) Minowa, T.; Kawano, K.; Kuribayashi, H.; Shiraishi, K.; Sugino, T.; Hattori, Y.; Yokoyama, M.; Maitani, Y. *Br. J. Cancer* **2009**, *101*, 1884.
- (94) Murukesh, N.; Dive, C.; Jayson, G. C. *Br. J. Cancer* **2009**, *102*, 8.
- (95) Zhou, Y.; Wang, S.; Yu, Z.; Hoyt, R. F., Jr.; Sachdev, V.; Vincent, P.; Arai, A. E.; Kwak, M.; Burkett, S. S.; Horvath, K. A. *Biophys. Res. Commun.* **2009**, *390*, 902.
- (96) Bartusik, D.; Tomanek, B. *J. Pharm. Biomed. Anal.* **2010**, *51*, 894.

- (97) Giesel, F. L.; Mehndiratta, A.; Locklin, J.; McAuliffe, M. J.; White, S.; Choyke, P. L.; Knopp, M. V.; Wood, B. J.; Haberkorn, U.; Von Tengg-Kobligh, H. *Exp. Oncol.* **2009**, *31*, 106.
- (98) Tsai, C. S.; Lai, C. H.; Chang, T. C.; Yen, T. C.; Ng, K. K.; Hsueh, S.; Lee, S. P.; Hong, J. H. *Int. J. Radiat. Oncol., Biol., Phys.* **2009**, *76*, 477.
- (99) Lodygensky, G. A.; West, T.; Stump, M.; Holtzman, D. M.; Inder, T. E.; Neil, J. *J. Brain, Behav., Immun.* **2009**, *24* (5), 759.
- (100) Yadav, A.; Chaudhary, C.; Keshavan, A. H.; Agarwal, A.; Verma, S.; Prasad, K. N.; Rathore, R. K. S.; Trivedi, R.; Gupta, R. K. *Acad. Radiol.* **2010**, *17*, 194.
- (101) Yang, Y.; Yanasak, N.; Schumacher, A.; Hu, T. C. C. *Magn. Reson. Med.* **2010**, *63*, 33.
- (102) Blankenberg, F. G. *Anti-Cancer Agents Med. Chem.* **2009**, *9*, 944.
- (103) Burtea, C.; Laurent, S.; Lancelot, E.; Ballet, S.; Murariu, O.; Rousseaux, O.; Port, M.; Vander Elst, L.; Corot, C.; Muller, R. N. *Mol. Pharmaceutics* **2009**, *6*, 1903.
- (104) Sosnovik, D. E.; Garanger, E.; Aikawa, E.; Nahrendorf, M.; Figueiredo, J. L.; Dai, G.; Reynolds, F.; Rosenzweig, A.; Weissleder, R.; Josephson, L. *Circ. Cardiovasc. Imaging* **2009**, *2*, 460.
- (105) Hayashi, K.; Mani, V.; Nemade, A.; Silvera, S.; Fayad, Z. A. *Int. J. Cardiovasc. Imaging* **2010**, *26* (3), 309.
- (106) Volcik, K. A.; Campbell, S.; Chambless, L. E.; Coresh, J.; Folsom, A. R.; Mosley, T. H.; Ni, H.; Wagenknecht, L. E.; Wasserman, B. A.; Boerwinkle, E. *Atherosclerosis* **2010**, *210* (1), 188.
- (107) Solomon, I. *Phys. Rev.* **1995**, *99*, 559.
- (108) Igarashi, J.; Murayama, K.; Fulde, P. *Phys. Rev. B: Condens. Matter Mater. Phys.* **1995**, *52*, 15966.
- (109) Bloembergen, N. *J. Chem. Phys.* **1957**, *27*, 572.
- (110) Nolle, A. W.; Morgan, L. O. *J. Chem. Phys.* **1957**, *26*, 642.
- (111) Albrand, J. P.; Taieb, M. C.; Fries, P. H.; Belorizky, E. *J. Chem. Phys.* **1983**, *78*, 5809.
- (112) Freed, J. H. *J. Chem. Phys.* **1978**, *68*, 4034.
- (113) Hwang, L. P.; Freed, J. H. *J. Chem. Phys.* **1975**, *63*, 4017.
- (114) Harris, R. K.; Wasylshen, R. *Encyclopedia of Magnetic Resonance*; John Wiley: Chichester, 2009.
- (115) Laurent, S.; Forge, D.; Port, M.; Roch, A.; Robic, C.; Vander Elst, L.; Muller, R. N. *Chem. Rev.* **2008**, *108*, 2064.
- (116) Roch, A.; Gossuin, Y.; Muller, R. N.; Gillis, P. *J. Magn. Magn. Mater.* **2005**, *293*, 532.
- (117) Roch, A.; Muller, R. N.; Gillis, P. *J. Magn. Magn. Mater.* **2001**, *14*, 94.
- (118) Roch, A.; Gillis, P.; Ouakssim, A.; Muller, R. N. *J. Magn. Magn. Mater.* **1999**, *201*, 77.
- (119) Rinck, P. A.; Jones, R. A.; Kvaerness, J.; Southon, T. E.; De Francisco, P.; Muller, R. N.; Petersen, S. B. *Magnetic Resonance in Medicine*; Blackwell Scientific Publications: Oxford, 1993.
- (120) Artemov, D. *J. Cell. Biochem.* **2003**, *90*, 518.
- (121) Weinmann, H. J.; Ebert, W.; Misselwitz, B.; Schmitt-Willich, H. *Eur. J. Radiol.* **2003**, *46*, 33.
- (122) Wang, Y. X. J.; Hussain, S. M.; Krestin, G. P. *Eur. Radiol.* **2001**, *11*, 2319.
- (123) Bulte, J. W. M.; Zhang, S. C.; Van Gelderen, P.; Herynek, V.; Jordan, E. K.; Duncan, I. D.; Frank, J. A. *Proc. Natl. Acad. Sci. U. S. A.* **1999**, *96*, 15256.
- (124) Bulte, J. W. M.; Hoekstra, Y.; Kamman, R. L.; Magin, R. L.; Webb, A. G.; Briggs, R. W.; Go, K. G.; Hulstaert, C. E.; Miltenyi, S.; The, T. H.; De Leij, L. *Magn. Reson. Med.* **1992**, *25*, 148.
- (125) Artemov, D.; Mori, N.; Okollie, B.; Bhujwalla, Z. M. *Magn. Reson. Med.* **2003**, *49*, 403.
- (126) Jiang, H.; Williams, G. J.; Dhib-Jalbut, S. *Neurochem. Int.* **1997**, *30*, 449.
- (127) Won Kang, H.; Josephson, L.; Petrovsky, A.; Weissleder, R.; Bogdanov Jr, A. *Bioconjugate Chem.* **2002**, *13*, 122.
- (128) Zhao, M.; Beauregard, D. A.; Loizou, L.; Davletov, B.; Brindle, K. M. *Nat. Med.* **2001**, *7*, 1241.
- (129) Boutry, S.; Laurent, S.; Vander Elst, L.; Muller, R. N. *Contrast Media Mol. Imaging* **2006**, *1*, 15.
- (130) Radermacher, K. A.; Beghein, N.; Boutry, S.; Laurent, S.; Vander Elst, L.; Muller, R. N.; Jordan, B. F.; Gallez, B. *Invest. Radiol.* **2009**, *44*, 398.
- (131) Artemov, D.; Bhujwalla, Z. M.; Bulte, J. W. M. *Current Pharm. Biotechnol.* **2004**, *5*, 485.
- (132) Choi, H.; Choi, S. R.; Zhou, R.; Kung, H. F.; Chen, I. W. *Acad. Radiol.* **2004**, *11*, 996.
- (133) Reimer, P. *Radiology* **2004**, *231*, 1.
- (134) Choi, H.; Choi, S. R.; Zhou, R.; Kung, H. F.; Chen, I. W. *Acta Radiol.* **2004**, *11*, 996.
- (135) Remsen, L. G.; McCormick, C. I.; Roman-Goldstein, S.; Nilaver, G.; Weissleder, R.; Bogdanov, A.; Hellstrom, K. E.; Hellstrom, I.; Kroll, R. A.; Neuwelt, E. A. *Am. J. Neuroradiol.* **1996**, *17*, 411.
- (136) Oyewumi, M. O.; Yokel, R. A.; Jay, M.; Coakley, T.; Mumper, R. J. *J. Controlled Release* **2004**, *95*, 613.
- (137) Chertok, B.; Moffat, B. A.; David, A. E.; Yu, F. Q.; Bergemann, C.; Ross, B. D.; Yang, V. C. *Biomaterials* **2008**, *29*, 487.
- (138) Lubbe, A. S.; Alexiou, C.; Bergemann, C. *J. Surg. Res.* **2001**, *95*, 200.
- (139) Lubbe, A. S.; Bergemann, C.; Brock, J.; McClure, D. G. *J. Magn. Magn. Mater.* **1999**, *194*, 149.
- (140) Thierry, B.; Al-Ejeh, F.; Brown, M. P.; Majewski, P.; Griesser, H. J. *Adv. Mater.* **2009**, *21*, 541.
- (141) Mahmoudi, M.; Milani, A. S.; Stroeve, P. *Int. J. Biomed. Nanosci. Nanotechnol.* **2010**, *1*, 164.
- (142) Mahmoudi, M.; Sant, S.; Wang, B.; Laurent, S.; Sen, T. *Adv. Drug Delivery Rev.* **2010**, in press, doi: 10.1016/j.addr.2010.05.006.
- (143) Mahmoudi, M.; Simchi, A.; Imani, M. *J. Phys. Chem. C* **2009**, *113*, 9573.
- (144) Mahmoudi, M.; Simchi, A.; Imani, M.; Milani, A. S.; Stroeve, P. *J. Phys. Chem. B* **2008**, *112*, 14470.
- (145) Mahmoudi, M.; Simchi, A.; Milani, A. S.; Stroeve, P. *J. Colloidal Interface Sci.* **2009**, *336*, 510.
- (146) Hosseinkhani, H.; Hosseinkhani, M.; Vasheghani, E.; Nekoomanesh, M. *Adv. Sci. Lett.* **2009**, *2*, 70.
- (147) Emami, S. H.; Orang, F.; Mahmoudi, M.; Rafienia, M. *Polym. Adv. Technol.* **2008**, *19*, 167.
- (148) Hosseinkhani, H.; Aoyama, T.; Ogawa, O.; Tabata, Y. *J. Controlled Release* **2002**, *83*, 287.
- (149) Konishi, M.; Tabata, Y.; Kariya, M.; Hosseinkhani, H.; Suzuki, A.; Fukuhara, K.; Mandai, M.; Takakura, K.; Fujii, S. *J. Controlled Release* **2005**, *103*, 7.
- (150) Hosseinkhani, H.; Tabata, Y. *J. Controlled Release* **2005**, *108*, 540.
- (151) Hosseinkhani, H.; Tabata, Y. *J. Controlled Release* **2004**, *97*, 157.
- (152) Hosseinkhani, H.; Tabata, Y. *J. Controlled Release* **2003**, *86*, 169.
- (153) Subramani, K.; Hosseinkhani, H.; Khraisat, A.; Hosseinkhani, M.; Pathak, Y. *Curr. Nanosci.* **2009**, *5*, 134.
- (154) Aoyama, T.; Hosseinkhani, H.; Yamamoto, S.; Ogawa, O.; Tabata, Y. *J. Controlled Release* **2002**, *80*, 345.
- (155) Hosseinkhani, H.; Hosseinkhani, M. *Curr. Drug Safety* **2009**, *4*, 79.
- (156) Hosseinkhani, H.; Hosseinkhani, M.; Khademhosseini, A.; Gabrielson, N. P.; Pack, D. W.; Kobayashi, H. *J. Biomed. Mater. Res., Part A* **2008**, *85*, 47.
- (157) Hosseinkhani, H. *Int. J. Nanotechnol.* **2006**, *3*, 416.
- (158) Hosseinkhani, H.; Tabata, Y. *J. Nanosci. Nanotechnol.* **2006**, *6*, 2320.
- (159) Hosseinkhani, H.; Kushibiki, T.; Matsumoto, K.; Nakamura, T.; Tabata, Y. *Cancer Gene Ther.* **2006**, *13*, 479.
- (160) Hosseinkhani, H.; Azzam, T.; Tabata, Y.; Domb, A. *J. Gene Ther.* **2004**, *11*, 194.
- (161) Hosseinkhani, H.; Aoyama, T.; Ogawa, O.; Tabata, Y. *Proc. Japan Acad. Ser. B* **2001**, *77*, 161.
- (162) Hosseinkhani, H.; Aoyama, T.; Ogawa, O.; Tabata, Y. *Pharm. Res.* **2002**, *19*, 1469.
- (163) Hosseinkhani, H.; Aoyama, T.; Ogawa, O.; Tabata, Y. *J. Drug Targeting* **2002**, *10*, 193.
- (164) Kim, Y. S.; Shin, I. G.; Lee, Y. M. *J. Controlled Release* **1998**, *56*, 197.
- (165) Wallace, D. G.; Rosenblatt, J. *Adv. Drug Delivery Rev.* **2003**, *55*, 1631.
- (166) Vollath, D. D.; Szabo, V.; Haubelt, J. *J. Eur. Ceram. Soc.* **1997**, *17*, 1317.
- (167) Jones, M. C.; Leroux, J. C. *Eur. J. Pharm. Biopharm.* **1999**, *48*, 101.
- (168) Imrie, C. T.; Henderson, P. A. *Chem. Soc. Rev.* **2007**, *36*, 2096.
- (169) Tomalia, D. A.; Baker, H.; Dewald, G. R.; Hall, M.; Kallos, G.; Martin, S.; Roeck, J.; Ryder, J.; Smith, P. *Polym. J.* **1985**, *17*, 117.
- (170) Weissmann, G.; Troll, W.; Van Duuren, B. L.; Sessa, G. *Biochem. Pharmacol.* **1968**, *17*, 2421.
- (171) Ferreira, L.; Karp, J. M.; Nobre, L.; Langer, R. *Cell Stem Cell* **2008**, *3*, 136.
- (172) Ferreira, L. *J. Cell Biochem.* **2009**, *108*, 746.
- (173) Chithrani, B. D.; Ghazani, A. A.; Chan, W. C. W. *Nano Lett.* **2006**, *6*, 662.
- (174) Chithrani, B. D.; Chan, W. C. W. *Nano Lett.* **2007**, *7*, 1542.
- (175) Green, S. E.; Ropp, P. A.; Pohlhaus, P. D.; Luft, J. C.; Madden, V. J.; Napier, M. E.; DeSimone, J. M. *Proc. Natl. Acad. Sci. U. S. A.* **2008**, *105*, 11613.
- (176) Frank, J. A.; Anderson, S. A.; Kalsih, H.; Jordan, E. K.; Lewis, B. K.; Yocum, G. T.; Arbab, A. S. *Cytotherapy* **2004**, *6*, 621.
- (177) Bulte, J. W.; Kraitchman, D. L.; Mackay, A. M.; Pittenger, M. F. *Blood* **2004**, *104*, 3410.
- (178) Derfus, A. M.; Chan, W. C. W.; Bhatia, S. N. *Nano Lett.* **2004**, *4*, 11.
- (179) Mahmoudi, M.; Shokrgozar, M. A.; Simchi, A.; Imani, M.; Milani, A. S.; Stroeve, P.; Vali, H.; Hafeli, U. O.; Bonakdar, S. *J. Phys. Chem. C* **2009**, *113*, 2322.
- (180) Mahmoudi, M.; Simchi, A.; Imani, M.; Hafeli, U. O. *J. Phys. Chem. C* **2009**, *113*, 8124.



- (181) Hoseini, H. A.; Debnath, S.; Liu, G.; Strongin, D. R. *Biomol. Catal.* **2008**, *8*, 144.
- (182) Kas, R.; Sevinc, E.; Topal, U.; Acar, H. Y. *J. Phys. Chem. C* **2010**, *114*, 7758.
- (183) Mahmoudi, M.; Simchi, A.; Vali, H.; Imani, M.; Shokrgozar, M. A.; Azadmanesh, K.; Azari, F. *Adv. Eng. Mater.* **2009**, *11*, B243.
- (184) Mahmoudi, M.; Simchi, A.; Imani, M.; Stroeve, P.; Sohrabi, A. *Thin Solid Films* **2010**, *118*, 4281.
- (185) Rejman, J.; Oberle, V.; Zuhorn, I. S.; Hoekstra, D. *Biochem. J.* **2004**, *377*, 159.
- (186) Atanasijevic, T.; Shusteff, M.; Fam, P.; Jasanoff, A. *Proc. Natl. Acad. Sci. U. S. A.* **2006**, *103*, 14707.
- (187) Babes, L.; Denizot, B.; Tanguy, G.; Le Jeune, J. J.; Jallet, P. *J. Colloid Interface Sci.* **1999**, *212*, 474.
- (188) Bertin, A.; Steibel, J.; Michou-Gallani, A. I.; Gallani, J. L.; Felder-Flesch, D. *Bioconjugate Chem.* **2009**, *20*, 760–767.
- (189) Chen, T.-J.; Cheng, T.-H.; Chen, C.-Y.; Hsu, S. C. N.; Cheng, T.-L.; Liu, G.-C.; Wang, Y.-M. *J. Biol. Inorg. Chem.* **2009**, *14*, 253.
- (190) Gao, J. H.; Liang, G. L.; Cheung, J. S.; Pan, Y.; Kuang, Y.; Zhao, F.; Zhang, B.; Zhang, X. X.; Wu, E. X.; Xu, B. *J. Am. Chem. Soc.* **2008**, *130*, 11828.
- (191) Kim, E. H.; Lee, H. S.; Kwak, B. K.; Kim, B. K. *Proceedings of the 10th International Conference on Magnetic Fluids*; Guaraja, Brazil, 2004; p 328.
- (192) Koenig, S. H.; Kellar, K. E.; Fujii, D. K.; Gunther, W. H. H.; Briley-Saebo, K.; Spiller, M. *Contrast Media Research Meeting (CMR99)*, Woodstock, Vermont, 1999; p S50.
- (193) Morales, M. P.; Bomati-Miguel, O.; Perez de Alejo, R.; Ruiz-Cabello, J.; Veintemillas-Verdaguer, S.; O'Grady, K. *J. Magn. Magn. Mater.* **2003**, *266*, 102.
- (194) Nitin, N.; LaConte, L. E. W.; Zurkiya, O.; Hu, X.; Bao, G. *J. Biol. Inorg. Chem.* **2004**, *9*, 706.
- (195) Petoral, R. M.; Soderlind, F.; Klasson, A.; Suska, A.; Fortin, M. A.; Abrikosova, N.; Selegard, L.; Kall, P. O.; Engstrom, M.; Uvdal, K. *J. Phys. Chem. C* **2009**, *113*, 6913.
- (196) Stefania, R.; Tei, L.; Barge, A.; Crich, S. G.; Szabo, I.; Cabella, C.; Cravotto, G.; Aime, S. *Chem.-Eur. J.* **2009**, *15*, 76.
- (197) Tanaka, K.; Kitamura, N.; Morita, M.; Inubushi, T.; Chujo, Y. *Bioorg. Med. Chem. Lett.* **2008**, *18*, 5463.
- (198) Moroz, P.; Jones, S. K.; Gray, B. N. *Int. J. Hyperthermia* **2002**, *18*, 267.
- (199) Gonzales-Weimuller, M.; Zeisberger, M.; Krishnan, K. M. *J. Magn. Magn. Mater.* **2009**, *321*, 4.
- (200) Gazeau, F.; Levy, M.; Wilhelm, C. *Nanomedicine* **2008**, *3*, 14.
- (201) Nel, A. E.; Madler, L.; Velegol, D.; Xia, T.; Hoek, E. M. V.; Somasundaran, P.; Klaessig, F.; Castranova, V.; Thompson, M. *Nat. Mater.* **2009**, *8*, 543.
- (202) Decuzzi, P.; Ferrari, M. *Biomaterials* **2007**, *28*, 2915.
- (203) Gao, H.; Shi, W.; Freund, L. B. *Proc. Natl. Acad. Sci. U. S. A.* **2005**, *102*, 9469.
- (204) Gratton, S. E. A.; Ropp, P. A.; Pohlhaus, P. D.; Luft, J. C.; Madden, V. J.; Napier, M. E.; DeSimone, J. M. *Proc. Natl. Acad. Sci. U. S. A.* **2008**, *105*, 11613.
- (205) Lundmark, R.; Carlsson, S. R. *Semin. Cell Dev. Biol.* **2010**, *21* (4), 363.
- (206) Bosch, B.; Grigorov, B.; Senserrich, J.; Clotet, B.; Darlix, J. L.; Muriaux, D.; Este, J. A. *Antiviral Res.* **2008**, *80*, 185.
- (207) Trapani, J. A.; Sutton, V. R.; Thia, K. Y. T.; Li, Y. Q.; Froelich, C. J.; Jans, D. A.; Sandrin, M. S.; Browne, K. A. *J. Cell Biol.* **2003**, *160*, 223.
- (208) Singh, R. D.; Puri, V.; Valiyaveetil, J. T.; Marks, D. L.; Bittman, R.; Pagano, R. E. *Mol. Biol. Cell* **2003**, *14*, 3254.
- (209) Glebov, O. O.; Bright, N. A.; Nichols, B. J. *Nat. Cell Biol.* **2006**, *8*, 46.
- (210) Doherty, G. J.; Lundmark, R. *Biochem. Soc. Trans.* **2009**, *37*, 1061.
- (211) Gillingham, A. K.; Munro, S. *Annu. Rev. Cell Dev. Biol.* **2007**, *23*, 579.
- (212) Girao, H.; Geli, M. I.; Idrissi, F. Z. *FEBS Lett.* **2008**, *582*, 2112.
- (213) Kasai, K.; Shin, H. W.; Shinotsuka, C.; Murakami, K.; Nakayama, K. *J. Biochem.* **1999**, *125*, 780.
- (214) Jongen, N.; Donnet, M.; Bowen, P.; Lemaître, J.; Hofmann, H.; Schenk, R.; Hofmann, C.; Aoun-Habbache, M.; Guillemet-Fritsch, S.; Sarrias, J.; Rousset, A.; Viviani, M.; Buscaglia, M. T.; Buscaglia, V.; Nanni, P.; Testino, A.; Herguicela, R. *Chem. Eng. Technol.* **2003**, *26*, 304.
- (215) Donnet, M.; Jongen, N.; Lemaître, J.; Bowen, P. *J. Mater. Sci. Lett.* **2000**, *19*, 749.
- (216) Jongen, N.; Lemaître, J.; Bowen, P.; Hofmann, H. *Chem. Mater.* **1999**, *11*, 712.
- (217) Wang, L.; Muhammed, M. *J. Mater. Chem.* **1999**, *9*, 2871.
- (218) Ruzicka, J.; Hansen, E. H. *Talanta* **1982**, *29*, 157.
- (219) Harries, N.; Burns, J. R.; Barrow, D. A.; Ramshaw, C. *Int. J. Heat Mass Transfer* **2003**, *46*, 3313.
- (220) Cabanas, M. V.; Valletregi, M.; Labeau, M.; Gonzalezcalbet, J. M. *J. Mater. Res.* **1993**, *8*, 2694.
- (221) Kodas, T. T. *Aerosol Processing of Materials*; Wiley-VCH: New York, 1999.
- (222) Ude, S.; Fernandez De La Mora, J.; Alexander Iv, J. N.; Saucy, D. A. *J. Colloid Interface Sci.* **2006**, *293*, 384.
- (223) Kim, J. H.; Germer, T. A.; Mulholland, G. W.; Ehrman, S. H. *Adv. Mater.* **2002**, *14*, 518.
- (224) Dahl, J. K.; Weimer, A. W.; Lewandowski, A.; Bingham, C.; Bruetsch, F.; Steinfeld, A. *Ind. Eng. Chem. Res.* **2004**, *43*, 5489.
- (225) Prin, E. M.; Glikin, M. A.; Kutakova, D. A.; Kauffeldt, T. *J. Aerosol Sci.* **1998**, *29*.
- (226) Shafranovsky, E. A.; Petrov, Y. I. *J. Nanopart. Res.* **2004**, *6*, 71.
- (227) Shinde, S. R.; Banpurkar, A. G.; Adhi, K. P.; Limaye, A. V.; Ogale, S. B.; Date, S. K.; Mareest, G. *Mod. Phys. Lett. B* **1996**, *10*, 1517.
- (228) Usui, H.; Shimizu, Y.; Sasaki, T.; Koshizaki, N. *J. Phys. Chem. B* **2005**, *109*, 120.
- (229) Mafune, F.; Kohno, J. Y.; Takeda, Y.; Kondow, T. *J. Am. Chem. Soc.* **2003**, *125*, 1686.
- (230) Wang, Z.; Liu, Y.; Zeng, X. *Powder Technol.* **2006**, *161*, 65.
- (231) Sasaki, T.; Terauchi, S.; Koshizaki, N.; Umehara, H. *Appl. Surf. Sci.* **1998**, *127–129*, 398.
- (232) Cannon, W. R.; Danforth, S. C.; Flint, J. H.; Haggerty, J. S.; Marra, R. A. *J. Am. Ceram. Soc.* **1982**, *65*, 324.
- (233) Zbronec, L.; Sasaki, T.; Koshizaki, N. *Appl. Phys. A: Mater. Sci. Process.* **2004**, *79*, 1783.
- (234) Martelli, S.; Mancini, A.; Giorgi, R.; Alexandrescu, R.; Cojocaru, S.; Crunteanu, A.; Voicu, I.; Balu, M.; Morjan, I. *Appl. Surf. Sci.* **2000**, *154*, 353.
- (235) Pratsinis, S. E.; Vemury, S. *Powder Technol.* **1996**, *88*, 267.
- (236) Wang, C.; Friedlander, S. K.; Mädler, L. *China Particuol.* **2005**, *3*, 243.
- (237) Ehbrecht, M.; Kohn, B.; Huysken, F.; Laguna, M. A.; Paillard, V. *Phys. Rev. B: Condens. Matter Mater. Phys.* **1997**, *56*, 6958.
- (238) Ledoux, G.; Guillois, O.; Porterat, D.; Reynaud, C.; Huysken, F.; Kohn, B.; Paillard, V. *Phys. Rev. B: Condens. Matter Mater. Phys.* **2000**, *62*, 15942.
- (239) Huysken, F.; Ledoux, G.; Guillois, O.; Reynaud, C. *Adv. Mater.* **2002**, *14*, 1861.
- (240) Bonetti, E.; Del Bianco, L.; Signoretti, S.; Tiberto, P. *J. Appl. Phys.* **2001**, *89*, 1806.
- (241) Tan, O. K.; Cao, W.; Zhu, W. *Sens. Actuators, B* **2000**, *63*, 129.
- (242) Cao, W.; Tan, O. K.; Zhu, W.; Jiang, B. *J. Solid State Chem.* **2000**, *155*, 320.
- (243) Jiang, J. Z.; Lu, S. W.; Zhou, Y. X.; Mørup, S.; Nielsen, K.; Poulsen, F. W.; Berry, F. J.; McMannus, J. *Mater. Sci. Forum* **1997**, *235–238*, 941.
- (244) Jiang, J. Z.; Lin, R.; Lin, W.; Nielsen, K.; Mørup, S.; Dam-Johansen, K.; Clasen, R. *J. Phys. D: Appl. Phys.* **1997**, *30*, 1459.
- (245) Senna, M. *J. Appl. Phys.* **1978**, *49*, 4580.
- (246) Zdujic, M.; Jovalekic, C.; Karanovic, L.; Mitric, M.; Poleti, D.; Skala, D. *Mater. Sci. Eng., A* **1998**, *245*, 109.
- (247) Sugimoto, T.; Matijevic, E. *J. Colloid Interface Sci.* **1980**, *74*, 227.
- (248) Massart, R. *IEEE Trans. Magn.* **1981**, *17*, 1247.
- (249) Itoh, H.; Sugimoto, T. *J. Colloid Interface Sci.* **2003**, *265*, 283.
- (250) Sen, T.; Magdassi, S.; Nizri, G.; Bruce, I. J. *Micro Nano Lett.* **2006**, *1*, 39.
- (251) Inouye, K.; Endo, R.; Otsuka, Y.; Miyashiro, K.; Kaneko, K.; Ishikawa, T. *J. Phys. Chem.* **1982**, *86*, 1465.
- (252) Muller, B. W.; Muller, R. H. *J. Pharm. Sci.* **1984**, *73*, 919.
- (253) Gupta, A. K.; Wells, S. *IEEE Trans. Nanobiosci.* **2004**, *3*, 66.
- (254) Bagwe, R. P.; Kanicky, J. R.; Palla, B. J.; Patanjali, P. K.; Shah, D. O. *Crit. Rev. Ther. Drug Carrier Syst.* **2001**, *18*, 77.
- (255) Langevin, D. *Annu. Rev. Phys. Chem.* **1992**, *43*.
- (256) Dimitrova, G. T.; Tadros, T. F.; Luckham, P. F.; Kipps, M. R. *Langmuir* **1996**, *12*, 315.
- (257) Landfester, K.; Bechthold, N.; Tiarks, F.; Antonietti, M. *Macromolecules* **1999**, *32*, 2679.
- (258) Perez-Luna, V. H.; Puig, J. E.; Castano, V. M.; Rodriguez, B. E.; Murthy, A. K.; Kaler, E. W. *Langmuir* **1990**, *6*, 5.
- (259) Jayakrishnan, J.; Shah, D. O. *J. Polym. Sci., Polym. Let. Ed.* **1984**, *22*, 31.
- (260) Ferrick, M. R.; Murtagh, J.; Thomas, J. K. *Macromolecules* **1989**, *22*, 3.
- (261) Antonietti, M.; Hentze, H. P. *Adv. Mater.* **1996**, *8*, 5.
- (262) Li, T.; Moon, J.; Morrone, A. A.; Mecholsky, J. J.; Talham, D. R.; Adair, J. H. *Langmuir* **1999**, *15*, 7.
- (263) Stathatos, E.; Lianos, P.; DelMonte, F.; Levy, D.; Tsiourvas, D. *Langmuir* **1997**, *13*, 4295.
- (264) Shiojiri, S.; Hirai, T.; Komazawa, I. *Chem. Commun.* **1998**, 1439.
- (265) Shah, D. O. *Micelles, Microemulsions, and Monolayers*; Marcel Dekker Inc.: New York, 1998.



- (266) Mahmoudi, M.; Stroeve, P.; Milani, A. S.; Arbab, S. A. *Superparamagnetic Iron Oxide Nanoparticles: Synthesis, Surface Engineering, Cytotoxicity and Biomedical Applications*; Nova Science Publisher: New York, 2010.
- (267) Bujdosó, E. *J. Radioanal. Nucl. Chem.* **1998**, *231*, 207.
- (268) Lawrence, M. J.; Rees, G. D. *Adv. Drug Delivery Rev.* **2000**, *45*, 89.
- (269) Liz, L.; Quintela, M. A. L.; Mira, J.; Rivas, J. J. *Mater. Sci.* **1994**, *29*, 3797.
- (270) Lopez-Quintela, M. A. *Curr. Opin. Colloid Interface Sci.* **2003**, *8*, 137.
- (271) Munshi, N.; De, T. K.; Maitra, A. J. *Colloid Interface Sci.* **1997**, *190*, 387.
- (272) Pang, Y. X.; Bao, X. J. *J. Mater. Chem.* **2002**, *12*, 3699.
- (273) Paul, B. K.; Moulik, S. P. *Curr. Sci.* **2001**, *80*, 990.
- (274) Perez, J. A. L.; Quintela, M. A. L.; Mira, J.; Rivas, J.; Charles, S. W. *J. Phys. Chem. B* **1997**, *101*, 8045.
- (275) Santra, S.; Tapecc, R.; Theodoropoulou, N.; Dobson, J.; Hebard, A.; Tan, W. H. *Langmuir* **2001**, *17*, 2900.
- (276) Sicoli, F.; Langevin, D. VII Conference of the European-Colloid-and-Interface-Society - Trends in Colloid and Interface Science VIII, Bristol, England, 1993; p 223.
- (277) Xiang, J. H.; Yu, S. H.; Liu, B. H.; Xu, Y.; Gen, X.; Ren, L. *Inorg. Chem. Commun.* **2004**, *7*, 572.
- (278) Zhi, J.; Wang, Y. J.; Lu, Y. C.; Ma, J. Y.; Luo, G. S. *React. Funct. Polym.* **2006**, *66*, 1552.
- (279) Matsuoka, K. *Bull. Chem. Soc. Jpn.* **1971**, *44*, 719.
- (280) Kholam, Y. B.; Dhage, S. R.; Potdar, H. S.; Deshpande, S. B.; Bakare, P. P.; Kulkarni, S. D.; Date, S. K. *Mater. Lett.* **2002**, *56*, 571.
- (281) Chen, D.; Xu, R. *Mater. Res. Bull.* **1998**, *33*, 1015.
- (282) Cote, L. J.; Teja, A. S.; Wilkinson, A. P.; Zhang, Z. J. *J. Mater. Res.* **2002**, *17*, 2410.
- (283) Giri, S.; Samanta, S.; Maji, S.; Ganguli, S.; Bhaumik, A. J. *Magn. Magn. Mater.* **2005**, *285*, 296.
- (284) Mao, B. D.; Kang, Z. H.; Wang, E. B.; Lian, S. Y.; Gao, L.; Tian, C. G.; Wang, C. L. *Mater. Res. Bull.* **2006**, *41*, 2226.
- (285) Sreeja, V.; Joy, P. A. *Mater. Res. Bull.* **2007**, *42*, 1570.
- (286) Wang, J.; Sun, J. J.; Sun, Q.; Chen, Q. W. *Mater. Res. Bull.* **2003**, *38*, 1113.
- (287) Xu, C. B.; Lee, J.; Teja, A. S. *J. Supercrit. Fluids* **2008**, *44*, 92.
- (288) Zhu, H. L.; Yang, D. R.; Zhu, L. M. *Surf. Coat. Technol.* **2007**, *201*, 5870.
- (289) Burda, C.; Chen, X. B.; Narayanan, R.; El-Sayed, M. A. *Chem. Rev.* **2005**, *105*, 1025.
- (290) Teja, A. S.; Koh, P. Y. *Prog. Cryst. Growth Charact. Mater.* **2009**, *55*, 22.
- (291) Shaw, R. W.; Brill, T. B.; Clifford, A. A.; Eckert, C. A.; Franck, E. U. *Chem. Eng. News* **1991**, *69*, 26.
- (292) Hyeon, T.; Lee, S. S.; Park, J.; Chung, Y.; Bin Na, H. *J. Am. Chem. Soc.* **2001**, *123*, 12798.
- (293) Butter, K.; Kassapidou, K.; Vroege, G. J.; Philipse, A. P. *J. Colloid Interface Sci.* **2005**, *287*, 485.
- (294) Grzeta, B.; Ristic, M.; Nowik, I.; Music, S. *J. Alloys Compd.* **2002**, *334*, 304.
- (295) Yokoi, H.; Kanto, T. *Bull. Chem. Soc. Jpn.* **1993**, *66*, 1536.
- (296) Angermann, A.; Topfer, J. *J. Mater. Sci.* **2008**, *43*, 5123.
- (297) Maity, D.; Choo, S. G.; Yi, J. B.; Ding, J.; Xue, J. M. *J. Magn. Magn. Mater.* **2009**, *321*, 1256.
- (298) Maity, D.; Kale, S. N.; Kaul-Ghanekar, R.; Xue, J. M.; Ding, J. J. *Magn. Magn. Mater.* **2009**, *321*, 3093.
- (299) Park, J.; An, K. J.; Hwang, Y. S.; Park, J. G.; Noh, H. J.; Kim, J. Y.; Park, J. H.; Hwang, N. M.; Hyeon, T. *Nat. Mater.* **2004**, *3*, 891.
- (300) Tartaj, P.; Morales, M. P.; Veintemillas-Verdaguer, S.; Gonzalez-Carreno, T.; Serna, C. J. *J. Phys. D: Appl. Phys.* **2003**, *36*, 182.
- (301) Sun, S.; Zeng, H. *J. Am. Chem. Soc.* **2002**, *124*, 2.
- (302) Zhao, S.; Wu, H. Y.; Song, L.; Tegus, O.; Asuha, S. *J. Mater. Sci.* **2009**, *44*, 926.
- (303) Gupta, A. K.; Gupta, M. *Biomaterials* **2005**, *26*, 3995.
- (304) Roca, A. G.; Morales, M. P.; O'Grady, K.; Serna, C. J. *Nanotechnology* **2006**, *17*, 2783.
- (305) Roca, A. G.; Morales, M. P.; Serna, C. J. *41st IEEE International Magnetism Conference (Intermag 2006)*, San Diego, CA, 2006; p 3025.
- (306) Bronstein, L. M.; Huang, X. L.; Retrum, J.; Schmucker, A.; Pink, M.; Stein, B. D.; Dragnea, B. *Chem. Mater.* **2007**, *19*, 3624.
- (307) Jung, H.; Park, H.; Kim, J.; Lee, J. H.; Hur, H. G.; Myung, N. V.; Choi, H. *Environ. Sci. Technol.* **2007**, *41*, 4741.
- (308) Samia, A. C. S.; Hyzer, K.; Schlueter, J. A.; Qin, C. J.; Jiang, J. S.; Bader, S. D.; Lin, X. M. *J. Am. Chem. Soc.* **2005**, *127*, 4126.
- (309) Jana, N. R.; Chen, Y. F.; Peng, X. G. *Chem. Mater.* **2004**, *16*, 3931.
- (310) Duraesa, L.; Costab, B. F. O.; Vasquesa, J.; Camposc, J.; Portugal, A. *Mater. Lett.* **2005**, *59*, 859.
- (311) Roy, R. A.; Roy, R. *Mater. Res. Bull.* **1984**, *19*, 169.
- (312) Ennas, G.; Musinu, A.; Piccaluga, G.; Zedda, D.; Gatteschi, D.; Sangregorio, C.; Stanger, J. L.; Concas, G.; Spano, G. *Chem. Mater.* **1998**, *10*, 495.
- (313) Guglielmi, M.; Principi, G. *J. Non-Cryst. Solids* **1982**, *48*, 161.
- (314) Raileanu, M.; Crisan, M.; Petrache, C.; Crisan, D.; Zaharescu, M. *J. Optoelectron. Adv. Mater.* **2003**, *5*, 693.
- (315) del Monte, F.; Morales, M. P.; Levy, D.; Fernandez, A.; Ocana, M.; Roig, A.; Molins, A.; O'Grady, K.; Serna, C. J. *Langmuir* **1997**, *13*, 3627.
- (316) Niznansky, D.; Rehspringer, J. L.; Drillon, M. *IEEE Trans. Magn.* **1994**, *30*, 821.
- (317) Bentivegna, F.; Ferre, J.; Nyvlt, M.; Jamet, J. P.; Imhoff, D.; Canva, M.; Brun, A.; Veillet, P.; Visnovsky, S.; Chaput, F.; Boilot, J. P. *J. Appl. Phys.* **1998**, *83*, 7776.
- (318) Durães, L.; Costa, B. F. O.; Vasques, J.; Campos, J.; Portugal, A. *Mater. Lett.* **2005**, *59*, 859.
- (319) Tillotson, T. M.; Gash, A. E.; Simpson, R. L.; Hrubesh, L. W.; Satcher, J. H.; Poco, J. F. *J. Non-Cryst. Solids* **2001**, *285*, 338.
- (320) Gash, A. E.; Tillotson, T. M.; Satcher, J. H.; Poco, J. F.; Hrubesh, L. W.; Simpson, R. L. *Chem. Mater.* **2001**, *13*, 999.
- (321) Cai, W.; Wan, J. Q. *J. Colloid Interface Sci.* **2007**, *305*, 366.
- (322) Liu, H.-L.; Ko, S. P.; Wu, J.-H.; Jung, M. H.; Min, J. H.; Lee, J. H.; An, B. H.; Kim, Y. K. *J. Magn. Magn. Mater.* **2007**, *310*, 815.
- (323) Tzitzios, V. K.; Petridis, D.; Zafropoulou, I.; Hadjipanayis, G.; Niarchos, D. *J. Magn. Magn. Mater.* **2005**, *294*, 95.
- (324) Siyaphus, R. J.; Kodama, D.; Matsumoto, T.; Sato, Y.; Jayadevan, B.; Tohji, K. *J. Magn. Magn. Mater.* **2007**, *310*, 2393.
- (325) Fievet, F.; Lagier, J. P.; Blin, B.; Beaudoin, B.; Figlarz, M. *Solid State Ionics* **1989**, *198*, 32.
- (326) Feldmann, C.; Jungk, G.-O. *Angew. Chem., Int. Ed.* **2001**, *40*, 359.
- (327) Kitamoto, Y.; Kimura, K.; Yamazaki, Y. *Funtai Oyobi Fumatsu Yakin/ J. Jpn. Soc. Powder Powder Metall.* **2009**, *56*, 121.
- (328) Kumar, R. V.; Koltypin, Y.; Xu, X. N.; Yeshurun, Y.; Gedanken, A.; Felner, I. *J. Appl. Phys.* **2001**, *89*, 6324.
- (329) Vijayakumar, R.; Koltypin, Y.; Felner, I.; Gedanken, A. *Mater. Sci. Eng., A* **2000**, *286*, 101.
- (330) Dang, F.; Enomoto, N.; Hojo, J.; Enpuku, K. *Chem. Lett.* **2008**, *37*, 530.
- (331) Suslick, K. S.; Hammerton, D. A.; Cline Jr, R. E. *J. Am. Chem. Soc.* **1986**, *108*, 5641.
- (332) Suslick, K. S.; Flint, E. B.; Grinstaff, M. W.; Kemper, K. A. *J. Phys. Chem.* **1993**, *97*, 3098.
- (333) Suslick, K. S.; Choe, S. B.; Cichowlas, A. A.; Grinstaff, M. W. *Nature* **1991**, *353*, 414.
- (334) Suslick, K. S.; Hyeon, T.; Fang, M.; Cichowlas, A. A. *Mater. Sci. Eng., A* **1995**, *204*, 186.
- (335) Pascal, C.; Pascal, J. L.; Favier, F.; Moubtassim, M. L. E.; Payen, C. *Chem. Mater.* **1999**, *11*, 141.
- (336) Amigo, R.; Asenjo, J.; Krotenko, E.; Torres, F.; Tejada, J.; Brillas, E. *Chem. Mater.* **2000**, *12*, 573.
- (337) Penner, R. M. *Acc. Chem. Res.* **2000**, *33*, 78.
- (338) Torres, F.; Amigo, R.; Asenjo, J.; Krotenko, E.; Tejada, J.; Brillas, E. *Chem. Mater.* **2000**, *12*, 3060.
- (339) Franger, S.; Berthet, P.; Berthon, J. *J. Solid State Electrochem.* **2004**, *8*, 218.
- (340) Therese, G. H. A.; Kamath, P. V. *Chem. Mater.* **2000**, *12*, 1195–1204.
- (341) Marken, F.; Patel, D.; Madden, C. E.; Millward, R. C.; Fletcher, S. *New J. Chem.* **2002**, *26*, 259.
- (342) Khan, H. R.; Petrikowski, K. *J. Magn. Magn. Mater.* **2002**, *249*, 458.
- (343) Philipse, A. P.; Maas, D. *Langmuir* **2002**, *18*, 9977.
- (344) Prozorov, T.; Mallapragada, S. K.; Narasimhan, B.; Wang, L. J.; Palo, P.; Nilsen-Hamilton, M.; Williams, T. J.; Bazylinski, D. A.; Prozorov, R.; Canfield, P. C. *Adv. Funct. Mater.* **2007**, *17*, 951.
- (345) Bharde, A. A.; Parikh, R. Y.; Baidakova, M.; Jouen, S.; Hannyoy, B.; Enoki, T.; Prasad, B. L. V.; Shouche, Y. S.; Ogale, S.; Sastry, M. *Langmuir* **2008**, *24*, 5787.
- (346) Bharde, A.; Rautaray, D.; Bansal, V.; Ahmad, A.; Sarkar, I.; Yusuf, S. M.; Sanyal, M.; Sastry, M. *Small* **2006**, *2*, 135.
- (347) Coker, V. S.; Telling, N. D.; van der Laan, G.; Patrick, R. A. D.; Pearce, C. I.; Arenholz, E.; Tuna, F.; Winpenny, R. E. P.; Lloyd, J. R. *ACS Nano* **2009**, *3*, 1922.
- (348) Amemiya, Y.; Arakaki, A.; Staniland, S. S.; Tanaka, T.; Matsunaga, T. *Biomaterials* **2007**, *28*, 5381.
- (349) Blakemore, R. P. *Annu. Rev. Microbiol.* **1982**, *36*, 20.
- (350) Matsunaga, T.; Kamiya, S. *Appl. Microbiol. Biotechnol.* **1987**, *26*, 328.
- (351) Emerich, D. F.; Thanos, C. G. *Expert Opin. Biol. Ther.* **2003**, *3*, 655.
- (352) Dubertret, P.; Norris, D. J.; Noireaux, V.; Brivanlou, A. H.; Libhaber, A. *Science* **2002**, *298*, 1759.
- (353) Jordan, A.; Scholz, R.; Wust, P.; Föhling, H.; Felix, R. *J. Magn. Magn. Mater.* **1999**, *201*, 413.

- (354) Petri-Fink, A.; Chastellain, M.; Juillerat-Jeanneret, L.; Ferrari, A.; Hofmann, H. *Biomaterials* **2005**, *26*, 2685.
- (355) Hilger, I.; Hergt, R.; Kaiser, W. A. *J. Magn. Magn. Mater.* **2005**, *293*, 314.
- (356) Oberdorster, G.; Oberdorster, E.; Oberdorster, J. *Environ. Health Perspect.* **2005**, *113*, 823.
- (357) Powers, K. W.; Palazuelos, M.; Moudgil, B. M.; Roberts, S. M. *Nanotoxicology* **2007**, *1*, 42.
- (358) Oberdorster, G.; Maynard, A.; Donaldson, K.; Castranova, V.; Fitzpatrick, J.; Ausman, K. D.; Carter, J.; Karn, B.; Kreyling, W.; Lai, D.; Olin, S.; Monteiro-Riviere, N.; Warheit, D.; Yang, H. *Part. Fibre Toxicol.* **2005**, *2*, 1.
- (359) Wittmaack, K. *Environ. Health Perspect.* **2007**, *115*, 187.
- (360) Nel, A.; Xia, T.; Madler, L.; Li, N. *Science* **2006**, *311*, 622.
- (361) Xia, T.; Kovochich, M.; Brant, J.; Hotze, M.; Sempf, J.; Oberley, T.; Sioutas, C.; Yeh, J. I.; Wiesner, M. R.; Nel, A. E. *Nano Lett.* **2006**, *6*, 1794.
- (362) Oberdorster, G.; Stone, V.; Donaldson, K. *Nanotoxicology* **2007**, *1*, 2.
- (363) Unfried, K.; Albrecht, C.; Klotz, L.; Von Mikecz, A.; Grether-Beck, S.; Schins, R. P. F. *Nanotoxicology* **2007**, *1*, 52.
- (364) Journeay, W. S.; Suri, S. S.; Morales, J. G.; Fenniri, H.; Singh, B. *Small* **2009**, *5*, 1446.
- (365) Journeay, W. S.; Suri, S. S.; Fenniri, H.; Singh, B. *Integr. Environ. Assess. Manage.* **2008**, *3*, 128.
- (366) Donaldson, K.; Stone, V. *Ann. Ist. Super. Santia.* **2003**, *39*, 405.
- (367) Donaldson, K.; Stone, V.; Clouter, A.; Renwick, L.; MacNee, W. *Am. J. Ind. Med.* **2001**, *58*, 211.
- (368) Donaldson, K.; Tran, L.; Jimenez, L. A.; Duffin, R.; Newby, D. E.; Mills, N.; MacNee, W.; Stone, V. *Part. Fibre Toxicol.* **2005**, *2*, 1.
- (369) Seaton, A.; MacNee, W.; Donaldson, K.; Godden, D. *Lancet* **1995**, *345*, 176.
- (370) Ghio, A. J.; Stonehurner, J.; Dailey, L. A.; Carter, J. D. *Inhalation Toxicol.* **1999**, *11*, 37.
- (371) Lucarelli, M.; Gatti, A.; Savarino, G.; Quattroni, P.; Martinelli, L.; Monari, E.; Boraschi, D. *Eur. Cytokine Network* **2004**, *15*, 339.
- (372) Dobrovolskaia, M. A.; McNeil, S. E. *Nat. Nanotechnol.* **2007**, *2*, 469.
- (373) Sayes, C. M.; Reed, K. L.; Warheit, D. B. *Toxicol. Sci.* **2007**, *97*, 163.
- (374) Sayes, C. M.; Marchione, A. A.; Reed, K. L.; Warheit, D. B. *Nano Lett.* **2007**, *7*, 2399.
- (375) Devlin, R. B.; Frampton, M. W.; Ghio, A. J. *Exp. Toxicol. Pathol.* **2005**, *57*, 183.
- (376) Worle-Knirsch, J. M.; Pulskamp, K.; Krug, H. F. *Nano Lett.* **2006**, *6*, 1161.
- (377) Stone, V.; Johnston, H.; Schins, R. P. F. *Crit. Rev. Toxicol.* **2009**, *39*, 613.
- (378) Stearns, R.; Paulauskis, J.; Godleski, J. *Am. J. Resp. Cell Mol.* **2001**, *24*, 108.
- (379) Teeguarden, J. G.; Hinderliter, P. M.; Orr, G.; Thrall, B. D.; Pounds, J. G. *Toxicol. Sci.* **2007**, *95*, 300.
- (380) Lewinski, N.; Colvin, V.; Drezek, R. *Small* **2008**, *4*, 26.
- (381) McAteer, J. A.; Davis, J. M. In *Basic Cell Culture: A Practical Approach*, 2nd ed.; Davis, J. M., Ed.; Oxford University Press: New York, 2002.
- (382) Kwon, Y.-M.; Xia, Z.; Glyn-Jones, S.; Beard, D.; Gill, H. S.; Murray, D. W. *Biomater. Mater.* **2009**, *4*, 025018.
- (383) Ding, L.; Stilwell, J.; Zhang, T.; Elboudware, O.; Jiang, H.; Selegue, J. P.; Cooke, P. A.; Gray, J. W.; Chen, F. F. *Nano Lett.* **2005**, *5*, 2448.
- (384) Driscoll, K. E. *Toxicol. Lett.* **2000**, *112–113*, 177.
- (385) Kobayashi, Y. *Crit. Rev. Immunol.* **2006**, *26*, 307.
- (386) Petri-Fink, A.; Hofmann, H. *IEEE Trans. Nanobiosci.* **2007**, *6*, 289.
- (387) Gould, P. *Nano Today* **2006**, *1*, 34.
- (388) Gupta, A. K.; Gupta, M. *Biomaterials* **2005**, *26*, 1565.
- (389) Gupta, A. K.; Wells, S. *IEEE Trans. Nanobiosci.* **2004**, *3*, 66.
- (390) Mahmoudi, M.; Simchi, A.; Imani, M. *J. Iran. Chem. Soc.* **2010**, *7*, S1.
- (391) Dutta, D.; Sundaram, S. K.; Teeguarden, J. G.; Riley, B. J.; Fifield, L. S.; Jacobs, J. M.; Addlemam, S. R.; Kayshen, G. A.; Moudgil, B. M.; Weber, T. J. *Toxicol. Sci.* **2007**, *100*, 303.
- (392) Mahmoudi, M.; Simchi, A.; Imani, M.; Milani, A. S.; Stroeve, P. *Nanotechnology* **2009**, *20*, 225104.
- (393) Mahmoudi, M.; Simchi, A.; Imani, M.; Shokrgozar, M. A.; Milani, A. S.; Hafeli, U. O.; Stroeve, P. *Colloids Surf., B* **2010**, *75*, 300.
- (394) Buyukhatipoglu, K.; Miller, T. A.; Clyne, A. M. *J. Nanosci. Nanotechnol.* **2009**, *9*, 6834.
- (395) Pelley, J. L.; Daars, A. S.; Saner, M. A. *Toxicol. Sci.* **2009**, *112*, 276.
- (396) Di Marco, M.; Sadun, C.; Port, M.; Guilbert, I.; Couvreur, P.; Dubernet, C. *Int. J. Nanomedicine* **2007**, *2*, 609.
- (397) Thorne, S. H.; Negrin, R. S.; Contag, C. H. *Science* **2008**, *311*, 1780.
- (398) Michalec, X.; Pinaud, F. F.; Bentolila, L. A.; Tsay, J. M.; Dooze, S.; Li, J. J.; Sundaresan, G.; Wu, A. M.; Gambhir, S. S.; Weiss, S. *Science* **2005**, *307*, 538.
- (399) Yang, C. Y.; Tai, M. F.; Chen, S. T.; Wang, Y. T.; Chen, Y. F.; Hsiao, J. K.; Wang, J. L.; Liu, H. M. *J. Appl. Phys.* **2009**, *105*, 07B314.
- (400) Cavella, C.; Geninatti Cich, S.; Corpillo, D.; Barge, A.; Ghirelli, C.; Bruno, E.; Lorusso, V.; Uggeri, F.; Aime, S. *Contrast Med. Mol. Imaging* **2006**, *1*, 15.
- (401) Heyn, C.; Ronald, J. A.; Mackenzie, L. T.; MacDonald, I. C.; Chambers, A. F.; Rutt, B. K.; Foster, P. J. *Magn. Reson. Med.* **2006**, *55*, 23.
- (402) Mailander, V.; Lorenz, M. R.; Holzapfel, V.; Musyanovych, A.; Fuchs, K.; Wiesneth, M.; Walther, P.; Landfester, K.; Schrezenmeier, H. *Mol. Imaging Biol.* **2008**, *10*, 138.
- (403) Huang, D. M.; Hsiao, J. K.; Chen, Y. C.; Chien, L. Y.; Yao, M.; Chen, Y. K.; Ko, B. S.; Hsu, S. C.; Tai, L. A.; Cheng, H. Y.; Wang, S. W.; Yang, C. S. *Biomaterials* **2009**, *30*, 3645.
- (404) Gyöngyösi, M.; Blanco, J.; Marian, T.; Trón, L.; Petneházy, O.; Petrasi, Z.; Hemetsberger, R.; Rodriguez, J.; Font, G.; Pavo, I. J.; Kertész, I.; Balkay, L.; Pavo, N.; Posa, G.; Emri, M.; Galuska, L.; Kraitchman, D. L.; Wojta, J.; Huber, K.; Glogar, D. *Circ. Cardiovasc. Imaging* **2008**, *1*, 94.
- (405) Ju, S.; Teng, G.; Zhang, Y.; Ma, M.; Chen, F.; Ni, Y. *Magn. Reson. Imaging* **2006**, *24*, 611.
- (406) Bulte, J. W. M.; Douglas, T.; Witwer, B.; Zhang, S. C.; Strable, E.; Lewis, B. K.; Zywickie, H.; Miller, B.; Van Gelderen, P.; Moskowitz, B. M.; Duncan, I. D.; Frank, J. A. *Nat. Biotechnol.* **2001**, *19*, 1141.
- (407) Jendelova, P.; Herynek, V.; DeCros, J.; Glogarova, K.; Andersson, B.; Hajek, M.; Sykova, E. *Magn. Reson. Imaging* **2003**, *50*, 767.
- (408) Lewin, M.; Carlesso, N.; Tung, C. H.; Tang, X. W.; Cory, D.; Scadden, D. T.; Weissleder, R. *Nat. Biotechnol.* **2000**, *18*, 410.
- (409) Lu, C. W.; Hung, Y.; Hsiao, J. K.; Yao, M.; Chung, T. H.; Lin, Y. S.; Wu, S. H.; Hsu, S. C.; Liu, H. M.; Mou, C. Y.; Yang, C. S.; Huang, D. M.; Chen, Y. C. *Nano Lett.* **2007**, *7*, 149.
- (410) Fleige, G.; Seeberger, F.; Laux, D.; Kresse, M.; Taupitz, M.; Pilgrimm, H.; Zimmer, C. *Invest. Radiol.* **2002**, *37*, 482.
- (411) Kirchner, C.; Liedl, T.; Kuder, S.; Pellegrino, T.; Javier, A. M.; Gaub, H. E.; Stölzle, S.; Fertig, N.; Parak, W. J. *Nano Lett.* **2005**, *5*, 331.
- (412) Wang, H. H.; Wang, Y. X. J.; Leung, K. C. F.; Sheng, H.; Zhang, G.; Lee, S. K. M.; Au, D. W. T.; Chak, C. P.; Qin, L.; Griffith, J. F. 5th Int. Conference on Information Technology and Applications in Biomedicine, ITAB and IS3BHE, 2008; p 187.
- (413) Wilhelm, C.; Gazeau, F. *Biomaterials* **2008**, *29*, 3161.
- (414) Babic, M.; Horak, D.; Trchova, M.; Jendelova, P.; Glogarova, K.; Lesny, P.; Herynek, V.; Hajek, M.; Sykova, E. *Bioconjugate Chem.* **2008**, *19*, 740.
- (415) Babic, M.; Horak, D.; Jendelova, P.; Glogarova, K.; Herynek, V.; Trchova, M.; Likavanova, K.; Lesna, P.; Pollert, E.; Hajek, M.; Sykova, E. *Bioconjugate Chem.* **2009**, *20*, 283.
- (416) Suh, J. S.; Lee, J. Y.; Choi, Y. S.; Yu, F.; Yang, V.; Lee, S. J.; Chung, C. P.; Park, Y. J. *Biochem. Biophys. Res. Commun.* **2009**, *379*, 669.
- (417) Schwarz, S.; Fernandes, F.; Sanroman, L.; Hostenius, M.; Lang, C.; Himmelreich, U.; Schmitz-Rode, T.; Schueler, D.; Hoehn, M.; Zenke, M.; Hieronymus, T. *J. Magn. Magn. Mater.* **2009**, *321*, 1533.
- (418) Wang, F. H.; Lee, I. H.; Holmstrom, N.; Yoshitake, T.; Kim, D. K.; Muhammed, M.; Frisen, J.; Olson, L.; Spenger, C.; Kehr, J. *Nanotechnology* **2006**, *17*, 1911.
- (419) Focke, A.; Schwarz, S.; Foerschler, A.; Scheibe, J.; Milosevic, J.; Zimmer, C.; Schwarz, J. *Magn. Reson. Med.* **2008**, *60*, 1321.
- (420) Xue, J.; Gao, P. Y.; Li, J.; Sun, C. R.; Huang, H.; An, Y. H. *Chin. J. Radiol.* **2006**, *40*, 122.
- (421) Lei, D.; Zhao, H.; Deng, X.; Liu, R.; Zhang, F.; Yao, D. *J. Huazhong Univ. Sci. Technol.* **2009**, *29*, 235.
- (422) Stuckey, D. J.; Carr, C. A.; Martin-Rendon, E.; Tyler, D. J.; Willmott, C.; Cassidy, P. J.; Hale, S. J. M.; Schneider, J. E.; Tatton, L.; Harding, S. E.; Radda, G. K.; Watt, S.; Clarke, K. *Stem Cells* **2006**, *24*, 1968.
- (423) Lee, J. H.; Smith, M. A.; Liu, W.; Gold, E. M.; Lewis, B.; Song, H. T.; Frank, J. A. *Nanotechnology* **2009**, *20*, 355102.
- (424) Makino, S.; Fukuda, K.; Miyoshi, S.; Konishi, F.; Kodama, H.; Pan, J.; Sano, M.; Takahashi, T.; Hori, S.; Abe, H.; Hata, J. I.; Umezawa, A.; Ogawa, S. *J. Clin. Invest.* **1999**, *103*, 697.
- (425) Nagaya, N.; Fujii, T.; Iwase, T.; Ohgushi, H.; Itoh, T.; Uematsu, M.; Yamagishi, M.; Mori, H.; Kangawa, K.; Kitamura, S. *Am. J. Physiol. - Heart C* **2004**, *287*, H2670.
- (426) Leite-Moreira, A. F. *Rev. Port. Cardiol.* **2003**, *22*, 589.
- (427) Perin, E. C.; Dohmann, H. F. R.; Borjovic, R.; Silva, S. A.; Sousa, A. L. S.; Mesquita, C. T.; Rossi, M. I. D.; Carvalho, A. C.; Dutra, H. S.; Dohmann, H. J. F.; Silva, G. V.; Belém, L.; Vivacqua, R.;

- Rangel, F. O. D.; Esporcatte, R.; Geng, Y. J.; Vaughn, W. K.; Assad, J. A. R.; Mesquita, E. T.; Willerson, J. T. *Circulation* **2003**, *107*, 2294.
- (428) Strauer, B. E.; Brehm, M.; Zeus, T.; Köstering, M.; Hernandez, A.; Sorg, R. V.; Kögler, G.; Wernet, P. *Circulation* **2002**, *106*, 1913.
- (429) Amsalem, Y.; Feinberg, M. S.; Landa, N.; Miller, L.; Holbova, R.; Shaharabani-Yosef, O.; Barbash, I. M.; Leor, J.; Mardor, Y.; Daniels, D.; Ocherashvilli, A. *Circulation* **2008**, *117*, e307.
- (430) Amsalem, Y.; Mardor, Y.; Feinberg, M. S.; Landa, N.; Miller, L.; Daniels, D.; Ocherashvilli, A.; Holbova, R.; Yosef, O.; Barbash, I. M.; Leor, J. *Circulation* **2007**, *116*, 138.
- (431) Sadek, H. A.; Garry, D. J. *Circulation* **2008**, *117*, e306.
- (432) Portet, D.; Denizot, B.; Rump, E.; Lejeune, J. J.; Jallet, P. *J. Colloid Interface Sci.* **2001**, *238*, 37.
- (433) Delcroix, G. J. R.; Jacquart, M.; Lemaire, L.; Sindji, L.; Franconi, F.; Le Jeune, J. J.; Montero-Menei, C. N. *Brain Res.* **2009**, *1255*, 18.
- (434) Politi, L. S. *Neuroradiology* **2007**, *49*, 523.
- (435) Guzman, R.; Uchida, N.; Bliss, T. M.; He, D.; Christopherson, K. K.; Stellwagen, D.; Capela, A.; Greve, J.; Malenka, R. C.; Moseley, M. E.; Palmer, T. D.; Steinberg, G. K. *Proc. Natl. Acad. Sci. U. S. A.* **2007**, *104*, 10211.
- (436) D'Ippolito, G.; Diabira, S.; Howard, G. A.; Menei, P.; Roos, B. A.; Schiller, P. C. *J. Cell Sci.* **2004**, *117*, 2971.
- (437) Tatard, V. M.; D'Ippolito, G.; Diabira, S.; Valeyev, A.; Hackman, J.; McCarthy, M.; Bouckenoghe, T.; Menei, P.; Montero-Menei, C. N.; Schiller, P. C. *Bone* **2007**, *40*, 360.
- (438) Wang, L.; Li, Y.; Chen, X.; Chen, J.; Gautam, S. C.; Xu, Y.; Chopp, M. *Hematology* **2002**, *7*, 113.
- (439) Pawelczyk, E.; Arbab, A. S.; Chaudhry, A.; Balakumaran, A.; Robey, P. G.; Frank, J. A. *Stem Cells* **2008**, *26*, 1366.
- (440) Heymer, A.; Haddad, D.; Weber, M.; Gbureck, U.; Jakob, P. M.; Eulert, J.; Nöth, U. *Biomaterials* **2008**, *29*, 1473.
- (441) Liu, Z. Y.; Wang, Y.; Liang, C. H.; Li, X. H.; Wang, G. Y.; Liu, H. J.; Li, Y. *Radiology* **2009**, *253*, 153.
- (442) Hong, H.; Yang, Y.; Zhang, Y.; Cai, W. *Curr. Pharm. Biotechnol.* **2010**, *11*, 685.
- (443) De Vries, I. J. M.; Lesterhuis, W. J.; Barentsz, J. O.; Verdijk, P.; Van Krieken, J. H.; Boerman, O. C.; Oyen, W. J. G.; Bonenkamp, J. J.; Boezeman, J. B.; Adema, G. J.; Bulte, J. W. M.; Scheenen, T. W. J.; Punt, C. J. A.; Heerschap, A.; Figdor, C. G. *Nat. Biotechnol.* **2005**, *23*, 1407.
- (444) Zhu, J.; Zhou, L.; XingWu, F. G. *New Engl. J. Med.* **2006**, *355*, 2376.
- (445) Song, M.; Moon, W. K.; Kim, Y.; Lim, D.; Song, I. C.; Yoon, B. W. *Korean J. Radiol.* **2007**, *8*, 365.

CR1001832